

UCSF

UC San Francisco Electronic Theses and Dissertations

Title

Excision repair and DNA synthesis after ultraviolet light exposure in African green monkey kidney CV-1 cells and simian virus 40 (SV40)

Permalink

<https://escholarship.org/uc/item/3f3469fs>

Author

Williams, John Ira

Publication Date

1977

Peer reviewed|Thesis/dissertation

EXCISION REPAIR AND DNA SYNTHESIS AFTER ULTRAVIOLET LIGHT EXPOSURE
IN AFRICAN GREEN MONKEY KIDNEY CV-1 CELLS AND SIMIAN VIRUS 40 (SV40)

by

Jon Ira Williams
B.S., Harvey Mudd College 1967

DISSERTATION

Submitted in partial satisfaction of the requirements for the degree of

DOCTOR OF PHILOSOPHY

in

BIOPHYSICS

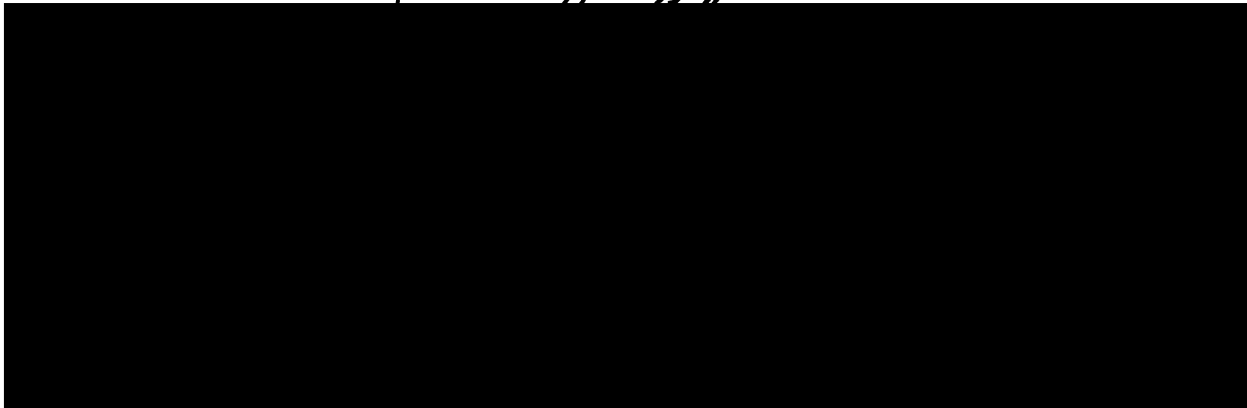
in the

GRADUATE DIVISION

(San Francisco)

of the

UNIVERSITY OF CALIFORNIA



Date

Librarian

APR 3 1977

Degree Conferred:

© 1977

JON IRA WILLIAMS

ALL RIGHTS RESERVED

...A virus is nothing but a part of a cell. We observe and recognize as viruses those parts independent enough to pass from cell to cell and we compare them with other parts that are more tightly tied up with the whole system. It is indeed this aspect of viruses that makes them invaluable to the biologist whom they present with the unique opportunity to observe in isolation the active determinants of biological specificity, which are truly the stuff of which all life is made.

p. 454, Luria and Darnell
General Virology

A b s t r a c t

The capacity of African green monkey kidney CV-1 cells to perform ultraviolet (UV) light-induced excision repair of cellular DNA and Simian Virus 40 (SV40) DNA was examined. The induction and kinetics of removal of UV (254 nm) lesions in CV-1 DNA was followed by assaying T4 endonuclease V-sensitive sites, repair replication and dimer removal. T4 endonuclease V substrate sites were induced at a rate of 1.36 sites per 10^8 daltons of DNA per J/m^2 and removed in a dose-dependent fashion. The loss of T4 endonuclease V substrate sites from CV-1 DNA was biphasic in the dose range 0-25 J/m^2 with a rapid initial rate and a slower rate 6-24 hours post-UV. The extent of T4 endonuclease V site loss saturated in the dose range 25-38 J/m^2 . UV-induced repair replication in CV-1 DNA also saturated in this dose range and exhibited a similar biphasic rate response. The estimated patch size from this data was about 30 nucleotides per repaired pyrimidine dimer. Dimer induction by UV light was followed by thin layer chromatography and occurred at a rate of 1.30 dimers per 10^8 daltons of DNA per J/m^2 . The rate of dimer removal was linear for the first 24 hours post-UV over the dose range 0-50 J/m^2 . This data favors a "patch-and-cut" mechanism for excision repair. Alternate mechanisms are discussed.

Excision repair in SV40 DNA was followed during a lytic infectious cycle in CV-1 cells by assaying T4 endonuclease V-sensitive sites and repair replication. T4 endonuclease substrate sites were induced at a rate of 1.42 sites per 10^8 daltons of DNA per J/m^2 and removed with biphasic kinetics in the dose range 25-38 J/m^2 . The kinetics of site

removal at lower doses was complex and probably reflected cytopathic cell changes during the lytic cycle. The extent of T4 endonuclease V-sensitive site removal in 24 hours compared favorably with the values found in CV-1 DNA. Repair replication in SV40 DNA could be detected using isopycnic gradients but the resolution of this technique was low. These experimental observations confirm intracellular SV40 DNA is subject to all stages of excision repair after UV light exposure.

DNA synthesis in UV-irradiated CV-1 cells was analyzed. Suppression of CV-1 DNA synthesis with UV light treatment and its recovery with post-UV incubation was established. SV40 DNA synthesis during a lytic infectious cycle in UV-irradiated CV-1 cells was then examined in detail by pulse-labelling techniques. SV40 DNA synthesis was depressed to 60% of control at 20 J/m^2 and 44% of control at 40 J/m^2 . The formation of Form I (supercoiled) SV40 DNA molecules was observed to be the most sensitive stage in the replication cycle: replicative intermediates (RIs) \rightarrow Form II (open circle) \rightarrow Form I. The relative proportion of RIs and Form II molecules increased with increasing UV dose. These results are interpreted as confirming UV lesions in SV40 DNA inhibit elongation but not initiation of DNA replication. Post-UV incubations of pulse-labelled SV40 DNA in unlabelled medium for one or three hours revealed a rapid decrease in RIs, a slow decrease in Form II molecules, and a rapid rise in Form I molecules. Two facts are deduced from this data: (1) CV-1 cells have the enzymatic capacity to bridge a small gap created opposite or near a pyrimidine dimer by two growing forks meeting at or near the dimer, and (2) replication is probably halted at or near a pyrimidine dimer on both parental strands.

TABLE OF CONTENTS

	<u>Page</u>
I. Introduction	1
1. Background	1
2. Molecular Biology and UV-Photobiology of Simian Virus 40 (SV40)	7
3. Problems in Excision Repair of Mammalian Cell Pyrimidine Dimers	15
4. Problems in Post-Replication Repair of Pyrimidine Dimers	19
II. Materials and Methods	24
1. Materials	24
(A) Biological Materials	24
(B) Chemicals	24
(C) Enzymes	25
2. Methods	25
(A) Conditions for Exposure to Ultra- violet (UV) Light	25
(B) Monkey Kidney CV-1 Cell Growth Characteristics	26
(C) Monkey Kidney CV-1 Cell Chromosome Analysis	27
(D) Monkey Kidney CV-1 Cell UV Survival Assay	27
(E) Cell Stock Growth and Storage by Freezing	28
(F) Viral Stock Growth	29
(G) Conditions for SV40 Infection of CV-1 Cells	29

	<u>Page</u>
(H) Hirt Extraction Procedure and Assay for Purity of SV40 DNA Obtained in the Hirt Supernatant	30
(I) Increase in Viral DNA in Cultures Infected at High Multiplicity	31
(J) Appearance of SV40 Plaque-Forming Units (PFUs) in Infected Culture Media	32
(K) SV40 Plaque Assays	33
(L) T4 Endonuclease V Assay for Endonuclease-Sensitive Sites in CV-1 DNA	33
(M) CV-1 DNA Repair Replication Studies	35
(N) Interference of ³ H-Decays or X-rays with UV Light-Induced Repair Replication	36
(O) Pyrimidine Dimer Removal from CV-1 Cells	37
(P) Induction of T4 Endonuclease V-Sensitive Sites and Kinetics of Site Removal in SV40 DNA	38
(Q) BrdUrd Photolysis Assay	38
(R) Repair Replication in SV40 DNA from Infected Cultures After Exposure to UV Light	39
(S) DNA Synthesis in CV-1 Cells after Exposure to UV Light	41
(T) SV40 DNA Replication in UV-Irradiated Cultures	43
3. Analytical Techniques	44
(A) T4 Endonuclease V Assay	44

	<u>Page</u>
(B) <u>Eco</u> RI Restriction Enzyme Assay	45
(C) Agarose Tube Gel Electrophoresis	46
(D) Neutral Sucrose Isokinetic Sedi- mentation	47
(E) Alkaline Sucrose Isokinetic Sedi- mentation	48
(F) Neutral CsCl Isopycnic Centrifu- gation	48
(G) CsCl-Ethidium Bromide Isopycnic Centrifugation	49
(H) CsCl-Propidium Iodide Equilibrium Density Gradient Ultracentrifu- gation	50
(I) Alkaline CsCl-CsSO ₄ Equilibrium Density Gradient Ultracentrifu- gation	50
(J) Thin-Layer Chromatography	51
III. Results	53
1. Monkey Kidney CV-1 Cell Characteristics in Culture	53
2. SV40 Productive Infectious Cycle in CV-1 Cells	54
3. Excision Repair in CV-1 Cells After Exposure to UV Light	57
4. Excision Repair in SV40 DNA After Ex- posure to UV Light	65
5. CV-1 DNA Synthesis UV-Irradiated Cultures .	71
6. SV40 DNA Synthesis in SV40-Infected CV-1 Cultures After Exposure to UV Light	72

	<u>Page</u>
IV. Discussion	78
1. Excision repair of CV-1 DNA	78
2. Excision repair of SV40 DNA	82
3. DNA synthesis in UV-irradiated CV-1 cells	85
4. DNA synthesis of UV-irradiated SV40 DNA	86
V. A Model for Post-Replication Repair in SV40 DNA.	96
VI. Appendices	99
A. Calculation of repair replication in SV40 DNA from infected cultures after exposure to UV light	99
B. Calculation of number average DNA molecular weight (M_n) and weight average DNA molecular weight (M_w) from SW40 rotor alkaline sucrose gradient radioactivity profiles.	101
C. Calculation of the number of T4 endonuclease V-sensitive sites per 10^8 daltons of CV-1 DNA from alkaline sucrose gradient radioactivity profiles	104
D. Calculation of the corrected percentage of tritium label found in the pyrimidine dimer peak on thin layer chromatograms.	107
E. Calculation of the maximum expected increase in DNA strand breakage by 313 nm light in SV40 DNA molecules which contain BrdUrd in place of dThd as a base residue in repaired regions of the SV40 genome.	109
F. Equations for the fraction of pulse label in UV-irradiated SV40 replicative intermediates (RIs) that persists for several hours after pulse-labelling	110
VII. List of References	113

ACKNOWLEDGEMENTS

I want to thank Drs. Alan Blumenthal, James Cleaver and Robert B. Painter of the Laboratory of Radiobiology for their generous donation of space and materials and their many helpful suggestions concerning this research. I also want to thank Elizabeth Clark, Gregory Thomas and Barbara Young for invaluable technical advice. Finally, my special thanks to Dr. Harvey Patt and all employees of the U.C. San Francisco Laboratory of Radiobiology with whom I have come into contact and without whom this research could never have been brought to a successful conclusion.

This research was performed under the auspices of National Institute of Health graduate training grant No. 5T01GM00829.

I. INTRODUCTION

1. Background

The physical and biochemical basis for the interaction of radiation and living tissue has occupied biologists since early in this century (1-4). Research prior to 1950 concentrated almost exclusively on effects of ionizing radiation on whole animals or animal tissue (5,6). The role of physical agents such as radiation could not be at the cellular level in animals until successful techniques for establishing eucaryotic cell cultures in defined media were widely available (7-10). A new type of biologist emerged, the cell biologist, who was dedicated to elucidating the subcellular events responsible for cell survival and propagation. Radiation became a popular means of perturbing cells for the examination of their response. Puck and his coworkers developed the first cell survival assay (11) and allowed the initial studies which indicated cell populations had a complex survival response to radiation (12,13). Complex theories to explain the shapes of survival curves were developed (14-16), but none of them predicted cellular recovery after radiation (12, 17).

Coincident with these early radiobiological studies, the concept of an action spectrum was developed for complex biological molecules such as proteins and nucleic acids as

well as for whole cells (18,19). The bacteriologists found that the action spectrum for killing of bacteria mimicked the absorption spectrum of nucleic acids (19). Although this does not hold for eucaryotic cells (20; for review also see (21)), attention was focussed on the response of nucleic acids in mammalian cells to all forms of radiation. Photobiology first concentrated on ultraviolet (UV) radiation in the wave length range around 260 nm, the absorption peak for nucleic acids. Survival curves for cells exposed to UV light from low pressure Hg lamps (germicidal lamps) emitting primarily at 254 nm showed much greater variation in shape than did curves produced by ionizing radiation (14, 22,23). The bacteriologists made the first observations of cellular recovery and repair after UV light exposure (for review see (24)). It was not until 1964 that the biochemical techniques of the bacteriologists were first applied to mammalian cells to confirm that mammalian cells have enzymes specific for damage in deoxyribonucleic acid (DNA) that are involved in recovery from UV-irradiation and removal of UV-induced lesions in DNA (25).

The biochemistry of UV damage was explored in the early 1960's as cell biology and radiobiology merged. Beuker and Berends (26,27) identified the primary photoproducts after UV-irradiation of frozen solutions of nucleic acids with a low pressure Hg lamp as the four isomeric cyclobutyl-

pyrimidine dimers; Setlow and Setlow later showed the importance of the cis-syn isomer in causing cell death (28). Several types of DNA restitution processes have been defined and confirmed in mammalian cells during the last decade: photoreversal, a non-enzymatic photochemical response (29); photoreactivation (30); excision repair (31, 32); and the repair response currently termed post-replication repair (33) (for reviews, see (17), (34) and (35)).

There are many questions about molecular repair processes in mammalian cells that are unanswered. One of these is what link (if any) the repair processes for UV-induced lesions have to those observed for lesions produced by ionizing radiation (34) or chemical carcinogen treatment (36, 37). Also, several recent experiments have introduced confusion over details of excision repair and post-replication repair. These topics are discussed in greater detail in the last two sections of the Introduction.

The importance of answering such questions is related to the clinical relevance of DNA repair experiments in UV photobiology. Cleaver observed (38) that cells from patients with the recessive disease Xeroderma Pigmentosum (XP) have a defect in DNA repair and a lower survival after UV light exposure than do normal human cells. This provided the first connection of molecular radiobiology to a known disease. In addition, the high incidence of all types of skin cancers in

XP patients suggested that DNA repair and malignancy may be related. Techniques for studying DNA repair after radiation have been modified and adopted on a large scale by cancer researchers (39). It is therefore all the more important that the molecular mechanisms for DNA repair after radiation treatment be as completely defined as possible, so that the mechanisms' relation to misrepair and mutation be clarified and the ultimate effects of incomplete restoration of cellular integrity be known.

One such ultimate effect is cell transformation (40, 41), a term encompassing a wide variety of in vitro observations thought to be closely related to the whole animal changes resulting in tumors and other malignant cell conditions that can ultimately lead to death of the animal. It is not known if simple or multiple mutations can lead to cell transformation, but a widely accepted non-viral theory of cancer, the somatic mutation theory (42), hypothesizes that the accumulation of mutations over the life of a cell can lead to the release of the cell from growth control and eventually to cell transformation and possibly malignancy. If this theory is correct, then much more information must be obtained on DNA repair and mutational events. This is especially pertinent to UV photobiology because of the universal exposure of people to sunlight at a dose rate equivalent to $0.1-0.2 \text{ J/m}^2/\text{min}$ (43) of 254 nm

UV light. This dose rate requires constant surveillance of DNA by DNA repair systems if cell lethality is to be avoided. It is possible that during the repair of DNA under these conditions in human epithelial cells or blood cells of the peripheral circulation that mutations may occur.

Bacterial studies reveal uncorrected errors in DNA replication can also lead to mutations (44). Such mutations are drastically increased by UV photoproducts in the DNA of a variety of organisms, including bacteria (45), plants (46), mammalian cells (47-49), and animal viruses (50). UV light thus poses a mutational threat to dividing tissues in mammals.

Repair deficient cell lines are necessary for molecular studies to correlate mutations with either misrepair or lack of repair. There are very few known mammalian cell lines deficient in repair. XP cells from complementation groups A-E (51) and the XP variant (52,53) as well as cells from patients with the disease ataxia telangiectasia (AT) (54) are the only verified repair deficient cell lines; characterization of AT cells has only begun. In addition, the variety of repair deficiencies in XP cells (55,56) and the demonstration that extracts of XP cells are not deficient in the endonucleolytic step of excision repair on isolated DNA (57) has raised the suspicion that XP cells may be deficient

in repair enzyme cofactors rather than in repair enzyme activity. Deliberate isolation of repair defective cell lines by such methods as ^3H suicide or viral infection has not yet succeeded (21).

A different approach to examining the relation of DNA repair systems to mutations has been explored over the last decade by virologists and cancer researchers. As an indication of repair in animal virus DNA, host cell reactivation after exposure to UV light has been demonstrated for herpes virus (58), adenovirus (59), and the papovavirus Simian Virus 40 (SV40) (60,61). These animal viruses are distinctive as a homogeneous set of haploid genomes which can be easily isolated away from host cell DNA and which can be mutated by single mutagenic events. These advantages suggest mutational events and properties of DNA repair may be more amenable to study in mammalian cell viruses than in mammalian cells. There have been only a few such studies of DNA repair for herpes virus (58,62), adenovirus (59,63), and SV40 (50,60,61,64,65).

The experimental efforts of this thesis have been: (1) to verify that a chosen animal virus-permissive host cell system, specifically SV40 productively infecting the established African green monkey kidney cell line CV-1, exhibits typical properties for repairing both CV-1 and SV40 DNA; (2) to closely examine excision repair in CV-1 cells

in an attempt to test the presently accepted heuristic model for excision repair (21); and (3) to study DNA replication in UV-irradiated SV40 DNA and to develop an improved model for post-replication repair in SV40 DNA. Fruitful experimental results in these three areas will serve in the future as a foundation for using the SV40 genome as a model mammalian cell replicon where the delicate interplay of DNA repair and mutational events may unravel some of the mysteries surrounding cell transformation and carcinogenesis.

2. Molecular Biology and UV-Photobiology of Simian Virus 40 (SV40)

SV40 was initially identified as a contaminant in monkey cell cultures used to grow and quantitate papovavirus vaccines (66). SV40 is a member of the papovavirus family of DNA tumor viruses and is grouped with polyoma virus because of the many similarities in their molecular biology. SV40 productively infects monkey cells in culture and is potentially capable of transforming cells in culture from humans, guinea pigs, mice, rats, hamsters and, in some cases, monkeys (67). SV40 causes tumors in all these animals except humans (67). There is also a recent report implicating SV40-like particles in cases of the rare neurological disease PML (progressive multifocal leukencephalopathy) (68).

The SV40 virion is about 45 nm in diameter and has 72 protein capsomers surrounding a DNA core. SV40 DNA is usually isolated from SV40 virions as a closed double-stranded DNA superhelix (Form I molecule) with a small percentage of open circle, double-stranded DNA molecules (Form II molecules) which have a break or gap in one DNA strand. There are about 20 superhelical turns per SV40 genome (67). Some linear DNA molecules are also found in SV40 virions (Form III molecules); these pseudovirions are non-infectious. The DNA of pseudovirions originates from host cell DNA and is only found in cultures where SV40 infection induces host cell DNA synthesis (67).

Table I on the next page lists the sedimentation constants for Form I, II and III SV40 DNA molecules under neutral or alkaline ($\text{pH} \geq 10.6$) pH conditions on isokinetic sucrose gradients. The large differences in sedimentation constants on alkaline sucrose gradients for the various SV40 DNA forms favors alkaline conditions for analysis of mixtures of SV40 DNA. Purification of SV40 away from host cell DNA for preparative purposes is favored on neutral pH sucrose gradients because of the narrow sedimentation region (14-20 S) within which all SV40 DNA forms are found.

SV40 DNA has a molecular weight of about 3.6×10^6 daltons, a G-C content of 41%, and a genome length of 5100 base pairs (67). The G-C content of host (monkey)

Sedimentation Constants for SV40 DNA Molecules

(in Svedbergs)

	<u>Neutral pH</u>	<u>Alkaline pH</u>
Form I	20	53
Form II	16	18
Form III	14	16

Table I

cell DNA is 42-44% (67). The coding capacity of SV40 is 3-5 genes for proteins with molecular weight of about 40,000 daltons; this agrees with the five complementation groups defined by exhaustive search for temperature-sensitive SV40 mutants (60). SV40 DNA is found to be packed in virions with all host cell histones except H1 (70). The small coding capacity of SV40 DNA (67) probably requires the virus to use host cell DNA replication and repair enzymes.

SV40 virions penetrate permissive cells very rapidly after adsorption and probably reach the nucleus within a few minutes (71), but SV40 DNA is not uncoated until 18-24 hours after infection (67). SV40 DNA is released in the host cell nucleus as a Form I molecule and is complexed with histones and other proteins into chromatin structures remarkably similar to eucaryotic chromatin (72). Initiation of SV40 DNA replication requires the A gene product (73) and begins at a single site about 0.65 genome units clockwise from the single EcoRI restriction enzyme substrate site. Replication is bidirectional and discontinuous on both parental strands (67). There is no specific termination site for replication (74); instead replication halts at or near a position 180° from the initiation site. There is no natural or UV-induced recombination between replicating SV40 DNA molecules (75). A gap of about 70 nucleotides is left in one strand of one or both of the near-completed daughter SV40

genomes. The gap can be sealed in vitro by polymerization and ligation (76). This short-lived intermediate may be the source of the constant small fraction of Form II molecules observed when SV40 DNA is isolated from infected host cells (77). Roman and Dulbecco have shown that the pool of replicating SV40 DNA molecules increases linearly and reaches a maximum size in only a few hours (78). They further observed that DNA molecules are randomly recruited into the pool of replicating molecules (78). This suggests that residual label is found in SV40 replicative intermediates long times after a "chase" has begun in pulse-"chase" experiments because some replicative intermediates have finished replication and later re-entered the replicating pool by random selection (77).

The total amount of SV40 DNA which accumulates in an infected culture is less than 20% of the total DNA (67) or 0.1-1.0 μg of SV40 DNA per 10^6 host cells. Infection of cultures at high multiplicity promotes the appearance of defective SV40 genomes which have large deletions and/or portions of host cell DNA covalently attached (79,80). The presence of host cell DNA in pseudovirions and virions with covalently attached viral DNA argues for the covalent integration of SV40 DNA in host cell chromosomes sometime during the lytic infection cycle. Evidence of up to 20,000 such integrated copies has been reported from hybridization studies (81), but more recent reports (82,83)

disagree and attribute the presence of viral DNA in precipitates of infected cell lysates spun at high speed to the sedimentation of dimer and higher multimers of SV40 DNA trapped in the sedimenting matrix of high molecular weight host cell molecules. However, there must be some period of covalent attachment to explain the presence of hybrid genomes, although the number of integrated genomes must be smaller than first reported. It is an attractive hypothesis to assume that covalent integration of SV40 chromatin into host cell chromosomes comes about much like phage λ integrates into the E. coli chromosome (84), but there is no evidence for such a process. In fact, hybridization studies of SV40-transformed cells show that different portions of the SV40 genome are present in different numbers of copies (85), so that covalent integration by simple breakage and attachment at a single site in both SV40 and host cell DNA may not explain how SV40 DNA becomes linked to host cell DNA in SV40-transformed cells.

Components of the SV40 virion assemble in the nucleus beginning about two days after infection (67). The assembled virions are exported to the extracellular medium at this time and export continues for several days. About 10^5 physical particles are produced per infected cell of which only 1% are capable of plaque formation and are thus classified as infectious.

Detailed genetic and biochemical studies of the SV40 genome have made SV40 the best-known animal tumor virus. Bacterial restriction enzymes have been used to map the SV40 genome in an attempt to relate genome structure and organization to function. Several restriction enzymes have been used on SV40 DNA creating up to 16 genome fragments (86). P. Berg and D. Nathans have independently developed techniques using restriction enzymes to artificially create deletions of 50 or more base pairs at specific SV40 genome sites (64,87, 88). The order of restriction enzyme substrate sites is known so that any SV40 fragment of only a few tens of base pairs can be isolated with precision, partly due to advances in agarose (89) and agarose-acrylamide gel zone electrophoresis. These techniques have aided in mapping the transcription order in SV40 DNA (73,90) as well as accelerated the new field of recombinant DNA biochemistry.

Information on the UV-photobiology of SV40 is scanty. Laterjet in 1967 showed that the transforming ability of SV40 is 5 times more resistant to UV-irradiation than plaque formation and argued on target theory grounds that only one-fifth of the SV40 genome was needed for transformation (91). Later workers found transformation of infected cultures with SV40 was increased by caffeine treatment after UV light exposure (92); caffeine is a specific inhibitor of post-replication repair (93). Black and coworkers demonstrated induction of

infectious SV40 from high yield clones of SV40-transformed hamster cells with UV light and showed this induction to be cell cycle-specific for late S-phase (94,95), the same period when these cells are most resistant to cell killing with UV light. They concluded that cellular repair systems may be involved in SV40 induction from host cell DNA.

Photoreactivation of UV-irradiated SV40 has not been studied. Two photoreactivation experiments with herpes virus in normal and XP fibroblasts are the only evidence on this repair system in mammalian cells using an animal virus and the conclusions from these two groups are in direct conflict (96,97). The difference may be related to the reported culture medium dependence of photoreactivation in mammalian cells (98,99).

Host cell reactivation of SV40 cannot be directly demonstrated in monkey cells since appropriate repair-deficient monkey cell mutants are lacking. However, an ingenious approach (61) using mixed cultures of monkey and human (XP or normal) cells has shown infectious double-stranded SV40 DNA carrying UV lesions is more easily rescued from normal human cells than from XP cells. This implies UV-irradiated SV40 DNA undergoes host cell reactivation in human cells. In agreement with this result for SV40, host cell reactivation has been observed in adenovirus after

UV light (59) or psoralen plus near-UV light (63). Recombination rather than repair is an unlikely explanation for these observations since recombination does not occur in UV-irradiated cells infected with a mixture of two SV40 temperature-sensitive mutants from different complementation groups (75).

3. Problems in Excision Repair of Mammalian Cell Pyrimidine Dimers

Excision repair of pyrimidine dimers is the best understood process of DNA damage removal in mammalian cells. Using techniques developed to study excision repair in microorganisms (21), mammalian cell radiobiologists have defined four basic steps in excision repair: endonucleolytic cleavage at or near the pyrimidine dimer site, removal of damaged bases, repair synthesis in the damaged DNA strand and ligation of the newly synthesized DNA.

Perhaps the most critical step in excision repair is endonucleolytic cleavage at or near the pyrimidine dimer. DNA damage produced by ionizing radiation or certain carcinogen treatments requires repair in states sharing several features of excision repair for pyrimidine dimers (base removal, repair synthesis, DNA ligation) (34) but does not require an endonuclease activity. Setlow et al (100) have suggested the endonuclease active after UV-irradiation

(UV-endonuclease) may be non-specific and recognize several or all types of DNA damage which distort the shape of the DNA double helical backbone, but there is as yet no confirmation of this hypothesis. The UV-endonucleases from phage T4 and M. luteus have been extensively purified and have well-defined specificities for pyrimidine dimers (101). However, XP cells which are deficient in excision repair of pyrimidine dimers are also deficient in excision of DNA base adducts produced by treatment with carcinogens which do not produce strand breaks (102). This implies that dimer specificity may not be a necessary property of mammalian cell UV-endonucleases. In vitro approaches to isolation of human UV-endonucleases are being developed (57,103) which will be used for repair enzyme purification. One attractive in vitro analogue to eucaryotic chromatin may be SV40 DNA complexed with histones since a single endonucleolytic cleavage in a Form I SV40 DNA molecule produces a Form II molecule. However, it must first be shown that pyrimidine dimers in SV40 DNA are susceptible to mammalian cell excision repair enzymes.

UV-photoproducts are excised in vitro in oligonucleotides about 8 bases long (104) with up to 100 bases removed in a single in vivo repair patch (21). These numbers contrast with the 0-6 bases removed at the site of DNA strand

breaks after ionizing radiation (105) and the single base residues expected from the exonuclease activity of a DNA polymerase (44). Purified mammalian UV-exonucleases are needed to decide if a single enzyme removes several types of damaged DNA bases and if UV-exonucleases are only active on certain chromatin conformations. As with mammalian UV-endonucleases, SV40 DNA and SV40 DNA complexed with histones may be excellent substrates for a detailed biochemical study of this excision repair step.

Excision repair measured by unscheduled DNA synthesis or repair replication saturates at UV fluences below 40 J/m^2 (21). This indicates there may be a limited supply of one or more of the enzymes or enzyme cofactors in the excision repair system within the cell. The existence of a rate-limiting step in excision repair is also suggested in most cell lines by comparing the constant rate of dimer removal from acid-insoluble DNA during the 24 hours after UV-irradiation (21) to the rapid decrease in repair replication and UV-endonuclease sites during the first few hours after UV-irradiation (21). It should be noted, however, that repair replication is still detectable at low UV fluences up to 24 hours after UV-irradiation (106) despite the sharp decline in the early rate of repair replication. Similarly, some UV-endonuclease sites persist for long times after UV-irradiation (107,108). A biphasic repair response

thus seems to prevail.

Rapid turnover of some repair enzymes has been ruled out as an explanation by Gautschi et al (109). They found that 65% of the initial repair activity in HeLa S3 and CHO cells still remained 20 hours after UV-irradiation even though protein synthesis had been suppressed with cycloheximide. This leaves at least six other hypotheses to explain why the rate of excision repair is biphasic and is detectable long times after UV-irradiation:

(1) DNA replication interferes with excision repair at the site of a UV-photoproduct;

(2) "Patch-and-cut" repair may occur in mammalian cells in which some or all dimers are excised in long, acid-insoluble nucleotides;

(3) Excision repair enzyme cofactors and not the enzymes themselves may be rate limiting;

(4) Different UV-photoproducts are repaired with different rates;

(5) Cell regulation of excision repair may slow the repair process as pyrimidine dimers are removed; and

(6) Different cell types exhibit different patterns of excision repair.

Hypothesis (6) was tested by measuring UV-endo-nuclease sensitive sites, repair replication and dimer excision in African green monkey kidney CV-1 cells

and carefully comparing the results. This approach was motivated by failures to analyze excision repair by all these techniques in a single cell line in the same laboratory. These experiments are described in the Results section of this thesis.

4. Problems in Post-Replication Repair of Pyrimidine Dimers

Early experiments on the response of mammalian cells to UV light revealed DNA replication was intimately involved in repair and recovery of mammalian cells after UV-irradiation (110). Various workers (93,111-113) performed pulse-labelling experiments after UV-irradiation that confirmed earlier observations on the DNA of microorganisms (114) which suggested nascent DNA is smaller in irradiated cells than in unirradiated cells. Pulse-"chase" experiments revealed that the smaller daughter DNA strands eventually return to control DNA size over a period of several hours (111). Using the BrdUrd photolysis technique (115) in mouse L5178Y cells, Lehmann observed gaps of 800-1000 nucleotides adjacent to the smaller daughter DNA strands (112). This study also showed that these nascent strands are joined by de novo synthesis and not by recombination, unlike the bacterial rec repair system, and that gap filling is inhibited by hydroxyurea (as is semiconservative DNA replication). The number and size of daughter strand gaps agrees well with the number of and distance between pyrimidine dimers (112,116). Other co-

workers have also observed these gaps (117,118). Edenberg has recently confirmed by fiber autoradiography that mammalian cell daughter DNA strands are indeed smaller in UV-irradiated cells, similar in size to the calculated intra-strand dimer distance, and remain smaller for up to 90 minutes after UV-irradiation at doses below 20 J/m^2 (119). A reasonable model for these observations is that DNA replication is interrupted at a pyrimidine dimer in the UV-damaged parental DNA and replication reinitiated several hundred nucleotides beyond. The gap opposite the pyrimidine dimer is eventually filled by de novo synthesis in an unknown fashion. The possibility that nascent DNA is replicating more slowly in UV-irradiated cells and that the above model is based on an artifact of the pulse-labelling experiments has been eliminated (120,121).

This model does not agree with pulse labelling experiments done several hours after UV-irradiation in which the nascent DNA is of control size on UV-damaged templates (111, 122,123). The time elapsed between UV light exposure and pulse labelling in these experiments is too short for complete removal of pyrimidine dimers (see Figure 5, ref (21)). These observations have also been made in XP and mouse cells where excision repair does not take place (21). The model also predicts that pyrimidine dimers should be opposite gaps in the daughter DNA and that treatment of UV-damaged DNA

with UV-specific endonucleases should create double strand breaks in the UV-damaged DNA. These double strand breaks should be detectable by neutral sucrose isokinetic sedimentation of the DNA. Efforts using the UV-specific endonucleases from M. luteus and T4 phage have shown no such gaps opposite pyrimidine dimers (116,124). The M. luteus studies (116) confirm that the M. luteus UV-specific endonuclease is active on the UV-damaged DNA and favor the idea that negative results are not due to peculiar substrate properties. Modified models (116,117,119,125) postulate that pyrimidine dimers may be by-passed without removal after a pause of the growing fork at the pyrimidine dimer. This means "post-replication repair" may be a complex process unrelated to true repair. These new models also suggest "post-replication repair" may induce mutations since replication across damaged bases may be "error-prone." This agrees with observed increases in frequencies of mutation to 8-azaguanine resistance in XP variant cells relative to normal fibroblasts (126).

However, these new models still cannot adequately explain Lehmann's observation of large gaps in mammalian cell daughter DNA (112), the mammalian cell pulse-labelling experiments of Buhl et al and others (111,112,123) several hours after UV-irradiation showing control size nascent DNA in UV-irradiated cultures, or the rapid disappearance of single-stranded regions in parental DNA after UV-irradiation

(117). These models also cannot confirm that "post-replication repair" is responsible for S-phase recovery (21). Because of the confusion surrounding the molecular response of mammalian cells to pyrimidine dimers during S-phase, this thesis will use the general term "DNA replication of UV-irradiated DNA" in place of "post-replication repair" to describe the cellular processes occurring during DNA replication on UV-damaged templates.

A major drawback in working with replicating DNA from mammalian cells is its extreme complexity. The presence of multiple initiation sites within the genome of a single cell, the large fraction of repetitious DNA in mammalian cells, and the lack of detailed information on how eucaryotic chromatin is organized and replicates all contribute to the difficulty of understanding what happens to growing daughter strands of mammalian cell DNA which encounter UV-photoproducts in the parental template strands.

SV40 replication studies avoid these problems and offer several advantages: (1) SV40 DNA has a single initiation site and can be induced to replicate synchronously using one of several available SV40 replication mutants (69); (2) Detailed information on SV40 chromatin structures is now available (72); and (3) Single site mutations in SV40 DNA are easily scored as phenotypic changes through plaque assays. In addition, agarose gel techniques allow careful

resolution of SV40 replicative intermediates (77). These advantages suggest that several types of experiments described above may be fruitfully repeated with SV40 DNA to gain a greater understanding of "post-replication repair" and its potentially mutagenic consequences. Some of these experiments and their results are described below.

II. MATERIALS AND METHODS

1. Materials

(A) Biological Materials: African green monkey kidney CV-1 and BS-C-1 cell lines (American Tissue Culture Collection numbers CCL 70 and CCL 26) were a gift of Dr. James Cleaver (Laboratory of Radiobiology, University of California at San Francisco, San Francisco, CA, 94143); some experiments were performed with CV-1 cells donated by Dr. Joanne Leong (Department of Biochemistry, University of California at San Francisco). CV-1 and BS-C-1 cells were routinely grown in plastic Petri plates (Falcon) in Modified Eagle's medium (GIBCO, Grand Island, N.Y., 14072) supplemented with 15% (v/v) fetal calf serum, 2×10^{-3} M glutamine (GIBCO), penicillin (80 u/ml), and streptomycin (80 u/ml) (GIBCO); this medium is abbreviated below as mEm. Simian Virus 40 (SV40) viral stocks were prepared from a wild-type SV40 sample designated SV40-1 (127), a gift of Dr. James Cleaver. E. coli tRNA was bought from Schwarz Mann Biochemicals (Orangeburg, N.Y., 10962).

(B) Chemicals: Radiotracer grade cesium chloride (CsCl) and optical grade cesium sulfate (CsSO_4) were obtained from Harshaw Chemical Company (Solon, Ohio 44139). Propidium iodide (PI_2) and Ethidium Bromide (EtBr) were bought from Calbiochem (LaJolla, CA, 92037). Stock solu-

tions of methyl- ^3H -thymidine (^3H -dThd), methyl- ^{14}C -thymidine (^{14}C -dThd), 2- ^3H -5-bromo-2'-deoxyuridine (^3H -BrdUrd) and 6- ^{14}C -5-bromo-2'-deoxyuridine (^{14}C -BrdUrd) were bought from Schwarz Mann Radiochemicals. Unlabelled thymidine (dThd), deoxycytidine (dCyd), 5-fluoro-2'-deoxyuridine (FdUrd), and 5-bromo-2'-deoxyuridine (BrdUrd) were purchased from Calbiochem. Puck's Saline A was bought from GIBCO. Seakem agarose (ME) was bought as standard pure powder from Marine Colloids, Inc. (Rockland, Maine, 04841). Giemsa stain was prepared from Giemsa R66 stock solution (George T. Gurr, Ltd., London, England) by 1:50 dilution in 2.4% (v/v) methanol, 6.8% (v/v) 0.1 M citric acid, 9.2% (v/v) 0.2 M $\text{Na}_2\text{HPO}_4 \cdot 10^{-4}$ M. Colcemid was a gift of Dr. Sheldon Wolff (Laboratory of Radiobiology, University of California at San Francisco).

(C) Enzymes: T4 endonuclease V, fraction 2 (128) was a gift from Dr. Errol Friedberg (Department of Pathology, Stanford University School of Medicine, Stanford, CA, 94305). EcoRI restriction enzyme (6000 u/ml) was obtained from New England Biolabs (Beverly, Maine, 01915).

2. Methods

(A) Conditions for Exposure to Ultraviolet (UV) Light: The UV light system consisted of a bank of GE 15w germicidal lamps emitting primarily 254 nm

wavelength UV light and located about 60 cm from a rotating plexiglass platform where the samples to be irradiated were placed. A black shutter connected to an automatic timing mechanism controlled the amount of time of exposure to UV light. The UV fluence as measured by a Yellow Springs Instrument #65 radiometer (YSI-Kettering) was $1.25 \text{ J/m}^2/\text{sec}$. Experimental samples were thoroughly washed to remove photoactive chemicals such as serum proteins or phenol red. Irradiations were routinely done with a thin isotonic layer of Ca^{2+} and Mg^{2+} free Dulbecco's phosphate buffered saline (PBS) (129) covering the cultures to prevent cells from drying out or shrinking.

(B) Monkey Kidney CV-1 Cell Growth Characteristics: Monkey kidney CV-1 cells were trypsinized from stock cultures and plated at a density of 3×10^3 cells/cm² in 60-mm diameter plastic Petri plates (Falcon) containing 4.0 ml mEm. The culture medium was aspirated off pairs of plates at regular time intervals and cells were trypsinized 15 minutes. The cell solution was pipetted up and down several times to break up cell clumps, 0.50 ml of the cell solution was diluted in 10.0 ml physiological saline, and the diluted cell solution was counted in a Coulter counter. Cell counts were corrected for coincidence counts by standard tables.

(C) Monkey Kidney CV-1 Cell Chromosome Analysis:

The medium of a near-confluent culture of CV-1 cells (about 2×10^6 cells) in a 60-mm diameter plastic Petri plate (Falcon) was made 10^{-6} M in Colcemid and grown for 7 hours at 37°C . The medium was removed, the cells were scraped off into the plate medium, and the cell solution spun at 700g for 5 minutes. The cell pellet was resuspended in 5.0 ml 0.7xSSC (0.11 M NaCl, 0.011 M Na citrate) and left at room temperature for 25 minutes. The cells were again pelleted and the cells resuspended in 5.0 ml 3:1 acid fixative (methanol:glacial acetic acid). The cells were centrifuged a third time under the same conditions and the cell pellet resuspended this time under the same conditions and the cell pellet resuspended this time in 2.0 ml of fixative. Small drops of fixed cells were dripped several cm onto wet microscope slides and the slides were air dried overnight before staining the slides 5 minutes in 3% Giemsa and destaining one minute in distilled water. The slides were air dried again and karyotypes were done on several cells.

(D) Monkey Kidney CV-1 Cell UV Survival Assay: An initial tube of cells in mEm was prepared at a concentration of 5×10^5 cells/ml. Serial 1:5 or 1:10 dilutions were set up and various numbers of CV-1 cells were plated in 5.0 ml of mEm on 60-mm plastic Petri plates. The

number of cells per plate was estimated to allow 10, 100 or 1,000 cells to survive at a given UV dose. The CV-1 cultures were incubated overnight before all Petri plates were rinsed twice in PBS and the CV-1 cells were UV-irradiated under 2.0 ml of PBS. One plate was fixed to determine cell multiplicity at the time of UV-irradiation. The PBS was removed, 5.0 ml mEm were added and the plates were incubated 10-12 days before the number of colonies of CV-1 cells with 50 or more cells was scored.

(E) Cell Stock Growth and Storage by Freezing: CV-1 cells were grown in glass 4 oz prescription bottles in 10-15 ml mEm under a 5% CO₂ atmosphere. The cells were transferred every 2-4 days by two rinses in Saline A followed by trypsinization in 5.0 ml 0.25% trypsin/EDTA (GIBCO) for 10-20 minutes. An equal volume of mEm was then added and the cells diluted. Cultures were routinely discarded after 20 passages.

Frozen cell stocks were prepared by making the trypsinized cell solution 10% (v/v) DMSO in mEm (130) and putting 1-2 ml aliquots in plastic vials or in glass ampoules which were flame sealed. The ampoules or vials were frozen automatically at about 1° C. per minute or wrapped in cotton and stored overnight in a Revco refrigerator. The ampoules or vials were then transferred to a liquid nitrogen tank.

Frozen stocks were thawed by placing them in a 37° C. water bath until the last ice crystals disappeared. The cell stock was then diluted into 10-15 ml mEm and incubated for several hours before the medium was changed to minimize the cytotoxic effects of DMSO.

(F) Viral Stock Growth: A confluent roller bottle of CV-1 cells (about 10^8 cells/bottle) grown in Eagles mEm supplemented with 5% (v/v) fetal calf serum was washed once in 20 ml Saline A, infected at 0.005 PFU/cell in 10 ml Saline A, and automatically rolled for 1-2 hours at 37° C. The infecting solution was then removed and about 150 ml mEm supplemented with 2% fetal calf serum were added to the roller bottle. The viral stock was grown at 37° C. under a 5% CO₂ atmosphere with a change of mEm every 3-5 days until cytopathic effects (CPE) appeared. 50 ml mEm were then added every 3-5 days until CPE was seen in about 90% of the culture cells. The culture medium was freeze-thawed three times, sonicated 15 seconds with a Sonifier cell disruptor (Heat Systems-Ultrasonic Inc.:setting 3) and centrifuged 5 minutes at 700g, 20° C. The supernatant was frozen in 50 ml volumes and used as a SV40 stock solution without further treatment.

(G) Conditions for SV40 Infection of CV-1 Cells: Confluent Petri plates of CV-1 cells were rinsed once in

Saline A and then infected with 0.20 ml of SV40 stock solution at a multiplicity of infection of 5-10 plaque forming units (PFUs) per cell or 0.20 ml of Saline A (mock-infection). The plates were gently rocked and the cells rewetted with the infecting solution several times during incubation at 37° C. for 1-2 hours. The infecting solution was then removed, 4.0 ml mEm were added and the plates were stored at 37° C. under a 5% CO₂ atmosphere to allow viral growth.

(H) Hirt Extraction Procedure and Assay For Purity of SV40 DNA Obtained in the Hirt Supernatant: Cell cultures on 60-mm diameter plastic Petri plates were lysed by the method of Hirt (131). The cells were washed once with 2.0 ml Saline A before 1.6 ml of lysis solution (0.6% SDS, 10⁻² M EDTA, pH 7.5) was added and the culture left at room temperature for 15 minutes. The lysis solution was made 1.0 M in NaCl by adding one-fifth volume of 5.0 M NaCl and the plates were gently rocked several times before the cloudy, viscous solution was transferred to a Sorvall centrifuge tube. The solutions were stored overnight at 4° C. and centrifuged in a Sorvall centrifuge at 12,000 rpm for 45 minutes in the cold (4° C.). The supernatants were stored at 4° C. for analysis.

To test the effectiveness of this technique, either

mock-infected cultures were labelled with ^{14}C -thymidine or SV40-infected cultures were prelabelled with ^{14}C -dThd before being infected with SV40. The labelled cultures were Hirt extracted and the Hirt supernatant volumes were measured. The Hirt precipitate pellets were made up to an equal volume. The two solutions were then counted in PCS (Amersham Searle), and the acid soluble count contribution to the Hirt supernatant assumed negligible since all cultures were chased in unlabelled mEm 15-24 hours before lysis.

(I) Increase in Viral DNA in Cultures Infected at High Multiplicity: Confluent CV-1 cultures were infected 60-90 minutes with 0.20 wild-type SV40 stock (about 5 PFUs/cell) or mock-infected with 0.20 ml Saline A for 60-90 minutes. The infecting solution was aspirated off and one of two procedures was then followed:

(a) Continuous labelling: Immediately after infection, 5.0 ml mEm containing ^3H -dThd (1.0 $\mu\text{Ci}/\text{ml}$, 11 Ci/mmmole) plus 10^{-5} M dThd and 4×10^{-6} M dCyd were added to each culture. At various times after infection, the radioactive medium was removed from pairs of plates (one mock-infected) and SV40 DNA was isolated by the Hirt extraction procedure. 250 μl aliquots of each Hirt supernatant were immediately analyzed by 5-20% neutral sucrose isokinetic sedimentation in a Beckman SW40 rotor (39,000

rpm for $4\frac{1}{2}$ hours, 20° C.). Approximately 20 20-drop fractions were then collected into test tubes. The fractions were filtered as described in the centrifugation section below, dried and counted in a Packard liquid scintillation spectrometer in toluene containing Omnifluor (New England Nuclear). Total counts in the 14-25 S peak region were computed and plotted as a function of time after infection.

(b) Pulse labelling: 5.0 ml mEm were added to all cultures and incubation begun at 37° C. At various times after infection, the culture medium in pairs of plates (one mock-infected) was replaced with supplemented mEm containing $^3\text{H-dThd}$ ($5.0 \mu\text{Ci/ml}$, 55 Ci/mmole) for one hour before SV40 DNA was isolated by the Hirt extraction procedure. $250 \mu\ell$ aliquots of each Hirt supernatant were processed as described in procedure (a).

(J) Appearance of SV40 Plaque-Forming Units (PFUs) in Infected Culture Media: Several confluent CV-1 Petri plates were infected for one hour at a multiplicity of about 5 PFUs/cell with SV40 stock solution. At various times after infection, the culture medium was removed and frozen. The culture media accumulated from all plates were freeze-thawed three times in baths of dry ice-95% ethanol and boiling water and centrifuged at 1000g for

10 minutes at 20^o C. The supernatant was then treated as a crude infecting stock for titering by plaque assay.

(K) SV40 Plaque Assays: CV-1 cells were plated in 60-mm plastic Petri dishes and incubated in mEm to confluency. Several days after confluency was reached, the plates were rinsed once in Saline A and 0.20 ml of various viral dilutions was added to the plates. The plates were incubated 1-2 hours at 37^o C., rocking the plates frequently. The viral solution was then aspirated off and 4.0 ml of a 1:1 agar/mEm mixture (1.8% (w/v) bacto-agar (Difco):2x mEm) plus 1.0% DMSO were added to each plate (132). 2.0 ml of additional agar/mEm were added every 4-5 days to each plate. On day 11-14 after infection, 3.0 ml of an agar/mEm solution containing 0.01% neutral red were added to each plate, the plates were wrapped in aluminum foil, and the plates were left overnight in the CO₂ incubator. Clear plaques on the plates were scored the next day.

(L) T4 Endonuclease V Assay for Endonuclease-Sensitive Sites in CV-1 DNA: Monkey kidney CV-1 cells were grown at least 24 hours in mEm on 60-mm diameter plastic Petri dishes. ³H-dThd (50 μCi/ml, 11 Ci/mMole) in Saline A was added to bring the final ³H-dThd concentration up to 1.0 μCi/ml and the cells were labelled for 24 hours. The

culture medium was then replaced with unlabelled mEm and the cultures were incubated overnight to insure that radioactivity was only in high molecular weight CV-1 DNA. Cultures were then washed twice in BPS and exposed to UV light under a thin (0.7 mmole) layer of PBS. The PBS was replaced with mEm and the cultures incubated various lengths of time. The medium was then removed and cellular DNA isolated as follows (133): cultures were washed once in PBS before 2.0 ml hypotonic solution (10^{-1} M NaCl, 10^{-2} M Na_2 EDTA, 0.5% (v/v) Triton X-100, pH 8.0) was added to each culture. The hypotonic solution was removed after 2 minutes, the cells were scraped off in 1.0 ml 1x SSC (0.15 M NaCl, 0.015 M Na citrate), and the cells were transferred to test tubes. The cells were lysed by adding 0.20 ml 1% (w/v) sodium dodecyl sulfate (SDS) in 1x SSC and vortexing the solution. The lysate was incubated at least one hour in a 37^o C. water bath after adding 0.10 ml RNase (1.0 mg/ml). Pronase (0.05 ml, 10.0 mg/ml) was then added to each tube and the tubes were incubated overnight. CV-1 DNA was purified by two chloroform:isoamyl alcohol (24:1) extractions and dialyzed one day against 20 volumes of 1x SSC and a second day against 20 volumes of 2×10^{-2} M Tris-HCl, 10^{-2} M Na_2 EDTA, pH 7.78 (T4 buffer) before being analyzed for endonuclease-sensitive sites by the T4 endonuclease technique described below.

(M) CV-1 DNA Repair Replication Studies: Monkey kidney CV-1 cells were grown to confluency in 100-mm plastic Petri plates (about 10^7 cells/plate) in mEm. The medium was aspirated off prior to irradiation with UV light; two plates were exposed at each dose. The culture medium in all plates was replaced with mEm plus 10^{-5} M. BrdUrd and 2×10^{-6} M. FdUrd for one hour before labelling with radioactive precursors. This was done to prevent radioactive label entering the ends of replicons undergoing semi-conservative replication and to increase resolution of repair replication. At various times after UV exposure, this medium was replaced with mEm plus 10^{-5} M BrdUrd, 2×10^{-6} M FdUrd, 2×10^{-3} M hydroxyurea, ^{14}C -dThd (0.1 $\mu\text{Ci/ml}$, 56 mCi/mmol) and ^3H -hypoxanthine (2.0 $\mu\text{Ci/ml}$, 0.57 Ci/mmol). The cells were labelled for 3 hours (these nucleic acid precursors were chosen to examine both purine and pyrimidine base insertion in the same gradient). The cells were then washed once in Saline A, scraped off in 2.0 ml 1x SSC and transferred to test tubes; cells from the two plates paired at each dose were pooled in the same test tube. The cells were lysed by adding 0.40 ml 1% (w/v) SDS in 1x SSC plus 0.20 ml heat-treated RNase (1.0 mg/ml) and vortexing the solution. The solution was incubated at least one hour in a 37°C . water bath before adding 0.10 ml Pronase (10 mg/ml) and continuing incubation overnight. DNA

in these samples was sheared by five passages through a 25-gauge needle with a 3.0 ml disposable plastic syringe. The sheared DNA was isolated by two chloroform:isoamyl alcohol (24:1) extractions and dialyzed for two days against fifty volumes of 1x SSC. The DNA was then analyzed by alkaline CsCl-CsSO₄ isopycnic centrifugation (120). Fractions in the upper peak ($\rho = 1.668$) were pooled and the absorbance at 260 nm (A_{260}) as well as the radioactivity in 50 $\mu\ell$ aliquots was measured. Specific activities (cpm in 50 $\mu\ell \times A_{260}^{-1}$) were computed as measures of the amount of repair replication using purine and pyrimidine precursors.

(N) Interference of ³H-Decays or X-rays with UV Light-Induced Repair Replication: For examination of the effect of exposure to various doses of X-rays or a high level of ³H-dThd (5.0 $\mu\text{Ci/ml}$, 11 Ci/mmol) prior to UV-irradiation, two protocols were used:

(a) Pairs of confluent CV-1 cultures were given 0, 2, or 10 Krads of X-rays (300 Kvp, 2 mm Cu nominal filtration) through the top of the Petri plates and a 1.2 mm layer of mEm. The cultures were incubated another 24 hours before the medium was removed and the uncovered cultures exposed in pairs to 0 to 25 J/m² of UV light. Fresh mEm was added to all cultures and they were incubated for 0, 2 or 4 hours before the medium was removed from the paired

plates and mEm with 10^{-5} M BrdUrd and 2×10^{-6} M FdUrd was added (pre-labelling medium). The cultures were incubated for 0.8-2.0 hours before the pre-labelling medium was replaced with mEm plus 2×10^{-3} M hydroxyurea, 2×10^{-6} M FdUrd and ^{14}C -BrdUrd (0.1 $\mu\text{Ci/ml}$, 56 mCi/mmmole) for two hours. The cells were then rinsed once in 1x SSC, scraped off in 2.0 ml 1x SSC and transferred to test tubes with the cells from paired plates pooled in the same test tube. The cells were lysed with the addition of 0.20 ml 1% (w/v) SDS in 1x SSC and treated as described under CV-1 DNA repair replication (section M).

(0) Pyrimidine Dimer Removal from CV-1 Cells: CV-1 cells were grown at least 24 hours in 35-mm or 60-mm diameter Petri plates in mEm before adding 0.01 volume of ^3H -dThd (500 $\mu\text{Ci/ml}$, 11 Ci/mmmole). The cells were labelled for 24 hours before the culture medium on all plates was replaced with unlabelled medium. Incubation was continued overnight to deplete cellular nucleic acid precursor pools of radioactive label. The plates were washed twice in PBS and exposed in triplicate samples to UV light under a thin (0.5-0.7 mm) layer of PBS. The PBS was removed and some cultures were analyzed immediately for pyrimidine dimer content by thin layer chromatography. The remaining cultures were covered with mEm and incubated for 6 or 24 hours before chromatographic analysis.

(P) Induction of T4 Endonuclease V-Sensitive Sites and Kinetics of Site Removal in SV40 DNA: Confluent CV-1 cultures in 60-mm diameter Petri plates were infected with SV40 stock at a multiplicity of 5-10 PFUs/cell for 1-2 hours or mock-infected with 0.20 ml Saline A for the same period of time. The medium on all cultures was replaced with mEm containing $^3\text{H-dThd}$ (1.0 $\mu\text{Ci/ml}$, 11 Ci/mmmole) 24 hours after infection and incubation continued for 24-28 hours. The radioactive medium was then replaced with unlabelled medium for at least 16 hours. Cultures to be exposed to UV light were washed twice in PBS and irradiated under a thin layer (0.7 mm) of PBS for 0-30 seconds (0-37.5 J/m^2 of UV light). The PBS was removed and SV40 DNA isolated immediately from some plates by the Hirt extraction procedure. The remaining plates were incubated with mEm for 0-24 hours before SV40 DNA was isolated. The DNA samples were analyzed for T4 endonuclease V-sensitive sites as described below.

(Q) BrdUrd Photolysis Assay: SV40 DNA was labelled by adding 0.20 volumes $^3\text{H-dThd}$ (50 $\mu\text{Ci/ml}$, 11 Ci/mmmole) in Saline A to the medium over SV40-infected cultures one day after infection. Viral growth in the presence of $^3\text{H-dThd}$ was continued for 24-33 hours before the radioactive medium was replaced with unlabelled mEm for at least 16 hours.

Infected cultures were then washed twice in PBS, and exposed to UV light ($0-90 \text{ J/m}^2$) under a layer of PBS. The PBS was removed and the cultures covered with mEm containing either 10^{-4} M dThd or 10^{-4} M BrdUrd . The cultures were incubated for 7 or 29 hours in the dark before SV40 DNA was isolated by the Hirt extraction procedure and the Hirt supernatants dialyzed overnight under black plastic against 2 ℓ of T4 buffer. Thin layers (1.7 mm) of each dialyzed sample were then exposed to 313 nm light in the apparatus described by Povirk and Painter (134). The highest dose used was $15.24 \times 10^4 \text{ J/m}^2$ and was monitored by a YSI #65 radiometer. 50 $\mu\ell$ or 150 $\mu\ell$ aliquots of exposed samples were analyzed on 5-20% alkaline sucrose isokinetic gradients or by agarose tube gel electrophoresis in 1.5% (w/v) agarose.

(R) Repair Replication in SV40 DNA from Infected Cultures After Exposure to UV Light: SV40-infected or mock-infected CV-1 cultures were labelled for 48 hours after infection with $^{14}\text{C-dThd}$ (0.01-0.20 $\mu\text{Ci/ml}$, 57 mCi/mmol) in mEm. Thirty minutes prior to UV-irradiation, the medium on all cultures was replaced with mEm containing $3 \times 10^{-3} \text{ M}$ hydroxyurea and incubation was continued at 37° C . The cultures were then washed twice in PBS and UV-irradiated to a total fluence of $0-43 \text{ J/m}^2$ under a thin (0.7 mm) layer of PBS. The PBS was removed and 4.0 ml of mEm plus $2.5 \times 10^{-6} \text{ M}$

FdUrd, 3×10^{-3} M hydroxyurea and $^3\text{H-dThd}$ ($10 \mu\text{Ci/ml}$, 11 Ci/mmole) was added to each culture. The cultures were incubated for two hours at 37°C . before SV40 DNA was isolated by the Hirt extraction procedure, purified by 5-20% neutral sucrose sedimentation and analyzed on 5-20% alkaline sucrose gradients. The ratio of ^3H counts to ^{14}C counts in the SV40 Form I DNA peak was corrected as described in Appendix A and plotted as a function of UV fluence.

Two experiments used more conventional repair replication techniques (21). One experiment modified the above protocol by adding 10^{-5} M BrdUrd and 10^{-6} M FdUrd for one hour before UV-irradiation and pre-incubating 30 minutes before UV-irradiation with 3×10^{-3} M hydroxyurea. The medium used after UV-irradiation contained mEm with 10^{-5} M BrdUrd, 10^{-6} M FdUrd, 3×10^{-3} M hydroxyurea and $^3\text{H-BrdUrd}$ ($20 \mu\text{Ci/ml}$, 23 Ci/mmole). Isolated SV40 DNA was analyzed by CsCl isopycnic centrifugation and the corrected $^3\text{H}/^{14}\text{C}$ radioactivity ratio (Appendix A) in the upper (light-light) DNA band was scored.

A second experimental protocol required incubating SV40-infected or mock-infected CV-1 cultures for one hour with mEm plus 10^{-5} M BrdUrd and 2×10^{-6} M FdUrd about 72 hours after SV40 infection began. All cultures had been pre-labelled with $^{14}\text{C-dThd}$ ($0.1 \mu\text{Ci/ml}$, 57 mCi/mmole) 18-48 hours after infection. Cultures were washed twice in PBS

and UV-irradiated in pairs and SV40-infected cultures in triplicate. The PBS was replaced with mEm containing 9×10^{-6} M BrdUrd, 2×10^{-6} M FdUrd, 2×10^{-3} M hydroxyurea and ^3H -BrdUrd (25 $\mu\text{Ci/ml}$, 2.3 Ci/mmole) and incubation was continued at 37°C . SV40 DNA was isolated after four hours of post-UV incubation by the Hirt extraction procedure, sheared to linear DNA molecules and analyzed by alkaline CsCl-CsSO_4 isopycnic centrifugation. Appropriately paired or triplicate Hirt supernatants were pooled for isopycnic centrifugation to insure adequate counting statistics. The $^3\text{H}/^{14}\text{C}$ radioactivity ratio for light-light DNA was corrected (Appendix A) and plotted as an estimate function of UV fluence to the infected cells.

(S) DNA Synthesis in CV-1 Cells after Exposure to UV Light: DNA synthesis in CV-1 cultures was examined immediately after exposure to UV light by calculating the specific radioactivity of hybrid (light-heavy) density DNA ($\rho = 1.754$) in the alkaline CsCl-CsSO_4 isopycnic gradients used to examine CV-1 DNA repair replication after UV-irradiation (Section M). The ^3H or ^{14}C counts at the density of hybrid DNA were divided by the sum of the A_{260} of light-light DNA and the A_{260} of light-heavy DNA to obtain the specific activity of pyrimidine (^{14}C) or purine (^3H) uptake during semi-conservative DNA synthesis in the pres-

ence of 2×10^{-3} M hydroxyurea. The percent hybrid DNA specific activity compared to the hybrid DNA specific activity of control cultures was plotted as a function of UV dose.

DNA synthesis in CV-1 cultures 0, 24 or 72 hours after UV-irradiation was also determined. CV-1 cells were grown to confluency in 60-mm diameter Petri plates or microtiter test plate wells (Linbro). No significant difference was found between the results from Petri plates and the results from Linbro plates. All cultures were washed twice in PBS and exposed to a UV fluence in the range of 0-37.5 J/m². The PBS was removed and mEm was added. The cultures were incubated for 9, 24 or 72 hours at 37^o C. before the medium was removed and mEm plus ³H-dThd (10 μCi/ml, 11 Ci/mmole) was added. The cultures were labelled for one hour before the medium was replaced with ice-cold 4% PCA. The PCA was changed twice at ten minute intervals and the cultures were then stored overnight in the cold. The 4% PCA was removed the next morning and the cultures were washed once in 70% ethanol. The fixed CV-1 cells were dissolved in 0.5 ml 1 N. NaOH at room temperature for one hour. The alkaline cell lysates were transferred to test tubes and 0.5 ml salmon sperm DNA (200 μg/ml) in 0.1 N NaOH plus 0.5 ml of 6% Na pyrophosphate in 1.5 N HCl was added. The resulting acid solution was chilled, filtered onto Whatman

GF/C filters and washed successively with 4% PCA, 70% ethanol, 95% ethanol and 100% ethanol. The filters were air dried and counted in toluene containing Omnifluor (New England Nuclear).

Confirmation of radioactivity peak identification was sought by varying the length of the ^3H -dThd pulse and comparing the radioactivity profiles for cultures incubated 0, 60 or 180 minutes in unlabelled medium after the ^3H -TdR pulse. The efficiency of the "chase" in unlabelled medium was followed by adding the corrected $^3\text{H}/^{14}\text{C}$ ratios for all three SV40 peaks and comparing the sums as a function of time in unlabelled medium for all plates handled during a single experiment. The position of Form III (linear) SV40 DNA molecules of whole genome size was determined by running marker agarose tube gels containing Form I molecules cleaved by the EcoRI restriction enzyme; the EcoRI enzyme makes one double-stranded cut per SV40 genome 0.65 genome units clockwise from the origin of replication (135).

(T) SV40 DNA Replication in UV-Irradiated Cultures: ^{14}C -dThd (0.1 $\mu\text{Ci}/\text{ml}$, 55 Ci/mmole) in mEm was added to several SV40-infected CV-1 cultures in 60-mm diameter Petri plates and the cells were labelled overnight. Mock-infected cultures were treated in the same fashion. The radioactive medium was replaced with unlabelled medium for at least 16 hours to insure all radioactivity was only in

high molecular weight DNA. All plates were washed twice in PBS and triplicate cultures were irradiated with UV light under a thin (0.7 mm) layer of PBS. The PBS was removed, 2.5 ml pre-gassed mEm with ^3H -dThd (10.0 $\mu\text{Ci/ml}$, 11 Ci/mmole) was added, and the cultures were returned to the incubator. After 5-20 minutes of labelling some plates were washed once with Saline A and SV40 DNA was isolated by the Hirt extraction procedure. The medium on remaining plates was replaced with mEm containing 5×10^{-5} M dThd and 5×10^{-5} M dCyd and incubation continued for 1 or 3 hours before SV40 DNA was isolated from cultures by the Hirt extraction procedure. The Hirt supernatants were dialyzed overnight against 40 volumes of T4 buffer (2×10^{-2} M Tris-HCl, 10^{-2} Na₂ EDTA, pH 7.78) and analyzed in 1.0% agarose tube gels by gel electrophoresis. The $^3\text{H}/^{14}\text{C}$ ratio for each SV40 DNA conformation was calculated as a measure of its relative frequency.

3. Analytical Techniques

(A) T4 Endonuclease V Assay (124,128): 5-200 μl DNA samples dialyzed overnight against T4 buffer and containing about 4×10^5 cpm/ml were mixed with 75 μl T4 buffer and either 25 μl of a crude PEG isolate of T4 endonuclease V (128) or 25 μl of T4 buffer. Some experiments were done with 5 μl of DNA sample, 95 μl T4 buffer and either 5 μl of the T4 endonuclease V PEG isolate or 5 μl of T4 buffer.

The enzyme assay samples were incubated one hour at 37° C. before the reaction was stopped by either layering the samples on 12.4 ml 5-20% alkaline sucrose gradients with 100 µl alkaline lysis layers or layering the samples on 1.5% agarose tube gels and beginning electrophoresis immediately. In the case of alkaline sucrose gradients, lysis was allowed for one hour before loading the gradient tubes in a Beckman SW40 rotor and centrifuging in a Beckman L5-75 ultracentrifuge at 39,000 rpm for 3-5 hours. The centrifugation time was chosen to obtain radioactivity profiles which peaked near the center of the gradient. The number average DNA molecular weight M_n and the weight average DNA molecular weight M_w were calculated from the radioactivity profiles as described in Appendix B and the number of T4 endonuclease V-induced breaks per 10^8 daltons of DNA calculated as described in Appendix C.

(B) EcoRI Restriction Enzyme Assay (136): Samples of SV40 DNA were dialyzed overnight against 500 volumes of EcoRI buffer (10^{-1} M Tris-HCl, 5×10^{-2} NaCl, 5×10^{-3} M $MgCl_2$, pH 7.50). An incubation mixture was made up with 100 µl dialyzed SV40 DNA plus 2.0 µl E. coli tRNA (1 mg/ml) and 1.0 µl EcoRI enzyme (\geq 6000 units/ml). The incubation mixture was incubated at 37° C. for one hour to allow complete cleavage of Form I SV40 DNA molecules. The reaction

was stopped by adding 25 $\mu\ell$ stopping solution (10^{-1} M Tris-HCl, 10^{-1} M Na_2 EDTA, pH 7.40) followed by 50 $\mu\ell$ tracking dye (0.001% Bromphenol blue, 0.6% SDS, 30% (w/v) sucrose). Incubation mixtures were immediately analyzed by agarose tube gel electrophoresis.

(C) Agarose Tube Gel Electrophoresis (77): Tris gel buffer (3.6×10^{-2} M Tris-HCl, 3.0×10^{-2} M NaH_2PO_4 , 10^{-3} M Na_2 EDTA, pH 7.60) was prepared by diluting a 10x stock solution of buffer. Buffer to be used in the electrophoresis reservoirs was made 0.2% in sodium dodecyl sulfate (SDS). Agarose tube gels were prepared in 15 cm. pyrex tubes (5 mm inner diameter) by heating 1.0-1.5% (w/v) agarose in gel buffer and refluxing for 10-15 minutes. The agarose was cooled briefly and then poured into the gel tubes. The gel tubes were sealed on one end with parafilm and the gels were formed by forcing the agarose solution into the gel tubes with a 10 ml pipette. The gels were hardened in the cold for one hour, and one cm. cut from the top end with a scalpel blade.

The gels were then capped on the lower end by cheese-cloth held in place by a rubber band, and placed in the electrophoresis apparatus. The gels were prerun at constant voltage (8-10 V/tube) for 30 minutes at room temperature. A 100 $\mu\ell$ DNA sample was mixed with an equal

volume of dye (0.001% bromphenol blue, 0.6% SDS, 30% (w/v) sucrose) and left for 5-15 minutes at 37° C. before samples were added to the gels and electrophoresis begun. The bromphenol blue marker moved at a rate of about 8 cm/hour independent of gel concentration in the range 1.0-1.5%.

Gels were carefully removed onto filter paper after electrophoresis, cut in 3 mm slices, and placed in 10 ml PCS (Amersham Searle) scintillation fluid. The samples were left at room temperature for 2 days before counting in a Packard scintillation spectrometer (77).

(D) Neutral Sucrose Isokinetic Sedimentation:

100-200 μl DNA samples were layered over 100 μl of neutral lysis solution (1.0 M NaCl, 1% sarkosyl, 0.1% Na deoxycholate, 5×10^{-2} M Na_2 EDTA, 6% p-amino salicylate, 10^{-2} M Tris-HCl, pH 9.6) (137) above a 5-20% neutral sucrose (1 M NaCl, 10^{-2} M Tris-HCl, pH 8.0) SW40 gradient with a 0.60 ml CsCl ($\rho = 1.62$) cushion. The gradients were left standing one hour before centrifuging at 39,000 rpm for 4½ hours at 20° C. The gradients were then punctured from the bottom and approximately 25 equal drop fractions were collected into test tubes. 50-100 μl aliquots of each fraction were then counted on a Packard Tri-Carb scintillation spectrometer. The gradients were calibrated

for molecular weights using SV40 Form I (53 S) and Form II (18 S) DNA in conjunction with Studier's relation between sedimentation constant and molecular weight (see Appendix B).

(E) Alkaline Sucrose Isokinetic Sedimentation: 5-20% alkaline sucrose gradients were prepared in Beckman SW40 polyallomer tubes using a Beckman gradient former. The alkaline sucrose reservoir buffers for the gradient former contained 0.3 N NaOH, 0.8 M NaCl, 10^{-3} M Na_2 EDTA, and either 32% (w/v) or 0% (w/v) sucrose. All gradients had 0.60 ml cushions ($\rho = 1.62$) of CsCl in 0% alkaline sucrose buffer. 100-300 μl alkaline lysis layers (5×10^{-1} M NaOH, 2×10^{-2} M Na_2 EDTA, 0.1% (w/v) Triton X-100) were slowly added to the top of the alkaline sucrose gradients before the samples to be analyzed were layered over the lysis layer. The tubes were spun in a Beckman SW40 rotor at 39,000 rpm, 20 $^{\circ}$ C. for 4 hours. The tubes were then punctured from the bottom and equal drop fractions were collected directly into scintillation counting vials and counted in PCS (Amersham Searle) on a Packard liquid scintillation spectrometer.

(F) Neutral CsCl Isopycnic Centrifugation (138): 4.50 gm DNA samples in T4 buffer were mixed with 5.60 gm CsCl in a Beckman 50Ti polyallomer centrifuge tube and

mineral oil was layered on top to remove air bubbles from the tube. The centrifuge tubes were loaded in a Beckman 50Ti rotor and spun at 40,000 rpm for 40 hours, 20° C. The centrifuge tubes were punctured through the bottom and 7-drop fractions were collected into test tubes. 100 µl aliquots from each fraction were dried on Whatman GF/C glass filters, washed twice in 5% TCA and rinsed successively in 70%, 95% and 100% ethanol. The filters were redried and counted in toluene containing Omnifluor (New England Nuclear). The CsCl gradient fractions containing normal density DNA were pooled, dialyzed overnight against 1 l T4 buffer and sedimented in SW40 5-20% alkaline sucrose gradients for analysis.

(G) CsCl-Ethidium Bromide Isopycnic Centrifugation: All operations were carried out under yellow safety light. DNA samples in T4 buffer weighing 5.25 gm were mixed with 5.32 g CsCl and 0.25 ml Ethidium Bromide (EtBr) (10 mg/ml) in a 50Ti polyallomer tube. The mixture was centrifuged at 43-48,000 rpm for at least 46 hours at 20° C. in a Beckman 50Ti rotor. The lower DNA band, visualized by a bank of UV black lights, was collected by pipette and extracted three times with isopropanol:H₂O (9:1) to remove EtBr. These samples were dialyzed overnight against T4 buffer in the dark before exposure to a 313 nm UV light

source and analysis by agarose gel electrophoresis or alkaline sucrose isokinetic sedimentation.

(H) CsCl-Propidium Iodide Equilibrium Density Gradient Ultracentrifugation (139): DNA samples in T4 buffer weighing 6.10 gm were mixed with 5.75 g CsCl and 0.40 ml propidium iodide (PI₂) (6 mg/ml) in a Beckman 50Ti polyallomer centrifuge tube and centrifuged at 48,000 rpm for 41 hours, 20^oC in a Beckman 50Ti rotor. The DNA bands were visualized in the dark by exposure to a bank of black lights and the upper DNA bands (non-supercoiled DNA) were collected by pipette. These samples were extracted four times with isopropanol:H₂O (9:1) to remove PI₂ and dialyzed overnight against 1ℓ T4 buffer before treatment with T4 endonuclease V and assay by agarose tube gel electrophoresis.

(I) Alkaline CsCl-CsSO₄ Equilibrium Density Gradient Ultracentrifugation (37): DNA samples in 1x SSC weighing 4.50 gm were mixed with 1.00 gm CsSO₄, 4.60 gm CsCl, and 0.50 ml 1 N NaOH in 1x SSC in 50Ti polyallomer tubes and spun at 48,000 rpm for 66 hours, 20^o C. in a Beckman 50Ti fixed-angle rotor. The gradients were punctured through the bottom and approximately 20 10-drop fractions were collected. 50 μℓ aliquots of each fraction were dried on Whatman 3 mm paper filters, washed twice in 5% TCA and rinsed successively in 70%, 95% and 100% ehtanol. The filters were redried and

counted in toluene containing Omnifluor (New England Nuclear). Fractions of normal density DNA were then pooled as well as fractions of hybrid density DNA and optical densities (A_{260}) recorded for each DNA sample. 50 $\mu\ell$ aliquots of each pooled sample were counted on paper filters or 100 $\mu\ell$ aliquots on glass filters before washing the filters in 5% TCA and rinsing them in alcohol baths as described above. These filters were counted and ^3H or ^{14}C specific activities (counts per minute $\times A_{260}^{-1}$) calculated. The density gradient was determined by measuring the mass of 50 $\mu\ell$ aliquots for several fractions. The density of light-light DNA was $\rho = 1.668$ and of hybrid DNA was $\rho = 1.754$.

(J) Thin-Layer Chromatography (140): UV-irradiated CV-1 cells were scraped into 0.80 ml ice-cold PBS and transferred to combustion tubes. An equal volume of ice-cold 10% trichloroacetic acid (TCA) was added and the sample mixed. The samples were centrifuged 15 minutes at 400 g, 4°C . and the supernatant discarded. The cell pellet was dissolved in 0.20 ml cold 97% Formic acid and the combustion tubes were sealed. The sealed tubes were heated at 180°C . for one hour and cooled to room temperature. The hydrolysates were evaporated to dryness before redissolving them in 5.0 $\mu\ell$ of distilled water and spotting them 2.0 cm. from the bottom of 20.0 x 20.0 cm thin-layer plates.

Eight samples were spotted on a single plate and dried under a hair dryer. The plates were developed by ascending chromatography in a sealed glass chromatography tank (10 x 30 x 25 cm) containing 100 ml of freshly prepared ethyl acetate:n-propanol (4:1) saturated with water. Development was stopped when the solvent front moved 10.0 cm from the origin. Plates were air-dried and taped with Scotch Brand Magic Transparent Tape no. 810 along the direction of solvent movement. Samples 2.0 cm wide were separated and twenty-one 0.5 cm strips were cut beginning 0.5 cm behind the origin. Each strip was soaked in 1.0 ml distilled water for at least 30 minutes after removing the plastic backing. Ten volumes of PCS counting solution (Amersham Searle) was added to each sample and the samples counted in a Packard scintillation spectrometer. Fractions 1-2 (the origin), 11-14, 15-17, and 18-20 were pooled in single counting vials to reduce counting time. Control experiments showed counting efficiency was not reduced under these conditions. The corrected percentage of pyrimidine dimers was calculated by a modification of the method of Cook and Friedberg (140) (see Appendix D).

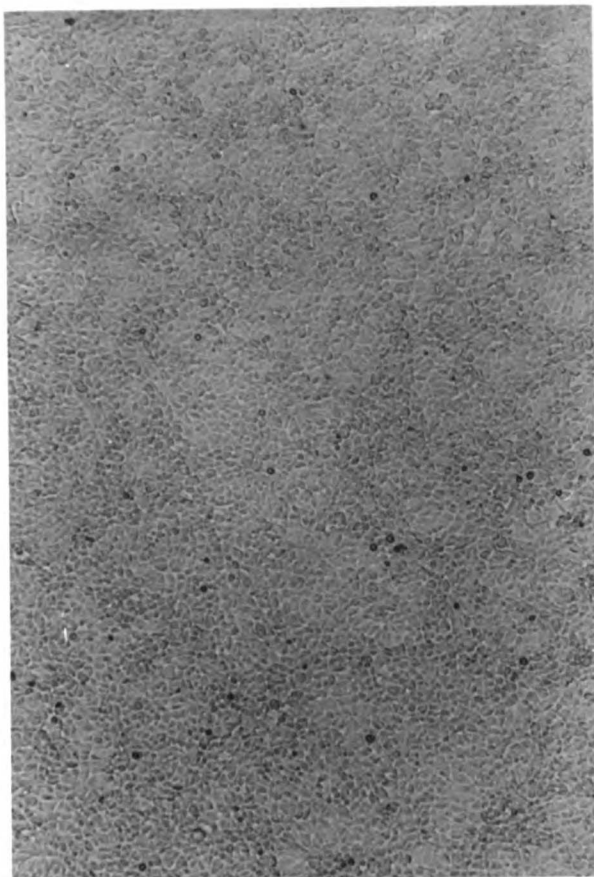
III. RESULTS

1. Monkey Kidney CV-1 Cells: Characteristics in Culture

Monkey kidney CV-1 cells are epithelial in shape and grow to high cell densities. Figure (1) shows a typical confluent CV-1 cell culture. The time course of CV-1 cell growth is shown in Figure (2a) for cells multiplying in 60-mm diameter plastic Petri dishes under a 5% CO₂ atmosphere. There is about a 15 hour division delay after replating CV-1 cells followed by an exponential cell increase with a doubling time of 19.4 hours, similar to the doubling time of 23.2 hours for monkey BS-C-1 cells, Figure (2b). The doubling time increases as cells reach a near-confluent density of about 7.1×10^4 cells/cm². Cell number reaches a maximum density of 1.6×10^5 /cm² and is maintained as long as the culture medium is replaced every three to four days.

Inhibition of mitosis in CV-1 cells with 10^{-6} M Colcemid allowed karyotype analysis. The variability in chromosome number seen in Figure (3) shows CV-1 culture cells have heterogeneous cell lineages and have adapted to prolonged culture with extreme aneuploidy. The American Tissue Culture Collection data (141) on the CV-1 cell line lists a chromosome range of 56-120, a similar range to that observed here.

Figure (1). Photomicrograph of a confluent African green monkey kidney cell culture. All photomicrographs were taken with a Reichert (Austria) Photo-Automatic camera mounted on a Reichert Biovert Microscope. Magnification is 170X.



Figures (2a-b):

(a) Growth curve of CV-1 cells. The data is a cumulative plot of four separate experiments and was fitted by eye to a smooth curve. The cell doubling time during the exponential portion of the growth curve was 19.4 hours.

(b) Growth curve of monkey BSC-1 cells. Data from two separate experiments was superimposed and fitted by eye to a smooth curve connecting data points. The doubling time during the exponential portion of the growth curve was 23.2 hours.

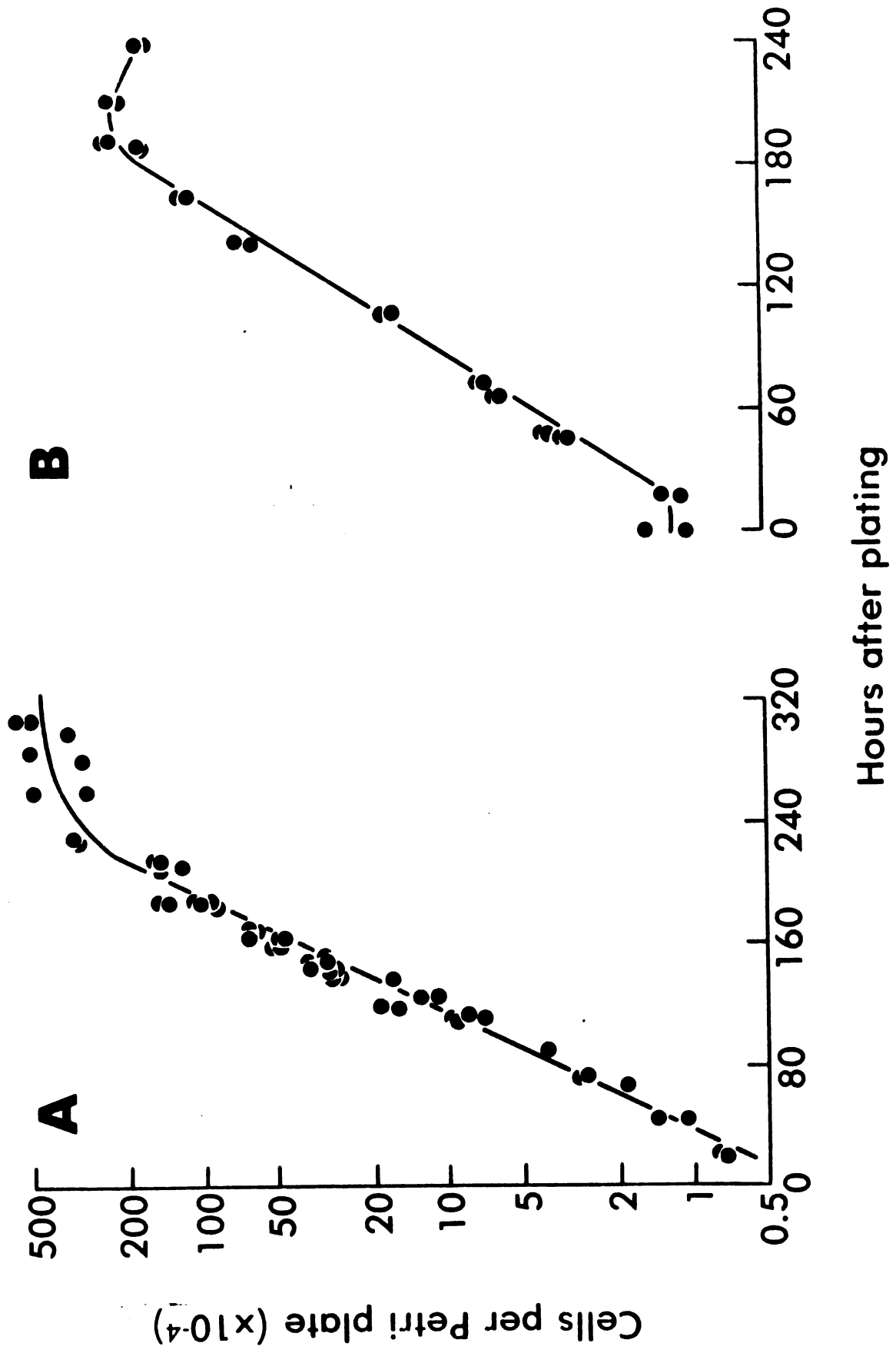
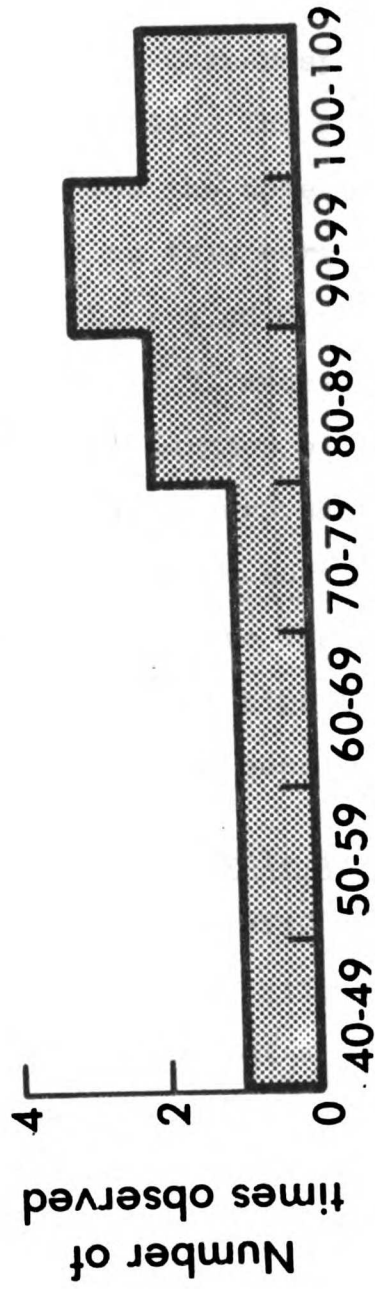


Figure (3). Histogram of metaphase chromosome number in CV-1 cells.



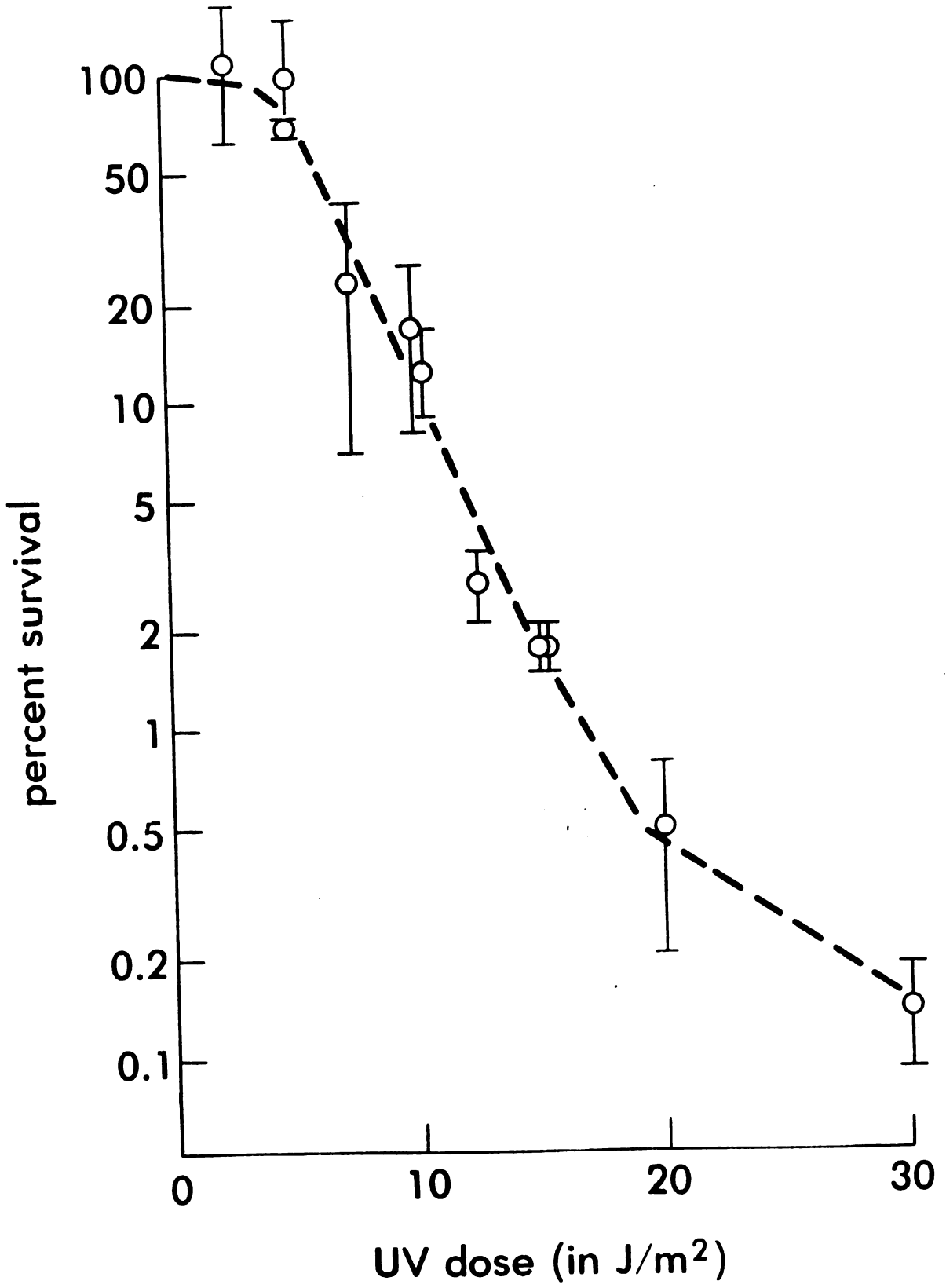
Number of metaphase chromosomes per cell

Irradiation of CV-1 cells in culture with UV light (predominantly 254 nm) from GE germicidal lamps reduced their capacity to form colonies of 50 cells or more after exposure to UV light (14). A dose-response curve for cell survival is shown in Figure (4). The slope of the exponential part of this curve gives the dose (D_0) required to reduce survival at any point on this curve to $e^{-1} = 0.37$ of that value. The measured $D_0 = 2.46$ Joules/meter² (J/m^2). The extrapolation number $n = 7.8$, where n is the ordinate intercept of the exponential portion of the dose-response curve when extrapolated back to zero dose. These two parameters define the dose-response or survival curve with the additional provision that the curve flattens at doses above $20 J/m^2$. The curve flattening at high UV doses is probably a technical artifact and has been seen before (152,153).

2. SV40 Productive Infectious Cycle in CV-1 Cells

The permissive or productive SV40 infectious cycle in monkey kidney CV-1 cells leads to lytic death of the host monkey cells. A pictorial record of a typical infection is shown in Figures (5-8). These pictures show that cell lysis or pathological cellular changes (cytopathic effects) is essentially complete within one week following infection at a high multiplicity of infection (m.o.i.) but gross cellular changes such as numerous intracellular vacuoles begin

Figure (4). CV-1 cell survival curve after treatment with UV light. All data points were corrected for cell multiplicity (14). The incident UV dose rate was 1.25 J/m^2 per second. Error bars indicate standard errors of the mean (S.E.M.) among five plates used to determine each data point.

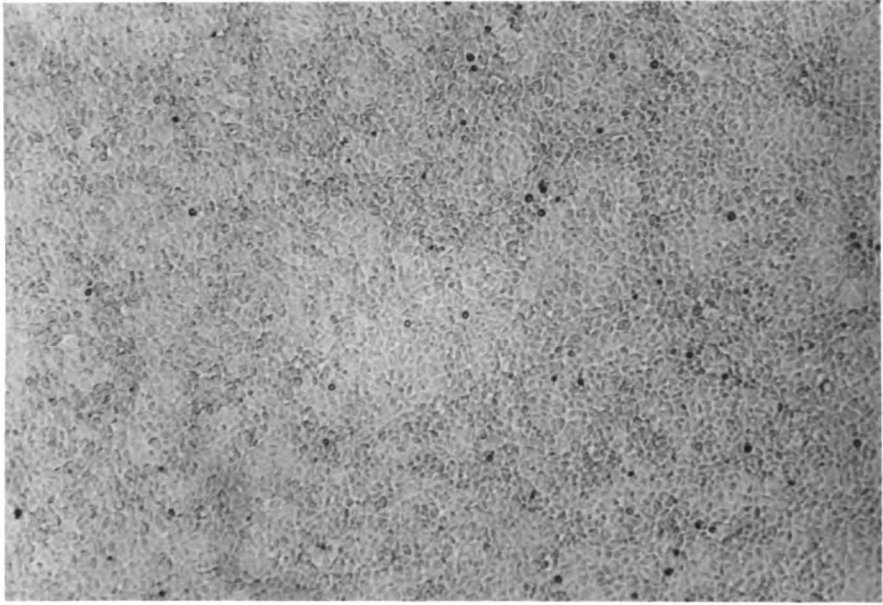


Figures (5a-b):

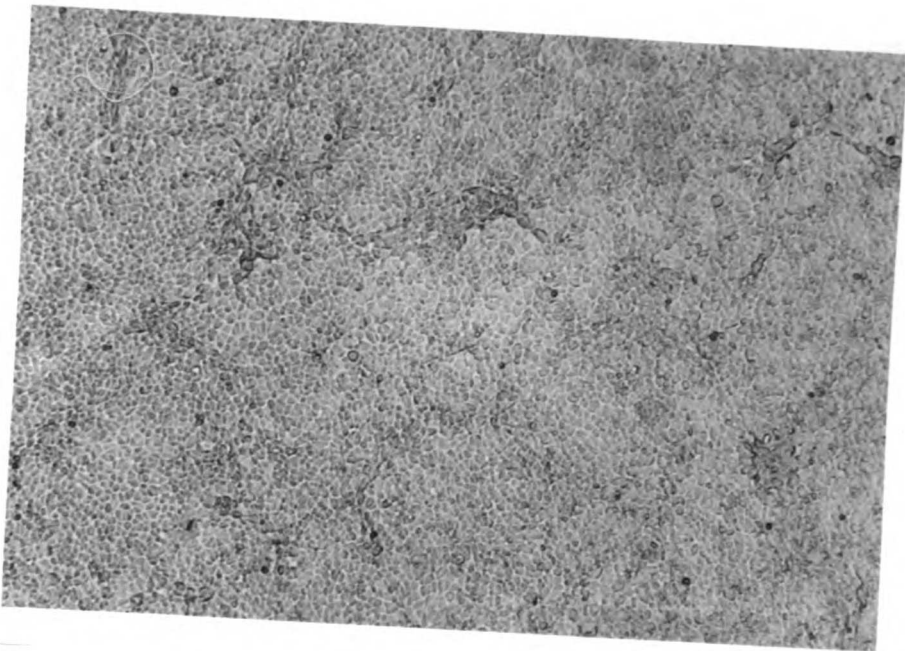
(a) Photomicrograph of a mock-infected CV-1 culture 24 hours after mock-infection.

(b) Photomicrograph of an SV40-infected CV-1 culture 24 hours after infection at a multiplicity of 5-10 PFUs per cell.

(A)



(B)

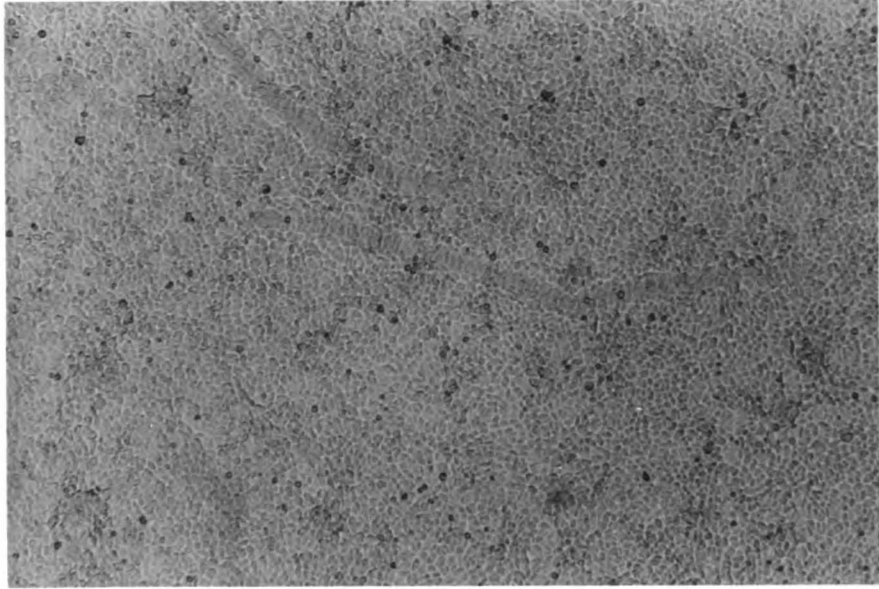


Figures (6a-b):

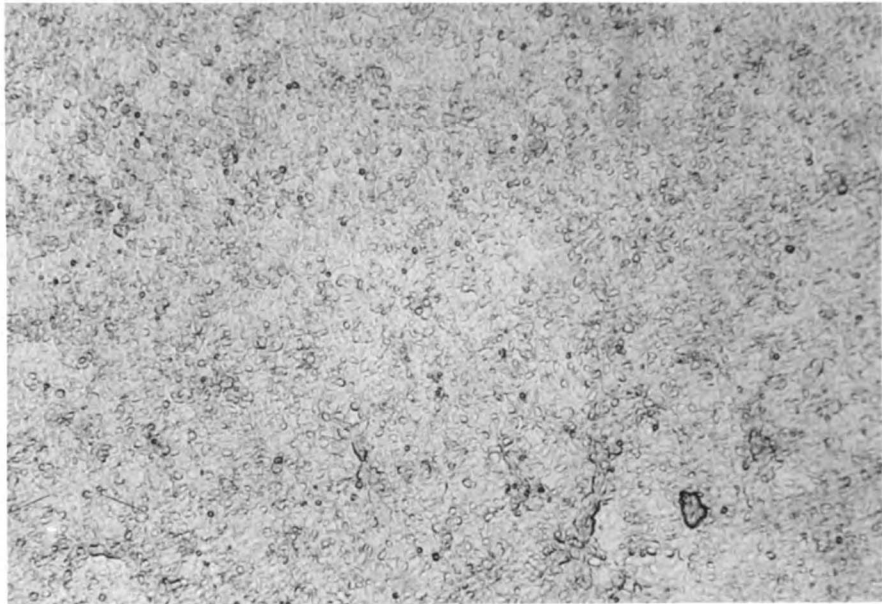
(a) Photomicrograph of a mock-infected CV-1 culture 48 hours after mock-infection.

(b) Photomicrograph of an SV40-infected CV-1 culture 48 hours after infection at a multiplicity of 5-10 PFUs per cell. Note there is no gross evidence of cytopathology at this stage of infection despite evidence of a high rate of SV40 DNA replication (cf Figure (9b); also (67)).

(A)



(B)

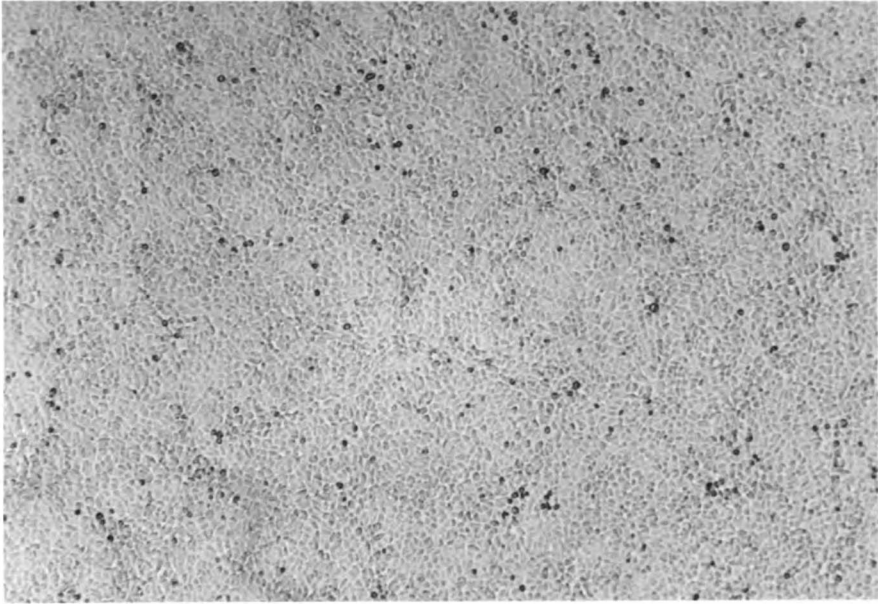


Figures (7a-b):

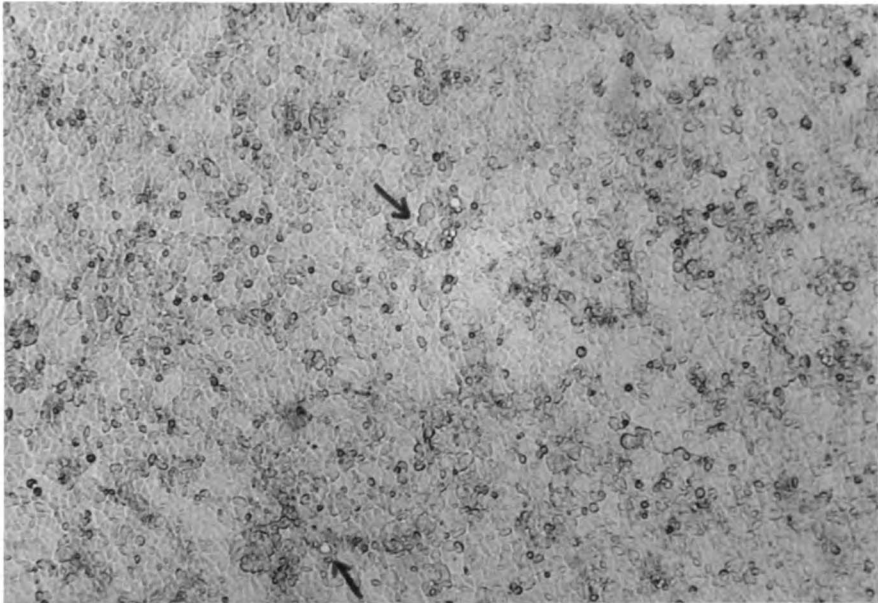
(a) Photomicrograph of a mock-infected CV-1 culture 72 hours after mock-infection.

(b) Photomicrograph of an SV40-infected CV-1 culture 72 hours after infection at a multiplicity of 5-10 PFUs per cell. Cytopathic effects are beginning to become visible as a "mottled" appearance to the culture in areas where cells begin to round up. Characteristic cytoplasmic vacuoles can be seen in cells indicated by arrows; these early vacuolations are the reason SV40 was first identified as "vacuolating virus" (66).

(A)



(B)

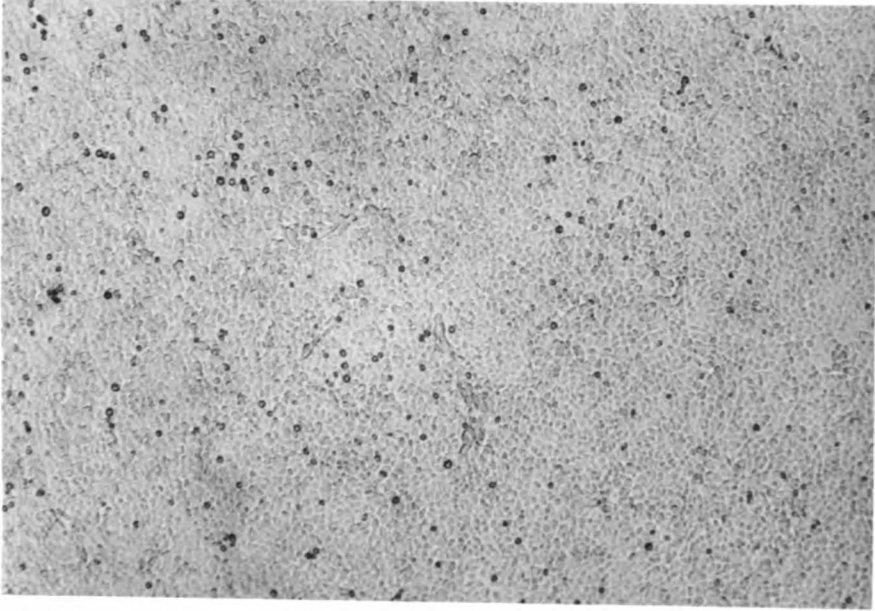


Figures (8a-b)

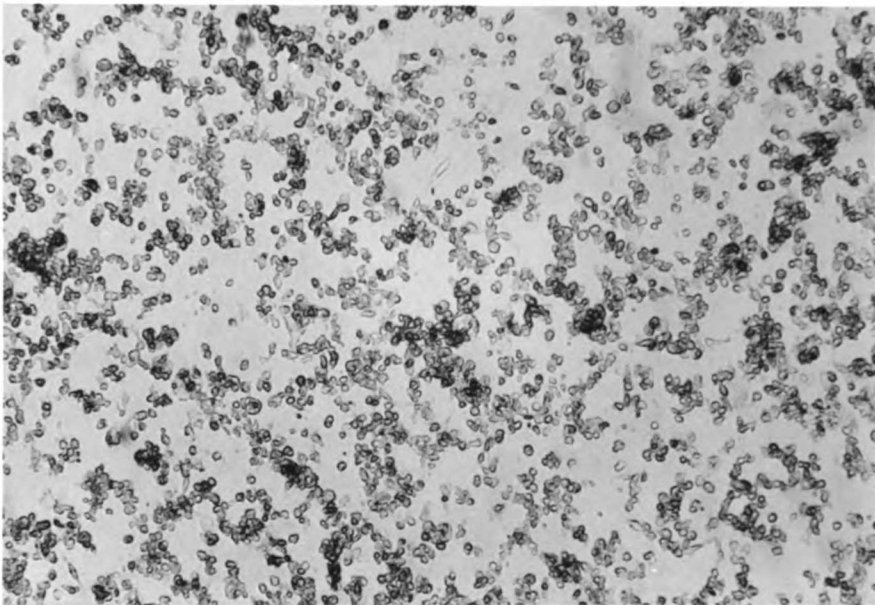
(a) Photomicrograph of a mock-infected CV-1 culture 8 days after mock-infection. No cell death is evident even though these cells have been refed only once in ten days.

(b) Photomicrograph of an SV40-infected CV-1 culture eight days after infection at a multiplicity of 5-10 PFUs per cell. Most cells have lysed or released attachment to the Petri plate and the SV40 infectious cycle has nearly run its course.

(A)



(B)



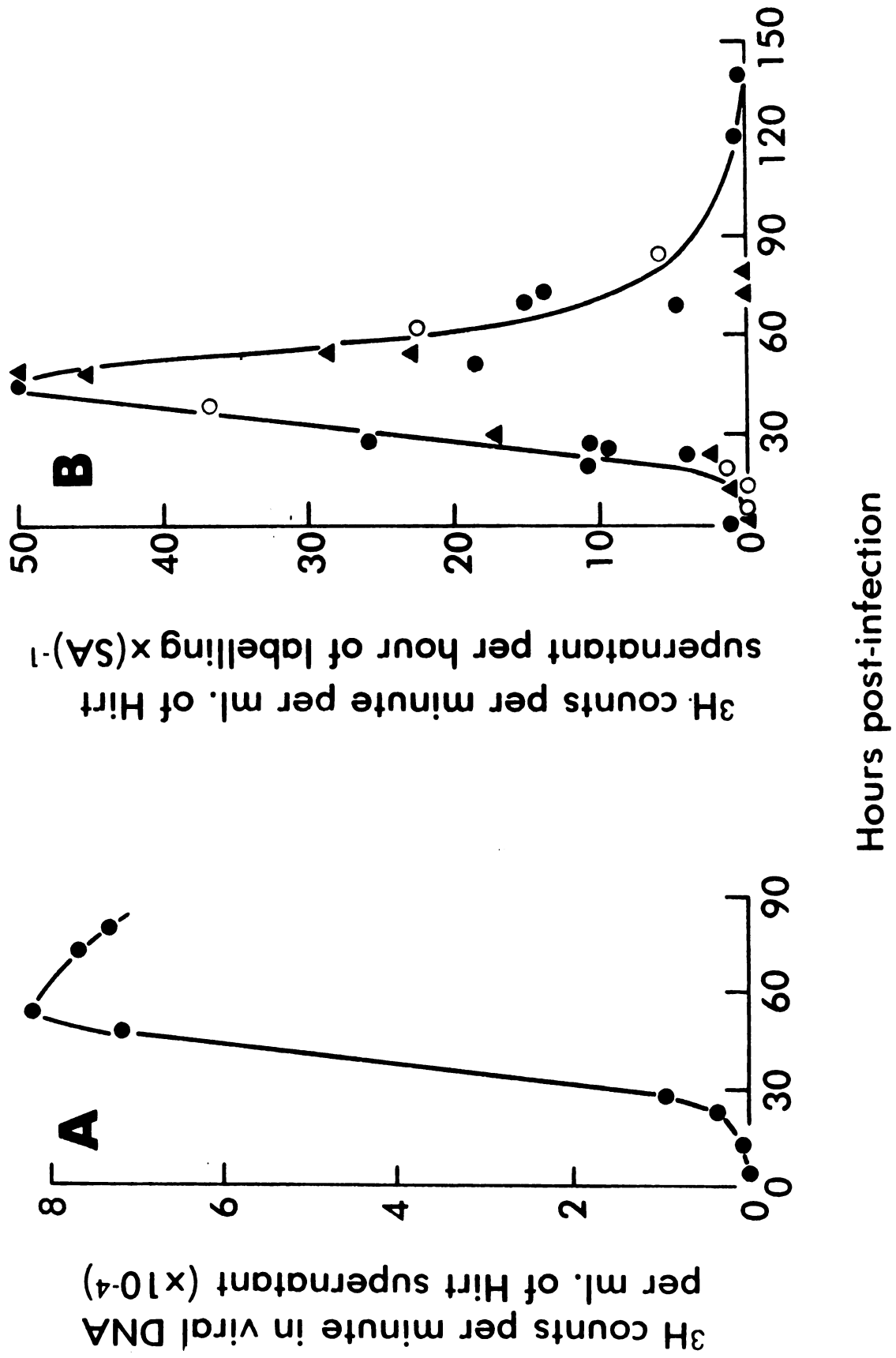
to appear only three days after infection. Since most of the experiments to be described in this thesis were completed by three days after infection, the repair competence of infected cultures probably remained intact during the experiments to be described.

Viral DNA replication is the primary synthetic task for the virus following adsorption and uncoating. The time course of increase in intracellular SV40 DNA in cultures infected at a m.o.i. of 4-5 per cell is shown in Figure (9a). This experiment was based on constant labelling with ^3H -dThd (1.0 $\mu\text{Ci/ml}$, 0.1 ci/mmol) in the presence of 10^{-6} M dThd and 4×10^{-6} M dCyd (the latter nucleotide was used to prevent thymidine starvation and interruption of cellular and viral DNA synthesis). The results show that viral DNA is not replicated in significant amounts during the first 15-20 hours following infection, but viral DNA synthesis then increases exponentially for at least 30 hours before the SV40 DNA synthesis rate begins to decrease. It is possible that uptake of ^3H -dThd from the culture medium becomes non-linear after this length of time as this radioactive precursor becomes depleted from the intracellular thymidine pool (154), so pulse labelling was used for additional study of SV40 DNA synthesis at later times post-infection. Adjustment of the continuous labelling data to the pulse labelling data on the basis of the 45 hour post-

Figures (9a-b)

(a) Tritium label appearing in SV40 DNA isolated in Hirt supernatants at various times post-infection with continuous labelling from time of infection. The tritium label was quantitated in the peak region at 10-25 S(vedbergs) on neutral sucrose isokinetic gradients. No peaks in this region were found for Hirt supernatants in mock-infected cultures. The decrease in label at late times after infection can be attributed to a combination of cell death and exhaustion of $^3\text{H-dThd}$ in the intracellular precursor pools.

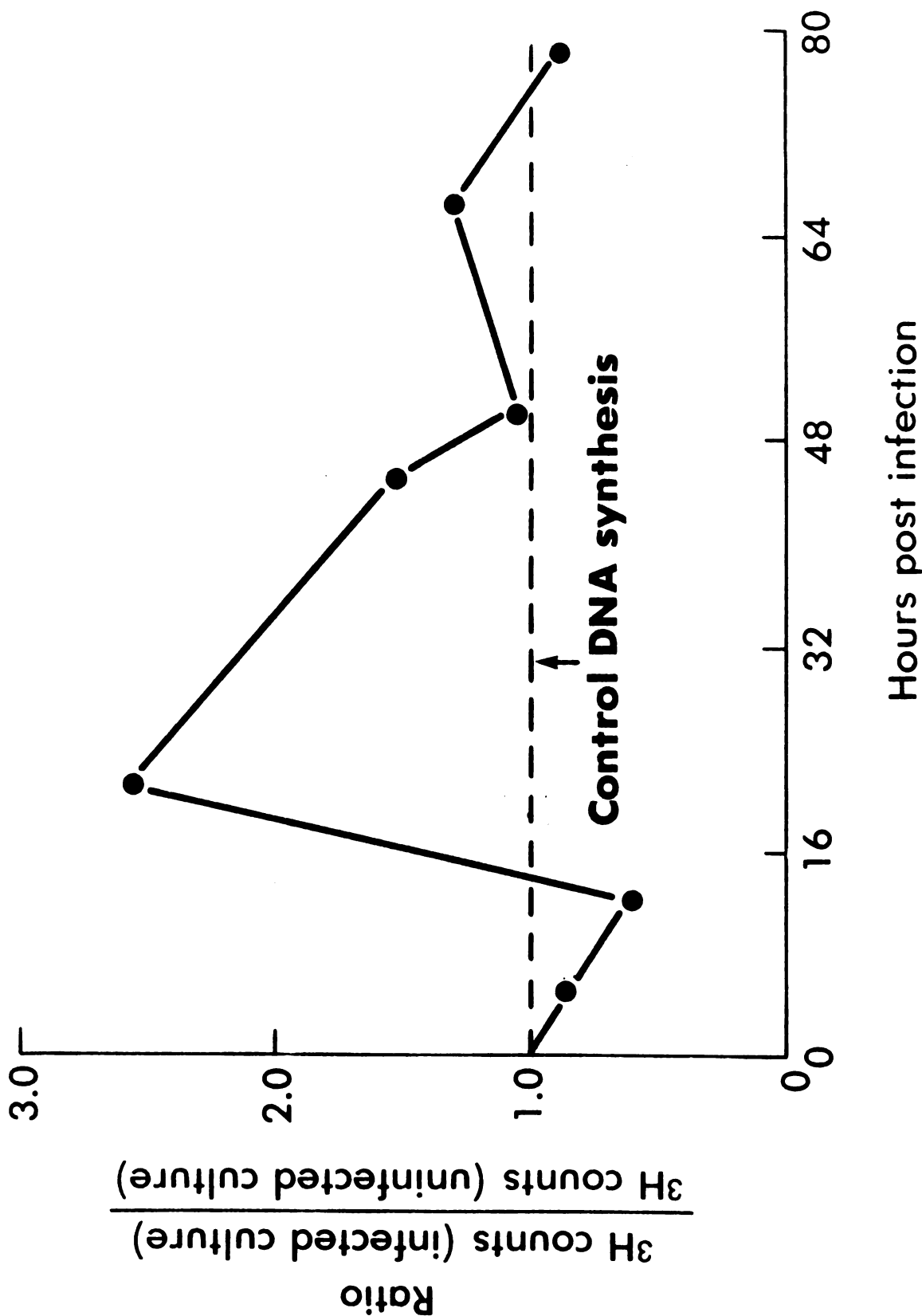
(b) Rate of tritium label appearance in Hirt supernatants from SV40-infected CV-1 cultures pulse-labelled 1-3 hours with $^3\text{H-dThd}$. Rates were corrected for the relative activity of tritium incorporated into DNA by dividing all rates by $\text{SA} = a \times b$; a is the activity of $^3\text{H-dThd}$ in the labelling medium in $\mu\text{Ci/ml}$ and b is the specific activity of thymidine in the medium in Ci/mmole . Values for a ranged from 1.0 to 10.0 $\mu\text{Ci/ml}$ and b ranged from 0.36 to 55 Ci/mmole . Data was obtained by either counting aliquots of the Hirt supernatnat (●—●—●) or quantitating tritium label appearing in the region of 10-25 S on neutral sucrose gradients (○—○—○). Rates from Figure (9a) (▲—▲—▲) were computed from successive values in the continuous labelling plot with a correction factor obtained by matching rate values for data from pulse labelling and continuous labelling at 45 hours post-infection.



infection labelling data points produces a smooth curve of SV40 DNA production rate (Figure (9b)). This plot suggests the SV40 DNA synthesis rate peaks about 45 hours post-infection and declines quickly thereafter. This data is more reliable than that in Figure (9a) since cell pool effects are minimized, but continuous labelling is apparently valid for up to 30 hours.

A poorly understood process following infection of monkey cells with SV40 is the transient stimulation of host cell DNA synthesis (142-144). This stimulation for an infected culture is reflected in the ratio of ^3H counts in DNA trapped in the SDS-salt precipitate from the Hirt extraction procedure to counts in an uninfected control (Figure (10)) at various times post-infection. This labeled DNA is essentially all host cell DNA since the Hirt extraction procedure will leave an SV40 DNA impurity of less than 2% in the host cell DNA trapped in the Hirt precipitate (131). Conversely, checks of the efficiency of host cell precipitation by the Hirt procedure showed less than 5% of all host cell DNA appeared in the Hirt supernatant ((131), this thesis). There is a delay in host cell DNA stimulation coincident with the eclipse phase of SV40 DNA production (Figure (10)). This is followed by a rise in host cell DNA synthesized after SV40 infection. The rate of host cell DNA synthesis then diminishes after about

Figure (10). Ratio of ^3H counts in Hirt precipitates from SV40-infected CV-1 cultures to counts in mock-infected cultures at various times post-infection. Tritium labelling was continuous with ^3H -dThd (1.0 $\mu\text{Ci/ml}$, 0.1 Ci/mmol) from time of infection. Data points are not connected by a smooth curve since they represent only single observations.



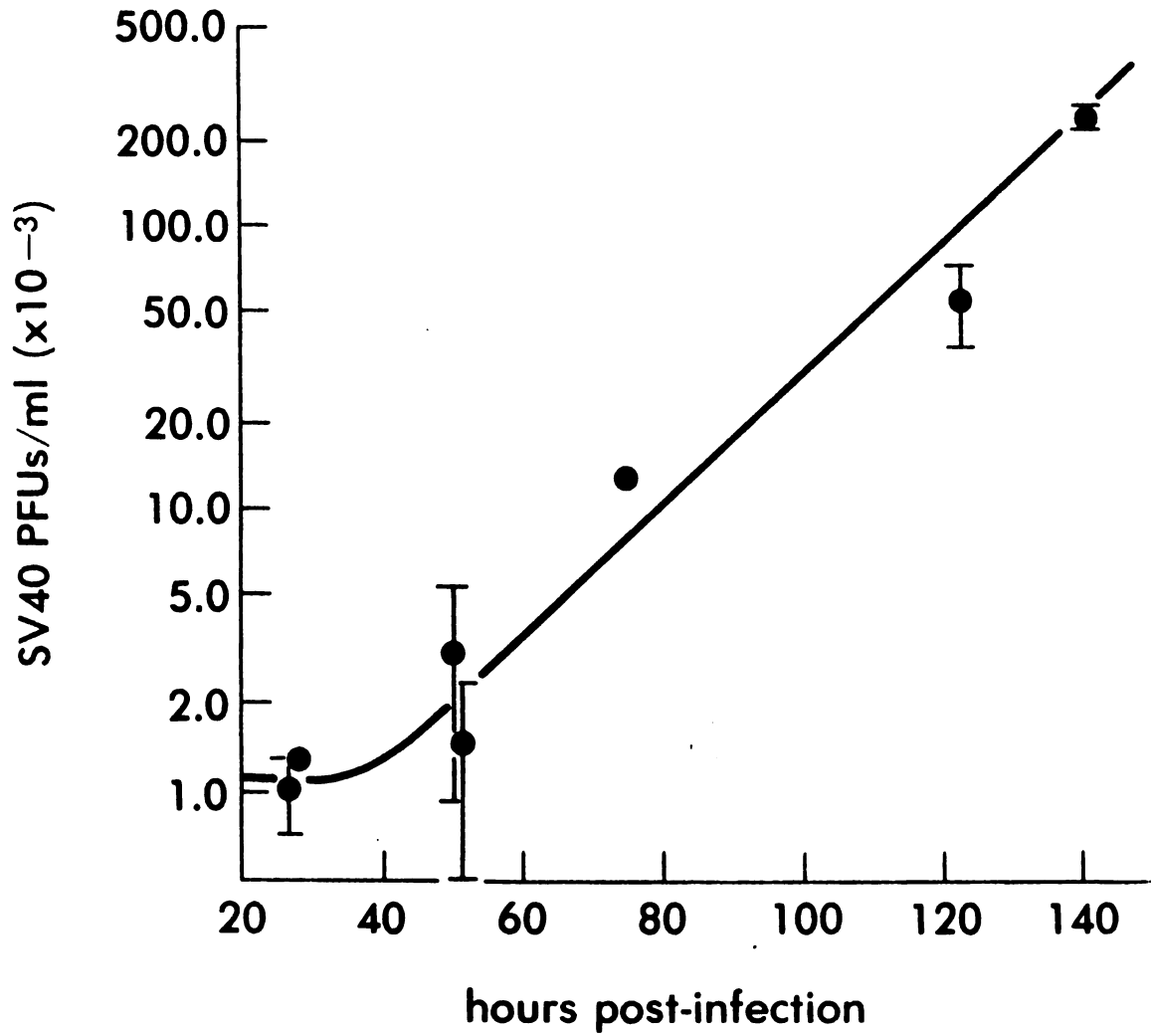
40 hours post-infection.

The final stages of the productive infectious cycle are packaging of the viral DNA and transport of mature viral particles to the extracellular medium. Figure (11) shows the appearance of plaque-forming units (PFUs) in the medium as a function of time after infection. There is a prolonged period with no appearance of new PFUs. The residual level of PFUs early after infection can be attributed to virions which reversibly adsorbed to CV-1 cells during early infection and re-entered the culture medium without penetrating a cell. New PFUs begin to appear 50 hours after infection and increase exponentially in number from that time on. Comparison of Figures (9a) and (11) show that there is a delay of about 20-30 hours between SV40 DNA replication and appearance of the packaged SV40 DNA in the culture medium. It is clear from Figures (9)-(11) that experiments completed three to four days post-infection maximize the amount of SV40 DNA affected and minimize problems of cell cytopathic changes. This observation guided the design of the experiments discussed below.

3. Excision Repair in CV-1 Cells After Exposure to UV Light

The earliest known step in excision repair after UV light is an endonucleolytic cleavage of the UV-damaged DNA strand near the pyrimidine dimer (21). The presence of UV-

Figure (11). Appearance of SV40 plaque-forming units (PFUs) in culture medium above SV40-infected CV-1 cells at various times after infection. Error bars indicate standard errors of the mean (S.E.M.) and were added to mean plaque values calculated from replicate cultures; two observations were on individual plaque assays and carry no error bars.



induced endonuclease-sensitive sites in CV-1 DNA was assayed with an excess of the T4 phage V gene product designated T4 endonuclease V (128) as a function of culture incubation time after exposure to UV light. Typical alkaline sucrose gradient profiles of UV-irradiated CV-1 DNA treated or not treated with T4 endonuclease V (PEG isolate) are shown in Figures (12a-c) for UV doses in the range 0-37.5 J/m². The number of breaks in the control profile corresponds to about 14 sites per 10⁸ daltons of DNA. The corrected number of T4 endonuclease-sensitive sites (Figure (13)) was 1.42 sites per 10⁸ daltons per J/m². This value compares favorably with the commonly quoted value of 50 pyrimidine dimers per J/m² per E. coli genome (145). If the E. coli genome is taken as 2.7 x 10⁹ daltons (146), then the latter value is equal to $50 \times \frac{10^8}{2.7 \times 10^9} = 1.85$ potential T4 endonuclease-V sensitive sites per 10⁸ daltons of DNA per J/m², or about 25% greater than the experimental value taken from Figure (13). The lowest UV fluence used in this set of experiments, 12.5 J/m², more than doubles the number of uncorrected breaks observed relative to the zero dose value (Figure (13)).

The sedimentation profiles in Figures (14a-b) show a change in the ability of T4 endonuclease V to nick CV-1 cell DNA exposed to 25 J/m² in cells and incubated for 0 or 6 hours after exposure to UV light. The extent of endonu-

Figures (12a-c). Alkaline sucrose isokinetic sedimentation profiles for CV-1 DNA exposed to UV fluences of (a) 0 J/m^2 , (b) 12.5 J/m^2 or (c) 37.5 J/m^2 and either treated with T4 endonuclease V for one hour (●.....●.....●) or T4 buffer for one hour (○—○—○) before analysis. Sedimentation is from left to right. Arrows indicate the position of either ^{14}C -labelled SV40 Form I DNA markers mixed with the CV-1 DNA sample before analysis (Figures (12a-b)) or the sedimentation position of 53 S molecules (Figure (12c)) determined by calibration curves of SV40 Form I DNA molecules sedimenting for various lengths of time. All data is corrected for background counts and ^{14}C spillover using external standards.

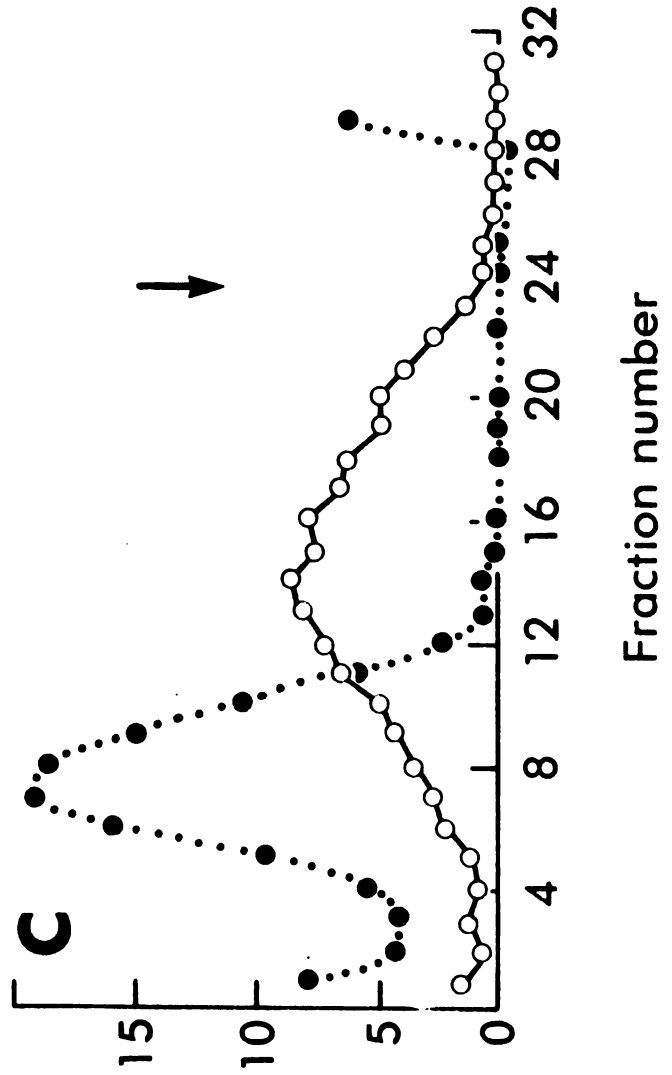
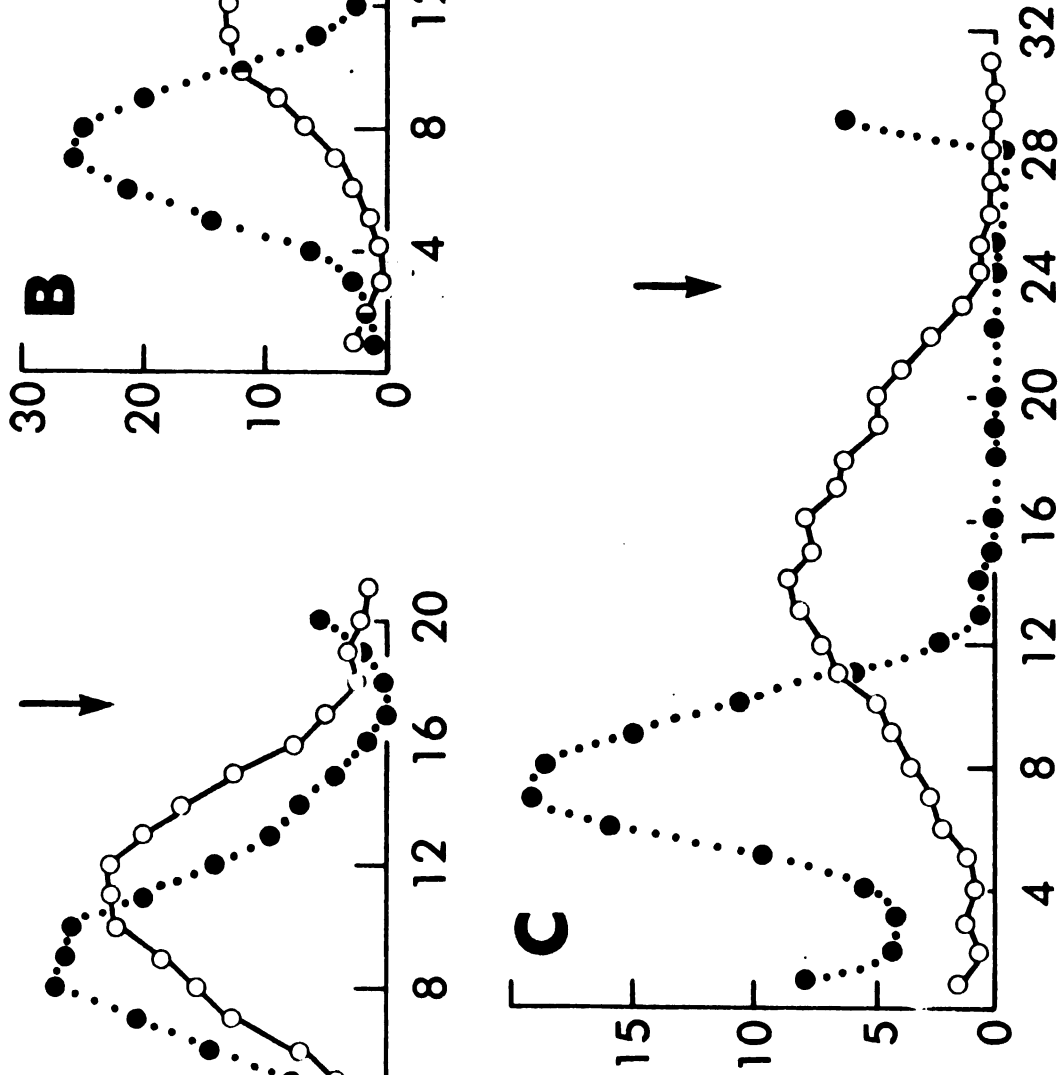
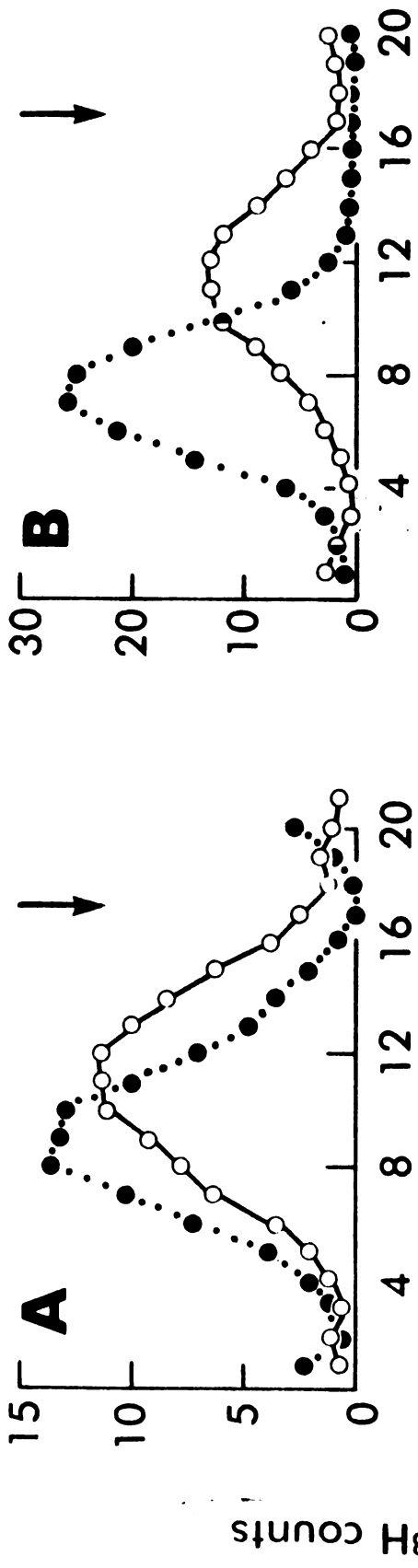
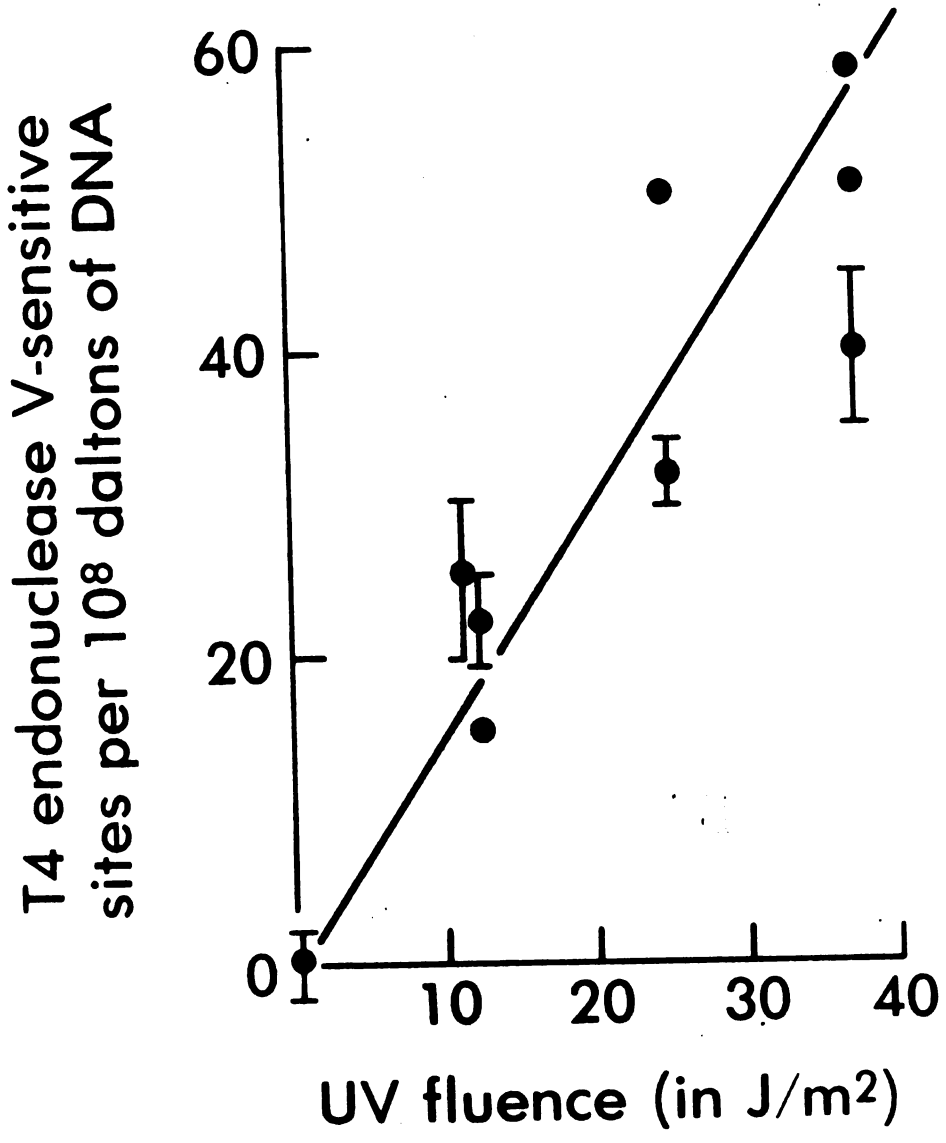
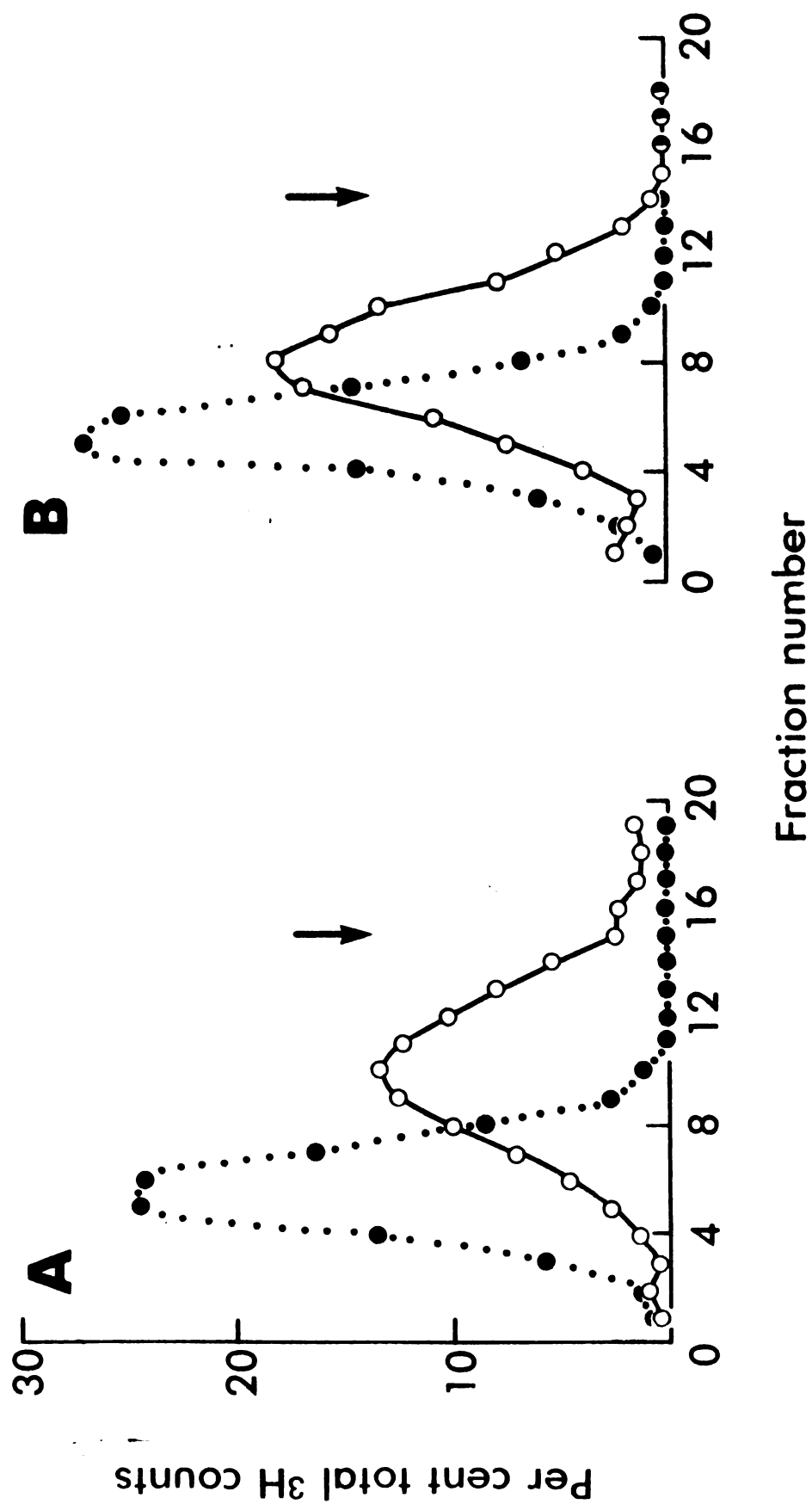


Figure (13). T4 endonuclease V-sensitive sites in CV-1 DNA as a function of UV fluence. All values were corrected for adventitious nicking and were calculated as described in Appendices B and C. A dose response line with slope of 1.42 sites per 10^8 daltons per J/m^2 was fitted to the data by eye. S.E.M. error bars were attached to data points for all samples analyzed more than once.



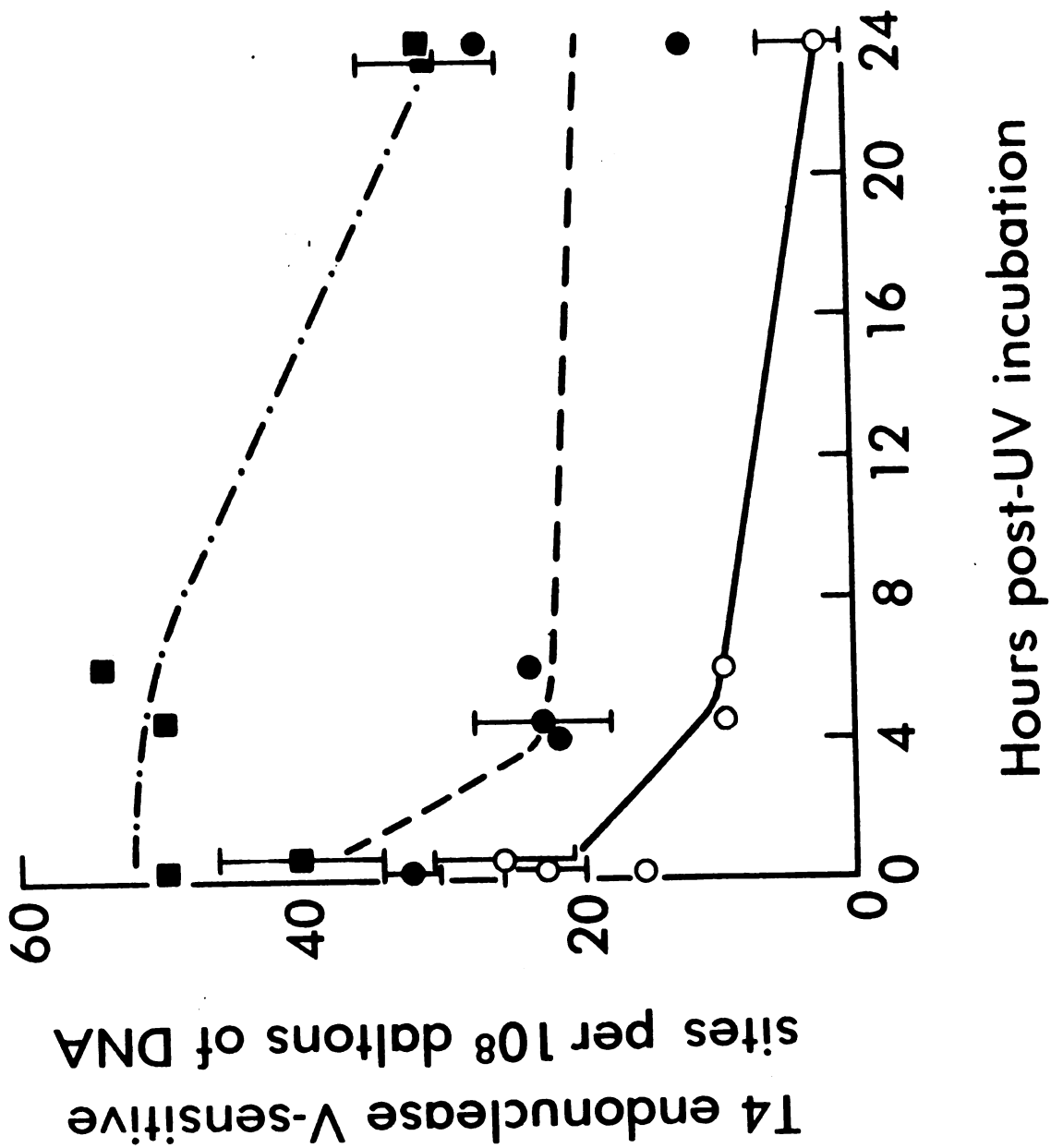
Figures (14a-b). Alkaline sucrose sedimentation profiles of CV-1 DNA from UV-irradiated cultures. Purified DNA from CV-1 cultures exposed to 25 J/m^2 of UV light was treated for one hour with either T4 buffer (○—○—○) or an excess of T4 endonuclease V (●.....●.....●) before analysis. CV-1 cultures were incubated (a) 0 hours or (b) 6 hours after exposure to UV light before the DNA was extracted. Sedimentation is from left to right. Arrows indicate the distance ^{14}C -labelled SV40 Form I molecules sedimented.



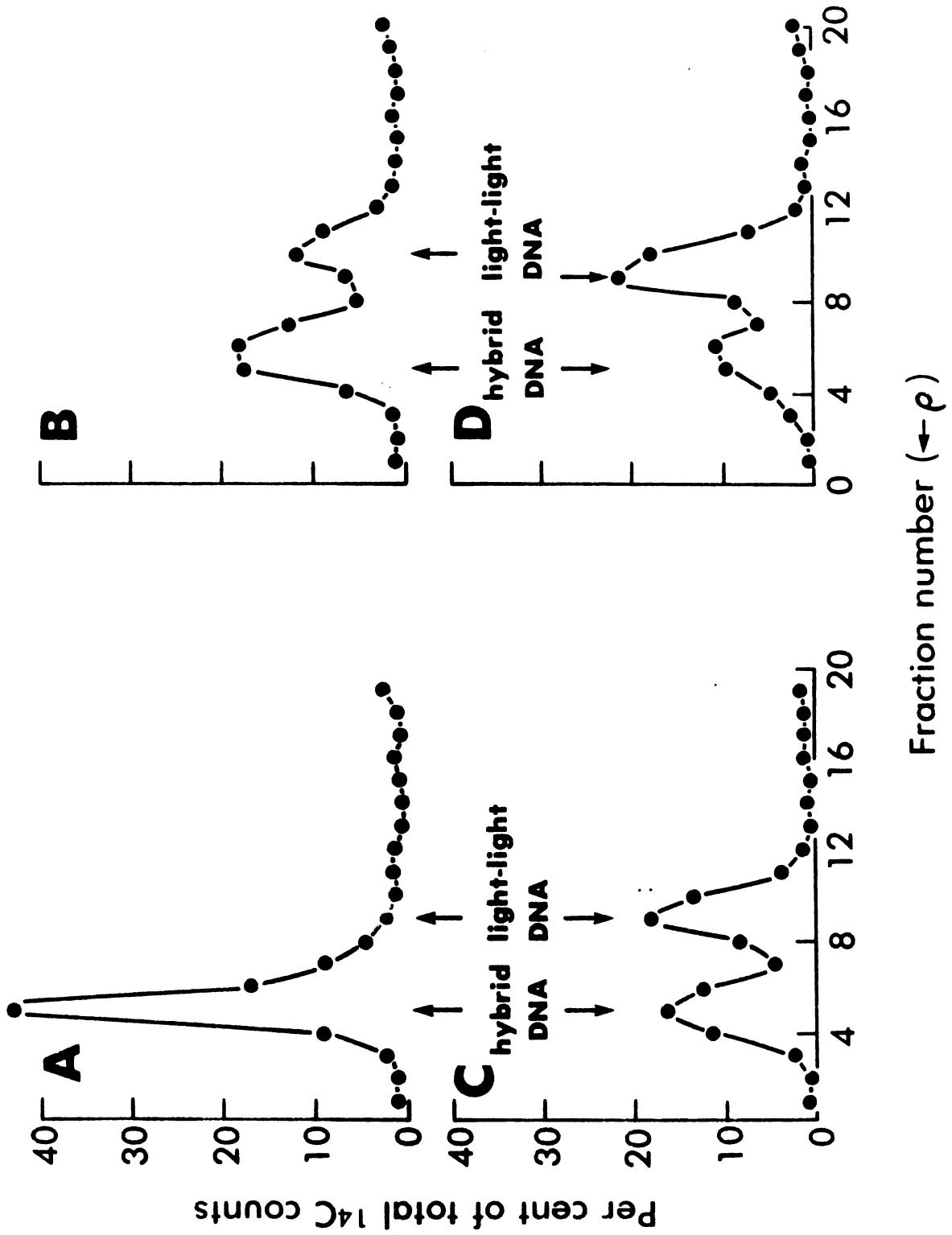
cleolytic cleavage of CV-1 DNA at various times after UV-irradiation (Figure (15)) shows a short initial period with a substantial decrease in number of T4 endonuclease V-sensitive sites followed by a slower rate of decrease in T4 endonuclease V-sensitive sites up to 24 hours of incubation. The data at a UV fluence of 37.5 J/m^2 suggests there may be inhibition of UV-endonuclease site removal at early times after UV-irradiation. The arguments for this hypothesis and for alternative hypotheses are weighed in the Discussion section of this thesis. The number of sites per 10^8 daltons of DNA which can be calculated from Figure (15) suggests that the decrease in T4 endonuclease V-sensitive sites saturates at a fluence below 25 J/m^2 .

The time course and dose response of these changes in number of UV-induced T4 endonuclease V-sensitive sites should resemble those observed during the insertion of new bases and the removal of damaged bases. The insertion of new bases was followed by repair replication studies as described in detail elsewhere (120). The alkaline CsCl-CsSO₄ isopycnic gradient profiles of Figures (16a-d) show changes in ¹⁴C-dThd uptake in the presence of BrdUrd in unsubstituted and hybrid density DNA as a function of UV dose to CV-1 cultures. It is apparent that ¹⁴C-dThd uptake into hybrid density DNA is suppressed with increasing UV dose, an expected result since hybrid density DNA is the

Figure (15). Decrease in number of T4 endonuclease V-sensitive sites in CV-1 DNA with post-UV incubation. Curves were fitted by eye to data obtained for cultures exposed to 12.5 J/m^2 (○—○—○), 25 J/m^2 (●—●—●), or 37.5 J/m^2 (■—■—■). Error bars represent S.E.M. for samples analyzed more than once.



Figures (16a-d). Alkaline CsCl-CsSO₄ isopycnic gradient profiles for isolated CV-1 DNA from cultures exposed to (a) 0 J/m², (b) 12.5 J/m², (c) 25 J/m², and (d) 37.5 J/m² before labelling with ¹⁴C-dThd (0.1 μCi/mo, 56 mCi/mmmole) plus 10⁻⁵ M BrdUrd for three hours. Density (ρ) increases from right to left. The density of unsubstituted (light-light) DNA was 1.668 and of unifilarly substituted (hybrid) DNA was 1.754.



product of semi-conservative DNA replication (150). The specific activity of light-light DNA (a measure of repair replication) increased with increasing UV dose (Figure (17)). Repair replication began to saturate in the UV dose range 25-35 J/m² for both ³H and ¹⁴C, suggesting that purines and pyrimidines are inserted by the same repair mechanism. The human cell line GM637 was studied as a control in one experiment. The human cell line was found to be less active in repair replication than the CV-1 cell line (Figure (17)).

A dose of 25 J/m² was used on replicate cultures to analyze the rate of repair replication at various times after the cultures were exposed to UV light. Figure (18) shows the rapid decrease in the rate of repair replication over the first seven hours followed by a slower rate up to 19 hours after UV-irradiation. This type of rate change agrees with that which would be predicted on the basis of the above experiments with T4 endonuclease V; that is, there is a relatively rapid repair phase where the major part of UV light-irradiated DNA damage is removed and a later, slower phase where damage removal and base insertion continue at a slower rate than observed at early times after CV-1 cells are exposed to UV light.

Removal of damaged bases after UV-irradiation is closely related to the polymerization of new bases to replace the damaged ones. Two mechanisms have been sug-

Figure (17). Repair replication in CV-1 DNA after exposure to UV light. The specific activity of ^{14}C (▲---▲---▲) or ^3H (○—○—○) counts incorporated into light-light DNA after exposure to various UV fluences was determined by counting 50 μl aliquots of pooled fractions of light-light DNA on Whatman 3 cm. paper filters and dividing the measured radioactivity by the optical density at 260 nm (A_{260}) for the appropriate fractions.

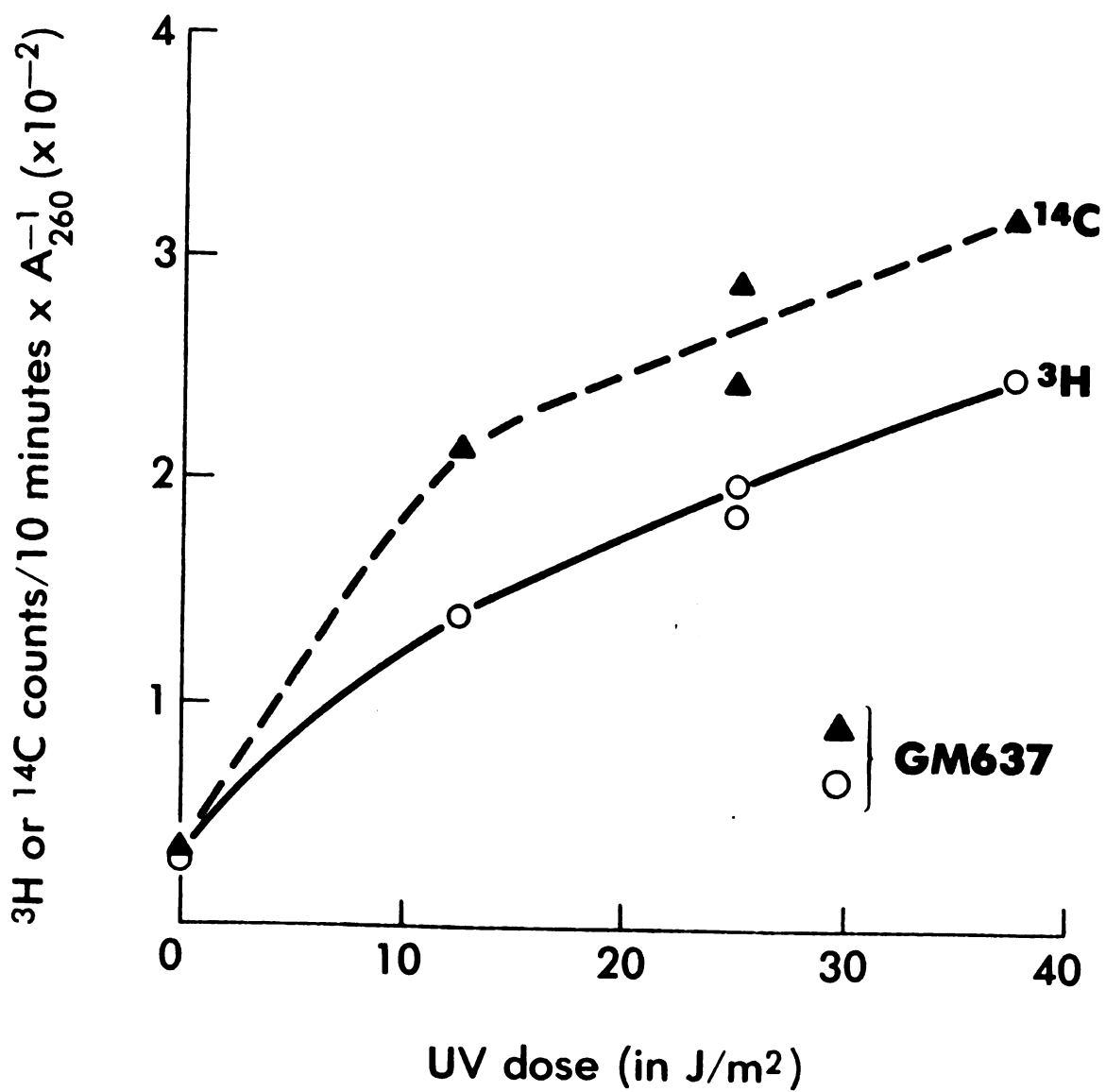
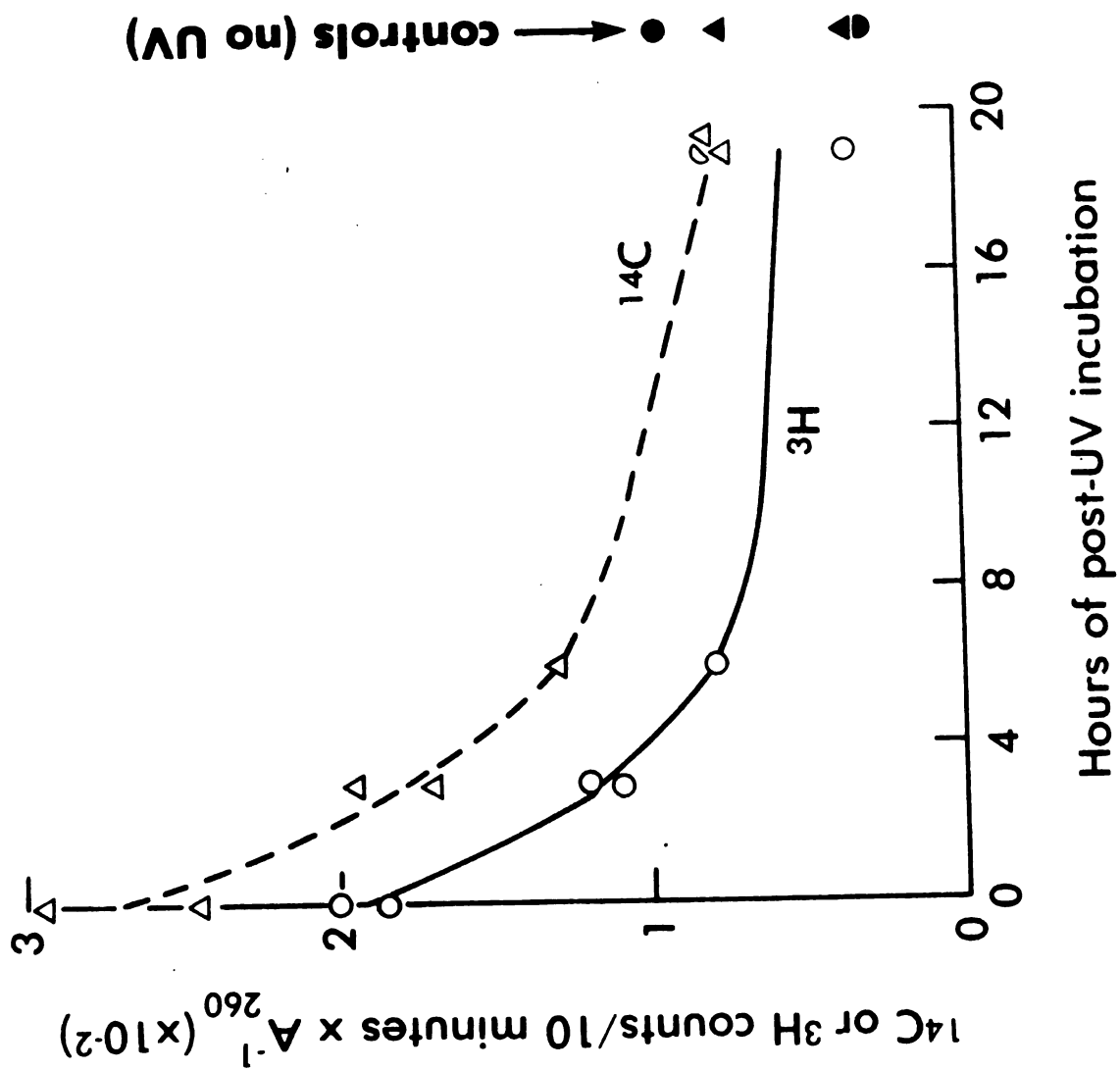
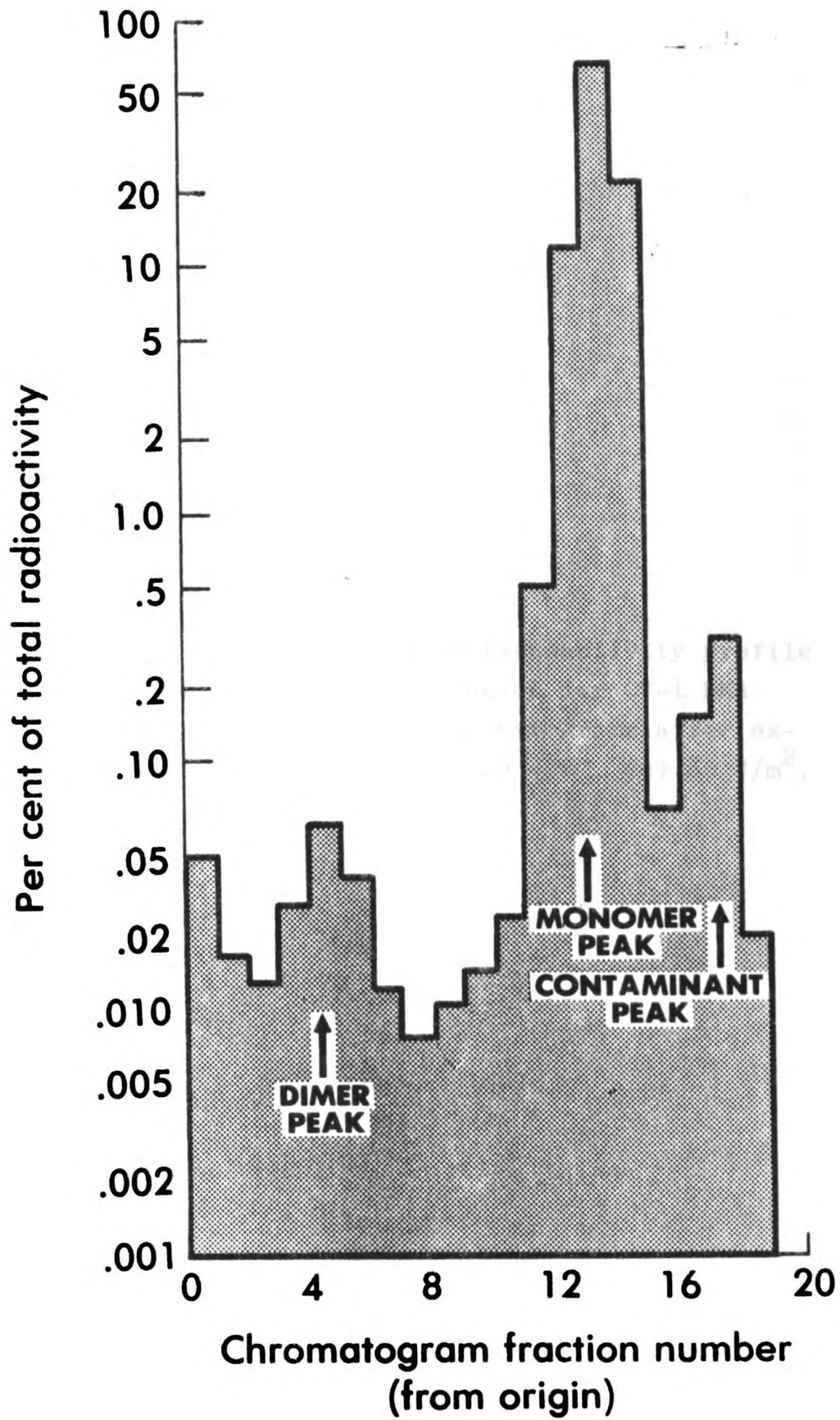


Figure (18). The rate of repair replication in CV-1 DNA with various lengths of post-UV incubation time. Specific activities of ^3H (\circ — \circ — \circ) or ^{14}C (Δ — Δ — Δ)-labelled light-light CV-1 DNA were plotted for cultures exposed to 0 J/m^2 (closed symbols) or 25 J/m^2 (open symbols) of UV light and incubated for various lengths of time before labelling with ^{14}C -dThd ($0.1 \mu\text{Ci/ml}$, 56 mCi/mmole) or ^3H -hypoxanthine ($2.0 \mu\text{Ci/ml}$, 0.57 Ci/mmole) in the presence of 10^{-5} M BrdUrd for three hours. Specific activities were computed as described in the legend for Figure (17).

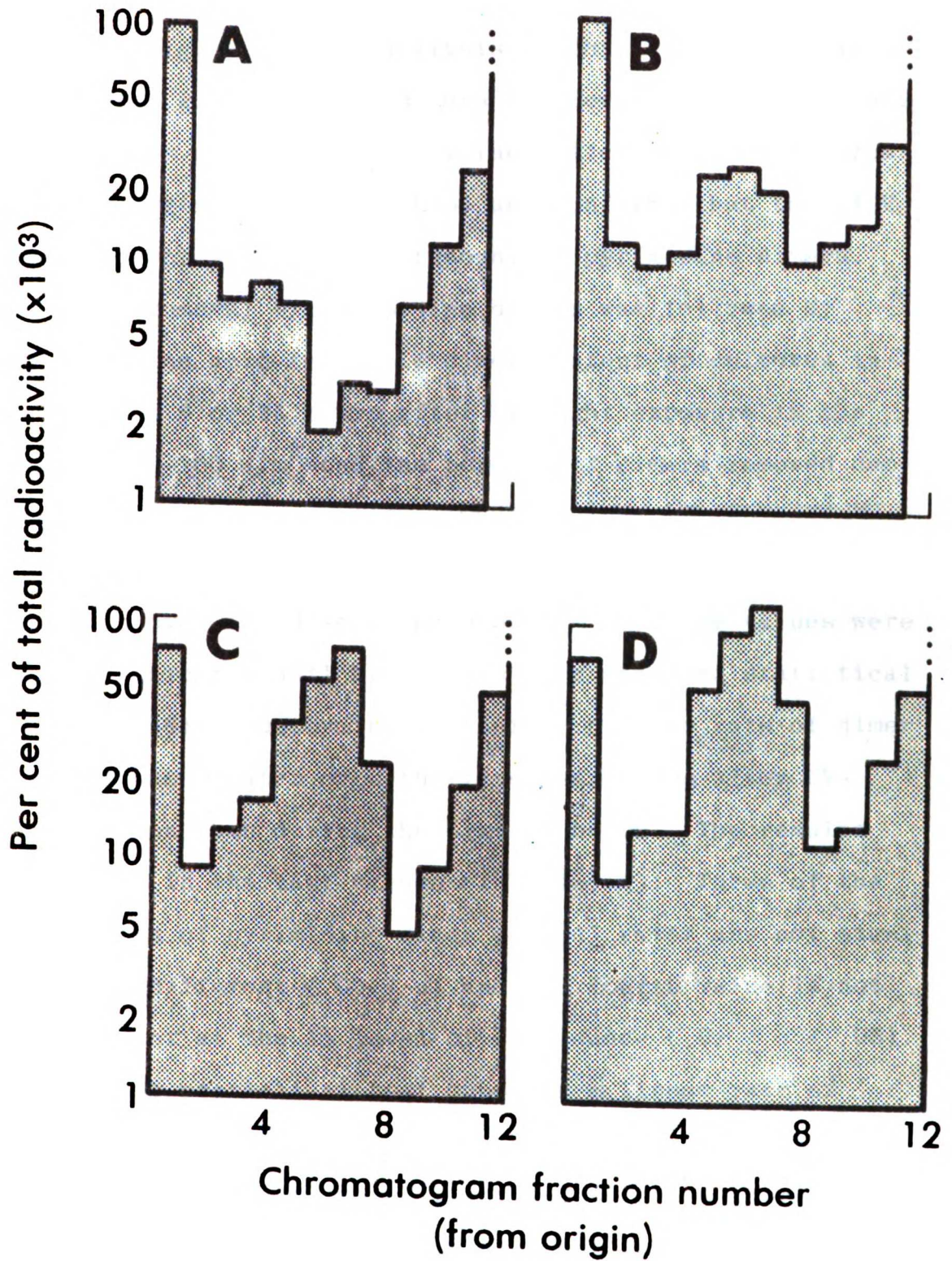


gested for this process (147). To test whether or not dimer removal kinetics are similar to the kinetics of UV-endo-nuclease site loss and repair replication, the persistence of pyrimidine dimers was followed in acid-insoluble CV-1 DNA by thin layer chromatography (140) and compared to the rate data for T4 endonuclease V-sensitive site loss and repair replication in CV-1 cells. Typical chromatographic radioactivity histograms are shown in Figures (19a-d) and (20) for several doses of UV light to CV-1 cultures heavily labelled in their DNA with ^3H -dThd. Fractions in the pyrimidine monomer peak were pooled for convenience in counting; control experiments showed the ^3H counting efficiency was not lowered by pooling three fractions at a time. Experiments were also done without pooling fractions and a ^3H -labelled contaminant peak was found that ran 2 or 3 fractions ahead of the monomer peak near the ethylacetate:n-propanol: H_2O (4:1:2) solvent front (Figure (19)), but the amount of this contaminant was not correlated with the length of exposure to UV light and never exceeded 0.1% of the total counts of the chromatogram. Counts in this region of the chromatogram were therefore routinely included with the monomer peak counts. The pyrimidine dimer peak was always spread over 4-7 fractions and the R_f of this peak relative to the monomer peak was in the range of 0.25-0.40. The percent of total chromatogram counts

Figure (19). Detailed tritium radioactivity profile of CV-1 DNA exposed to a UV fluence of 25 J/m^2 and analyzed by thin layer chromatography. Pyrimidine monomer and dimer positions are indicated by arrows. Chromatography is from left to right.



Figures (20a-d). Tritium radioactivity profiles in the pyrimidine dimer region for CV-1 DNA analyzed on thin layer chromatograms after exposure to (a) 0 J/m^2 , (b) 25 J/m^2 , (c) 50 J/m^2 , and (d) 100 J/m^2 .



in the pyrimidine dimer region increased with increasing UV fluence (Figure (21)). Analysis of this data by linear regression gives 0.0027% dimers ($\hat{\pi}$) per J/m^2 or $1.30 \hat{\pi}$ per 10^8 daltons per J/m^2 . This value differs by only 8% from that determined in Figure (13) and confirms that the T4 V gene product specifically recognizes pyrimidine dimers.

The removal of pyrimidine dimers was followed by assaying the acid-insoluble dimer content of cultures incubated 0, 6 or 24 hours after UV light exposure in the range of 0-100 J/m^2 and the percent of dimers removed during 24 hours of incubation. Table (2) lists the corrected percent of dimers removed per hour during 6 or 24 hours of incubation over the dose range 0-50 J/m^2 . These values were tested against a null hypothesis by a standard statistical t-test (148) to determine whether or not the rate of dimer removal was greater over the first six hours after UV-irradiation than during the next 18 hours. The results are shown in the last column of Table (2): Three of the four pairs of pyrimidine dimer removal rates are not significantly different ($.05 \leq \rho$) and the fourth value is not significant at the 1% level of confidence ($.01 \leq \rho \leq .05$). Thus, this statistical test supports a linear rate of dimer removal throughout the 24 hours of incubation after cultures are exposed to UV light and suggests there is a rate limiting cellular repair step not related to the endo-

Figure (21). Percentages of CV-1 DNA tritium counts found in the pyrimidine dimer region of thin layer chromatograms after UV fluences of 0-100 J/m^3 . Linear regression analysis was used to fit a smooth line to the data with a slope of 0.0027% dimers per J/m^2 . Each data point is a single observation and consequently carries no error bar.

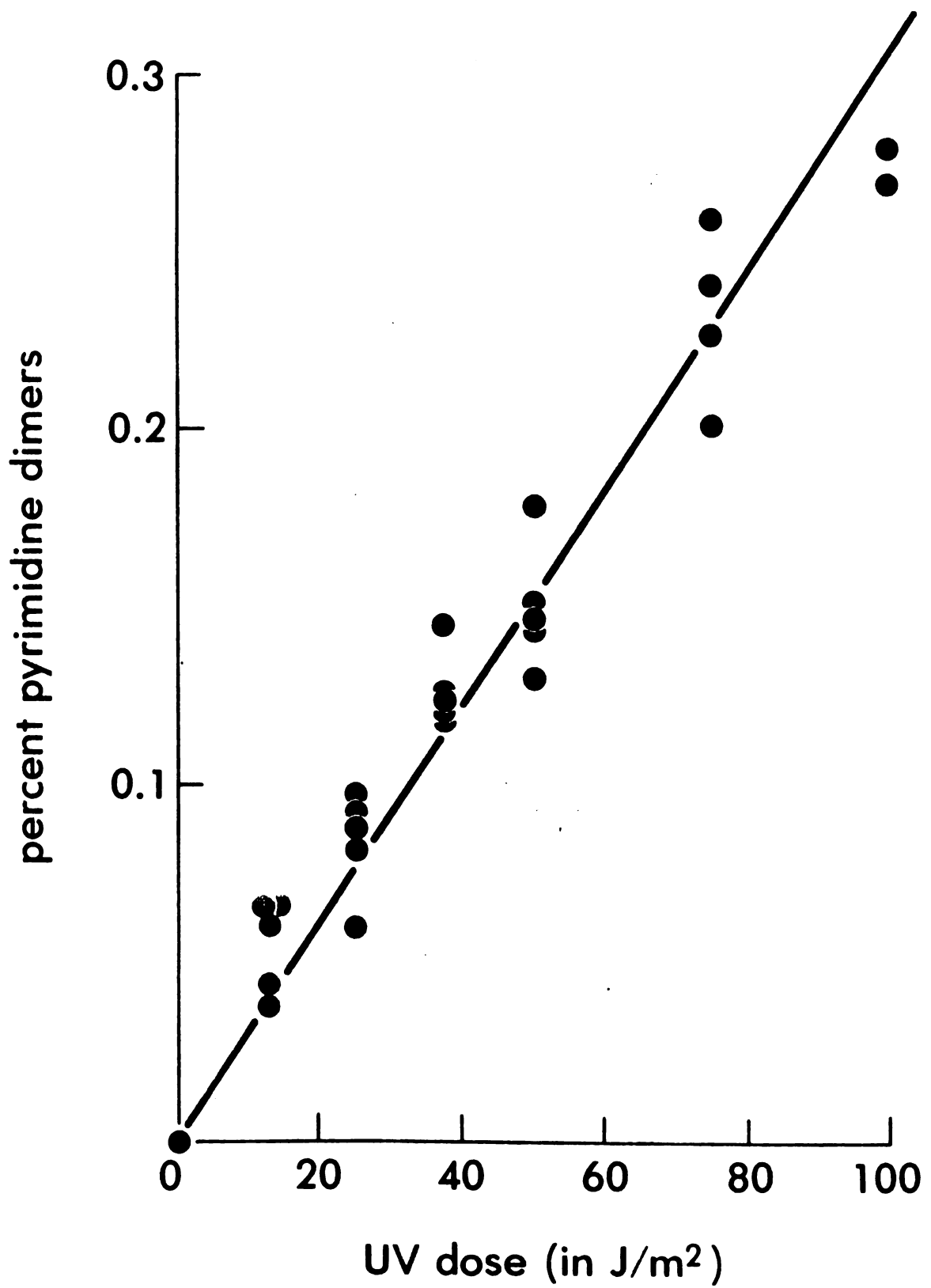


Table 2

Pyrimidine Dimer Contents of CV-1 Cultures Incubated
0, 6 or 24 Hours After Exposure to Various Doses of UV Light

(A) UV Dose (in J/m^2)	(B) % of Pyrimidine Bases Present as Dimers with Y Hours of Incubation after UV Light Exposure	(C) Y = (6)	(D) Y = (24)	(E) % of Dimers Removed in 24 Hours	(F) % of Pyrimidine Bases Pre- sent as Dimers Removed per Hour of Incubation	(G) 24 Hour Incubation
	Y = (0)	Y = (6)	Y = (24)		6 Hour Incubation	24 Hour Incubation
12.5	.054 \pm .006	.039 \pm .009	.020 \pm .004	63%	(2.5 \pm 1.0) $\times 10^{-3}$	(1.4 \pm 0.1) $\times 10^{-3}$
25.0	.084 \pm .006	.076 \pm .006	.048 \pm .006	43	(1.3 \pm 0.7) $\times 10^{-3}$	(1.5 \pm 0.2) $\times 10^{-3}$
37.5	.126 \pm .005	.102 \pm .008	.086 \pm .010	32	(4.0 \pm 1.0) $\times 10^{-3}$	(1.7 \pm 0.3) $\times 10^{-3}$
50.0	.150 \pm .008	.136 \pm .004	.096 \pm .005	36	(2.3 \pm 0.7) $\times 10^{-3}$	(2.3 \pm 0.2) $\times 10^{-3}$
75.0	.230 \pm .010	.244 \pm .004	.170 \pm .005	26	--	(2.5 \pm .03) $\times 10^{-3}$
100.0	.274 \pm .005	.316 \pm .009	.282 \pm .003	~0	--	--

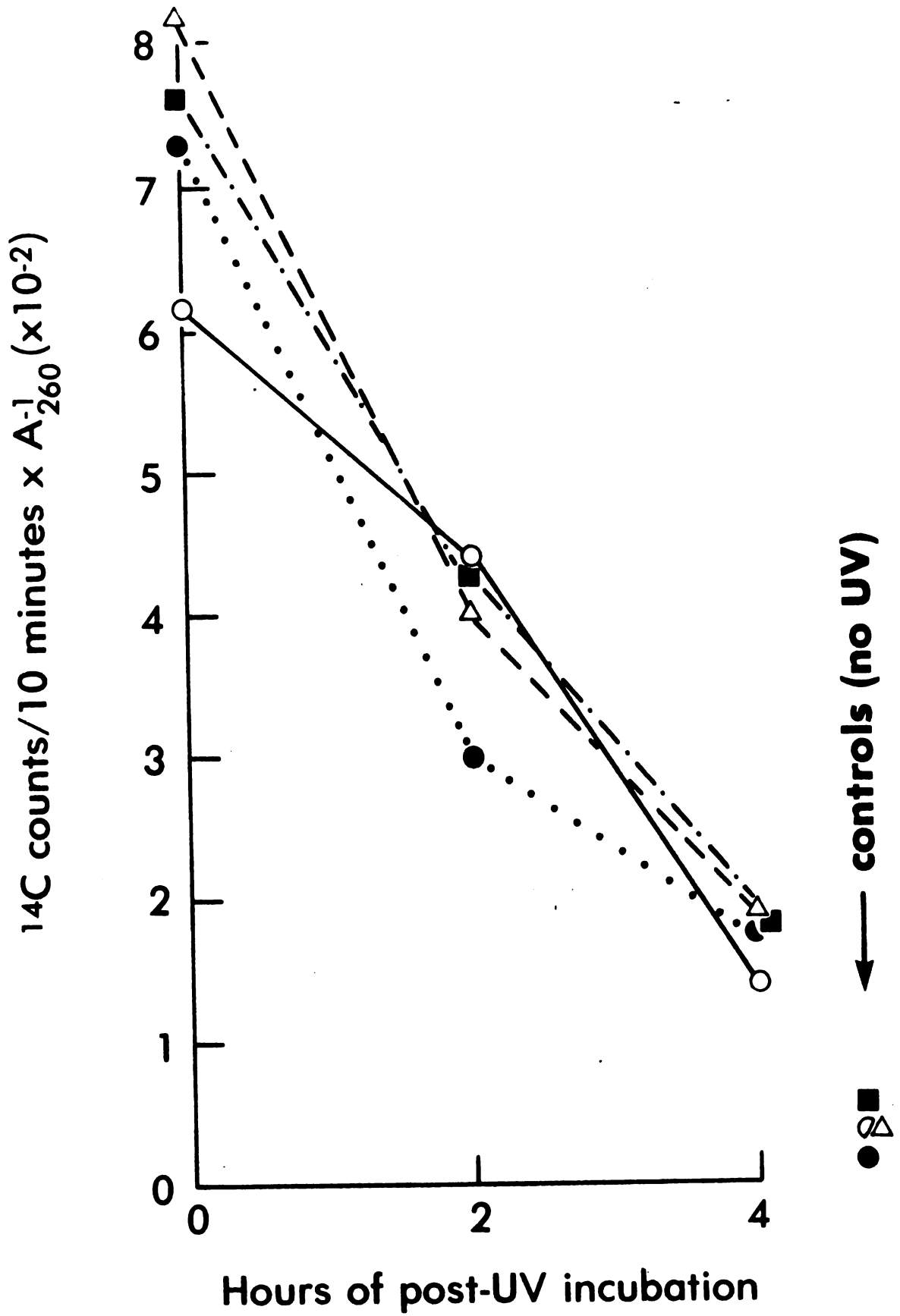
Note: All errors in columns (B) - (D) are standard errors of the mean (148) while errors in columns (F) and (G) are standard errors of the difference between the means.

nucleolytic cleavage and base insertion stages of excision repair.

An alternate hypothesis is the possibility an experimental artifact inherent to the thin layer chromatography protocol prevents the detection of pyrimidine dimer removal early after UV-irradiation. One such potential artifact that sets the chromatography protocol apart from the repair replication and endonuclease-sensitive site studies is the high level of ^3H -dThd taken up by CV-1 cultures used for thin layer chromatography. A ^3H -dThd concentration in the culture medium of 10 μCi per ml. is reduced to about 2 μCi per ml after 24 hours of labelling. The 8 μCi per ml of incorporated ^3H in the cellular DNA is equivalent to an X-ray dose rate of 2.7 krads per cell per day (130), a chronic radiation exposure which might inhibit excision repair.

To test this hypothesis, CV-1 cultures were exposed to 5.0 $\mu\text{Ci}/\text{ml}$ of ^3H -thymidine for 24 hours followed by an overnight "chase" with unlabelled medium or were X-irradiated and incubated for 24 hours before the radiation-damaged cultures were exposed to 0 or 25 J/m^2 of UV light. Repair replication was then measured as a function of time after UV-irradiation (see Materials and Methods). The results are shown in Figure (22) for ^3H -dThd exposure and 0, 2, or 10 krads of acute X-rays. The rate of repair replication

Figure (22). Rates of repair replication at various times after UV-irradiation with a fluence of 25 J/m^2 in CV-1 cultures treated one day before UV-irradiation with nothing ($\circ\text{---}\circ\text{---}\circ$), 2 Krads X-rays (300 Kvp, 2 mm Cu nominal filtration) ($\bullet\text{.....}\bullet\text{.....}\bullet$), 10 Krads X-rays ($\blacksquare\text{---}\blacksquare\text{---}\blacksquare$), or 24 hours incubation in mEm supplemented with $^3\text{H-dThd}$ ($5 \text{ }\mu\text{Ci/ml}$, 11 Ci/mmole) ($\triangle\text{---}\triangle\text{---}\triangle$). Cultures were labelled with mEm plus $^{14}\text{C BrdUrd}$ ($0.1 \text{ }\mu\text{Ci/ml}$, 56 mCi/mmole) in the presence of $2 \times 10^{-3} \text{ M}$ hydroxyurea for four hours at various times after UV-irradiation and ^{14}C specific activities of light-light DNA determined as described in the legend of Figure (17) (also see Materials and Methods).



after UV-irradiation in all cases decreases during the first six hours to about 20% of the initial rate. The initial rate of repair replication is also higher in all cases of previous X-ray or ^3H -dThd exposure and suggests a possible synergism between X-ray or ^3H decay damage and UV light damage. R. B. Setlow et al (100) claimed to observe a UV-like response 20 hours after γ -ray exposure of normal human and XP fibroblasts that may be a similar effect to that seen in Figure (22). On the other hand, the data scatter in Figure (22) is large enough that there may be no significant difference in the observed repair rates. In any event, it is clear that ^3H decays or X-irradiation prior to UV light exposure of CV-1 cell cultures do not impair CV-1 cell excision repair capacity as measured by repair replication.

4. Excision Repair of SV40 DNA After Exposure to UV Light

The small coding capacity of SV40 DNA requires CV-1 host cell DNA repair mechanisms to rescue SV40 DNA damaged by UV light. Excision repair of SV40 DNA was followed by assaying the induction and removal of T4 endonuclease V-sensitive sites from SV40 DNA after UV-irradiation of SV40-infected CV-1 cultures. Extracted SV40 DNA was either treated with T4 endonuclease V or an equal volume of T4 buffer (see Materials and Methods) and the DNA-enzyme

incubation mixture was analyzed on agarose tube gels or alkaline sucrose gradients for the conversion of SV40 Form I molecules to nicked Form II molecules. A typical set of agarose tube gel radioactivity profiles is shown in Figures (23a-c) for UV fluences of 0, 12.5 or 25 J/m^2 .

The percent of unnicked Form I molecules calculated with corrections for the initial percent of Form I molecules and non-specific nicking by T4 endonuclease V represents the O^{th} order term in a Poisson distribution with a mean value equal to the mean number of T4 endonuclease V-sensitive sites per SV40 DNA molecule. The mean number of sites should be linearly related to the UV dose if UV-induced endonuclease-sensitive sites are single hit events. Figure (24) displays the calculated mean values from the Poisson distribution for damaged SV40 DNA molecules extracted immediately after UV-irradiation from infected CV-1 cultures. The data was fitted by linear regression analysis to a line with a slope of 0.049 sites per SV40 genome per J/m^2 and a correlation coefficient $r = 0.936$ (148) which implies linearity. The line slope is equivalent to 1.36 sites per 10^8 daltons of DNA per J/m^2 . No difference was found in the results from alkaline sucrose velocity gradients or agarose tube gel electrophoresis up to a DNA sample:enzyme volume ratio of 20:1.

There are important changes in the mean number of T4

Figures (23a-c). Tritium radioactivity profiles for SV40 DNA analyzed on 1.5% agarose tube gels by electrophoresis after isolation from SV40-infected CV-1 cultures exposed to (a) 0 J/m^2 , (b) 12.5 J/m^2 , and (c) 25 J/m^2 . SV40 DNA samples were treated for one hour with T4 buffer (○—○—○) or an excess of T4 endonuclease V (●.....●.....●) before analysis. Electrophoresis is from left to right.

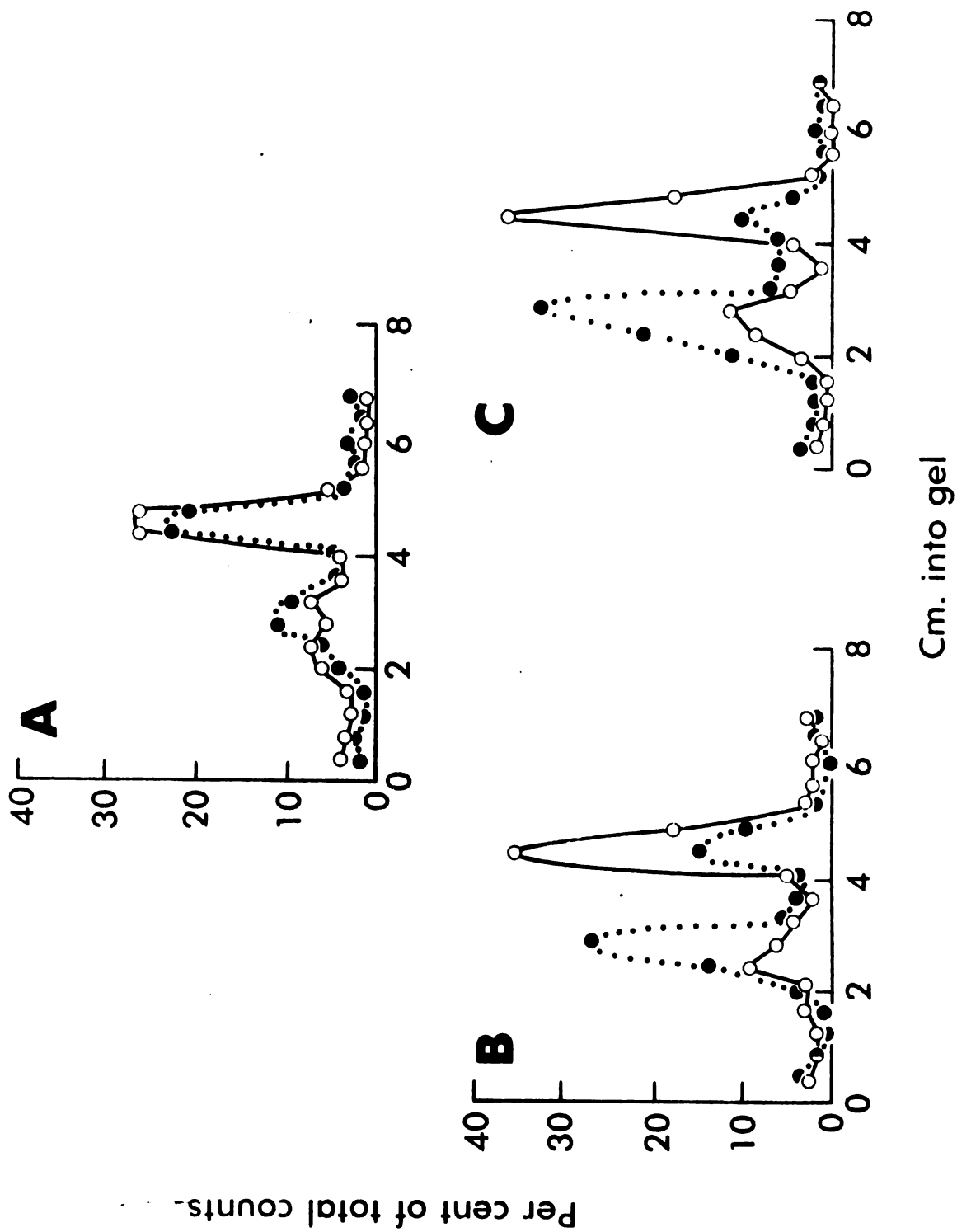
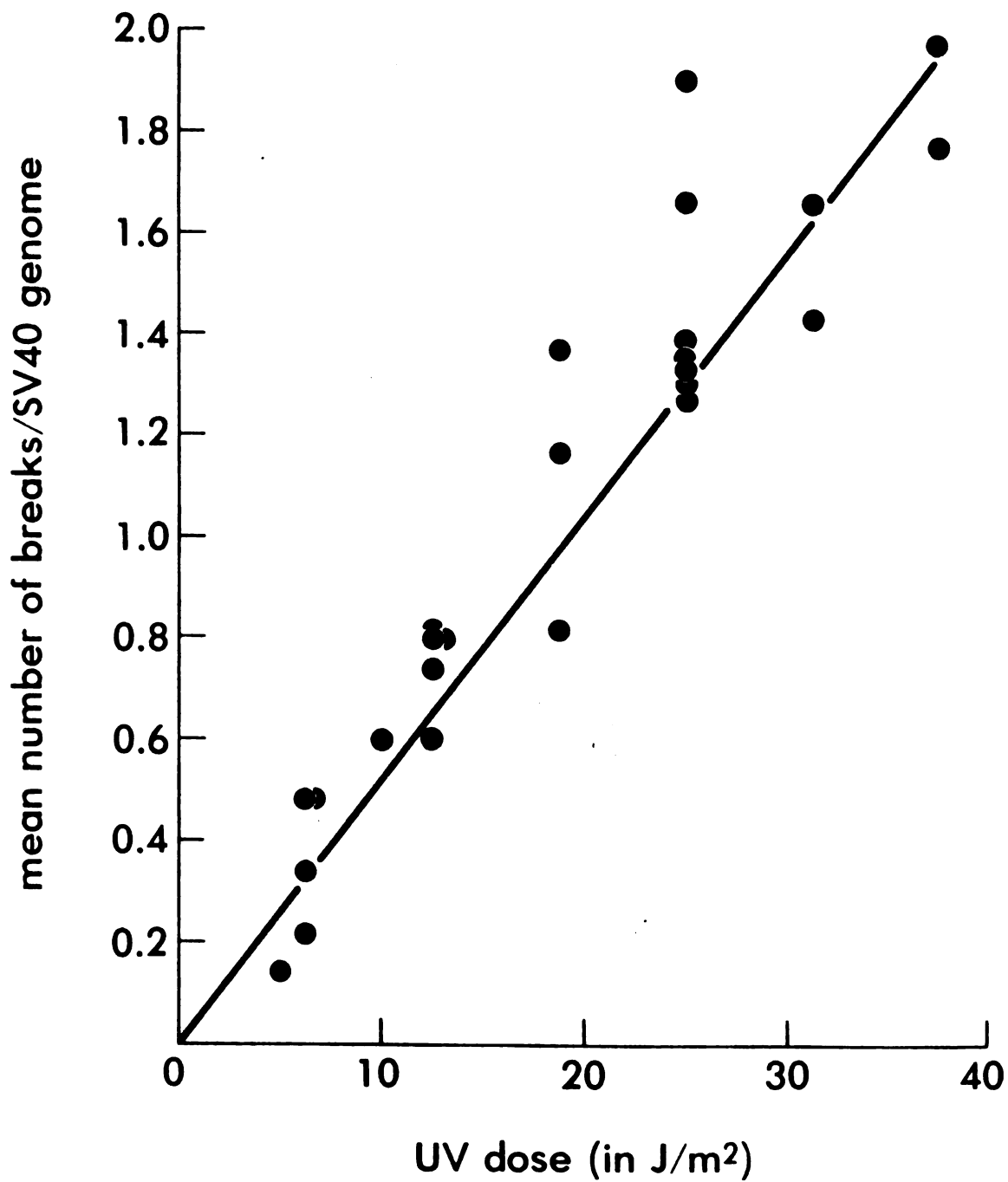


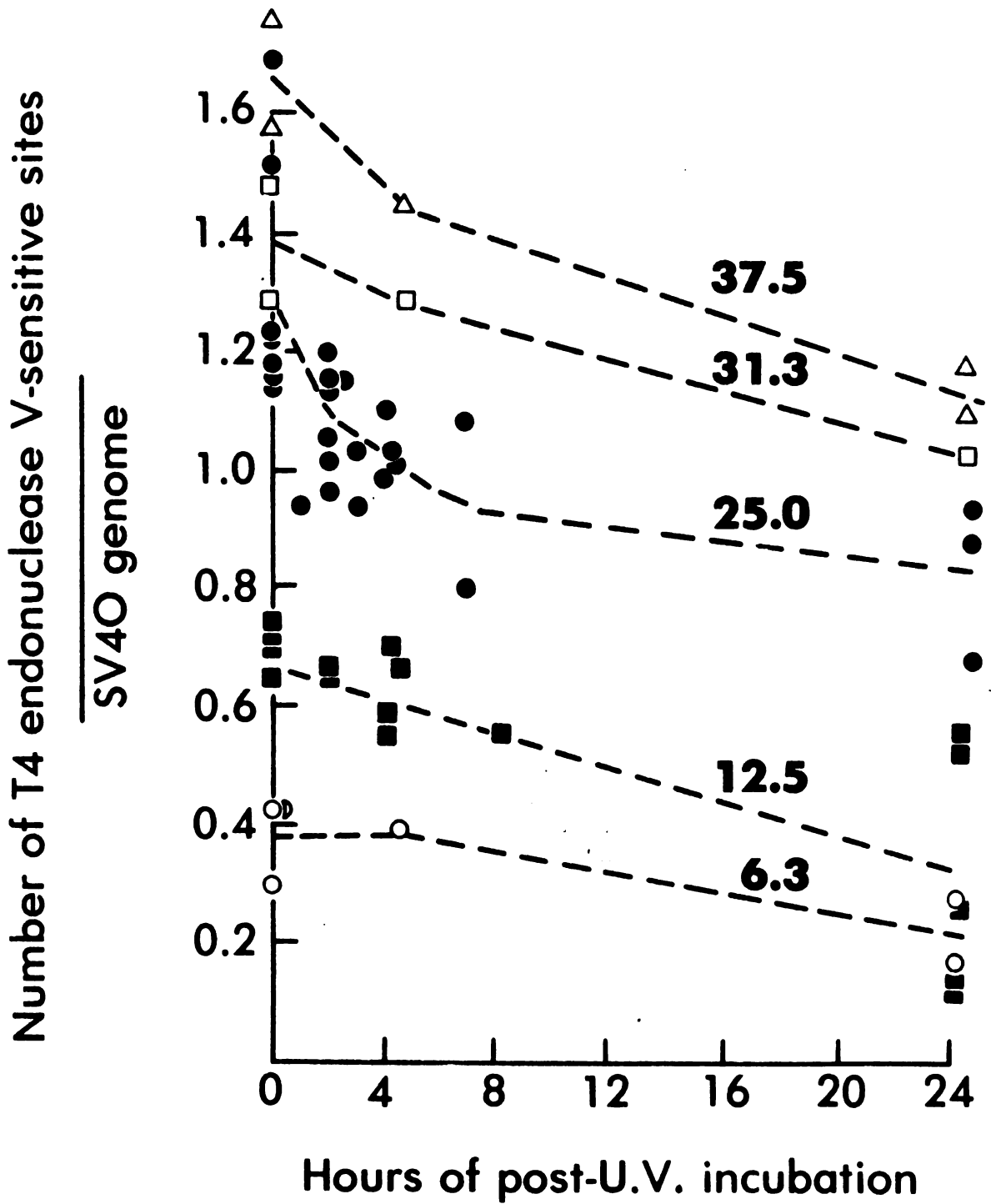
Figure (24). Mean values of number of T4 endonuclease V-sensitive sites in SV40 DNA immediately after exposure to various UV fluences. Mean values n were calculated using the Poisson distribution as $n = -\ln f$ where f was the fraction of SV40 Form I DNA molecules unnicked by T4 endonuclease V after correcting for adventitious nicking and the presence of SV40 Form II and Form III molecules. Linear regression analysis yielded a smooth line through the experimental data with a slope of 0.049 endonuclease-sensitive sites per SV40 genome per J/m^2 and a correlation coefficient of 0.936.



endonuclease V-sensitive sites per SV40 DNA molecule as a function of culture incubation time after UV-irradiation. Figure (25) summarizes these changes for 6.3, 12.5, 25, 31.3, and 37.5 J/m² of UV light. The number of endonuclease sites decreases in the 24 hours after UV-irradiation at a rate dependent on the UV dose used. At low doses, T4 endonuclease V-sensitive sites are removed essentially at a constant rate and to a lesser extent than at higher doses. There is a clear biphasic response at the extensively studied dose of 25 J/m² as well as at the higher dose of 37.5 J/m². The removal of T4 endonuclease V-sensitive sites at these doses is characterized by a fast initial removal of T4 endonuclease V-sensitive sites for the first 6-8 hours after exposure to UV light and a subsequent slow removal of remaining T4 endonuclease V-sensitive sites. This type of response suggests endonucleolytic cleavage may be rate-limited; that is, removal of UV light-induced endonuclease-sensitive sites at UV doses above 25 J/m² for SV40 infected CV-1 cultures may proceed unchecked until some type of feedback mechanism inhibits the efficiency of UV induced endonuclease-sensitive sites disappearance.

The removal of T4 endonuclease V-sensitive sites from Form I molecules with post-UV incubation is not synonymous with repair unless the Form I conformation is eventually restored during repair. If Form I molecules containing

Figure (25). Mean number of T4 endonuclease V-sensitive sites per SV40 genome at various times after UV-irradiation of SV40-infected CV-1 cultures. Corrected mean values were calculated as described in the legend for Figure (24). Experiments were conducted on cultures exposed to 6.3 J/m^2 (○---○), 12.5 J/m^2 (■---■), 25 J/m^2 (●---●), 31.3 J/m^2 (□---□), and 37.5 J/m^2 (△---△). Curves were fitted through average values at a single time point for a given UV fluence.



the bulk of T4 endonuclease V affinity sites are degraded or remain Form II molecules after enzymatic incision, then observations of a decrease in the mean number of T4 endonuclease V sites in Form I molecules are misleading. This alternative hypothesis was tested by examining the total radioactivity and the percent of Form I and Form II molecules in agarose tube gel profiles for SV40 DNA samples isolated from UV-irradiated cultures incubated for various lengths of time after irradiation. There was no trend towards lower total radioactivity with incubation time, suggesting SV40 DNA is not appreciably degraded after UV-irradiation. In addition, the percent of Form I molecules remained relatively constant and there was no buildup of Form II molecules. There was a minor increase in label in Form III (linear) molecules, but this has been attributed to host cell DNA of SV40 genome size that will be packaged in pseudovirions (67,155). The significance of these observations is that a decrease in T4 endonuclease V-sensitive sites confirms that three stages of excision repair (endonucleolytic cleavage, base removal, and ligation) definitely occur on SV40 DNA. Only base insertion has not been demonstrated by this technique.

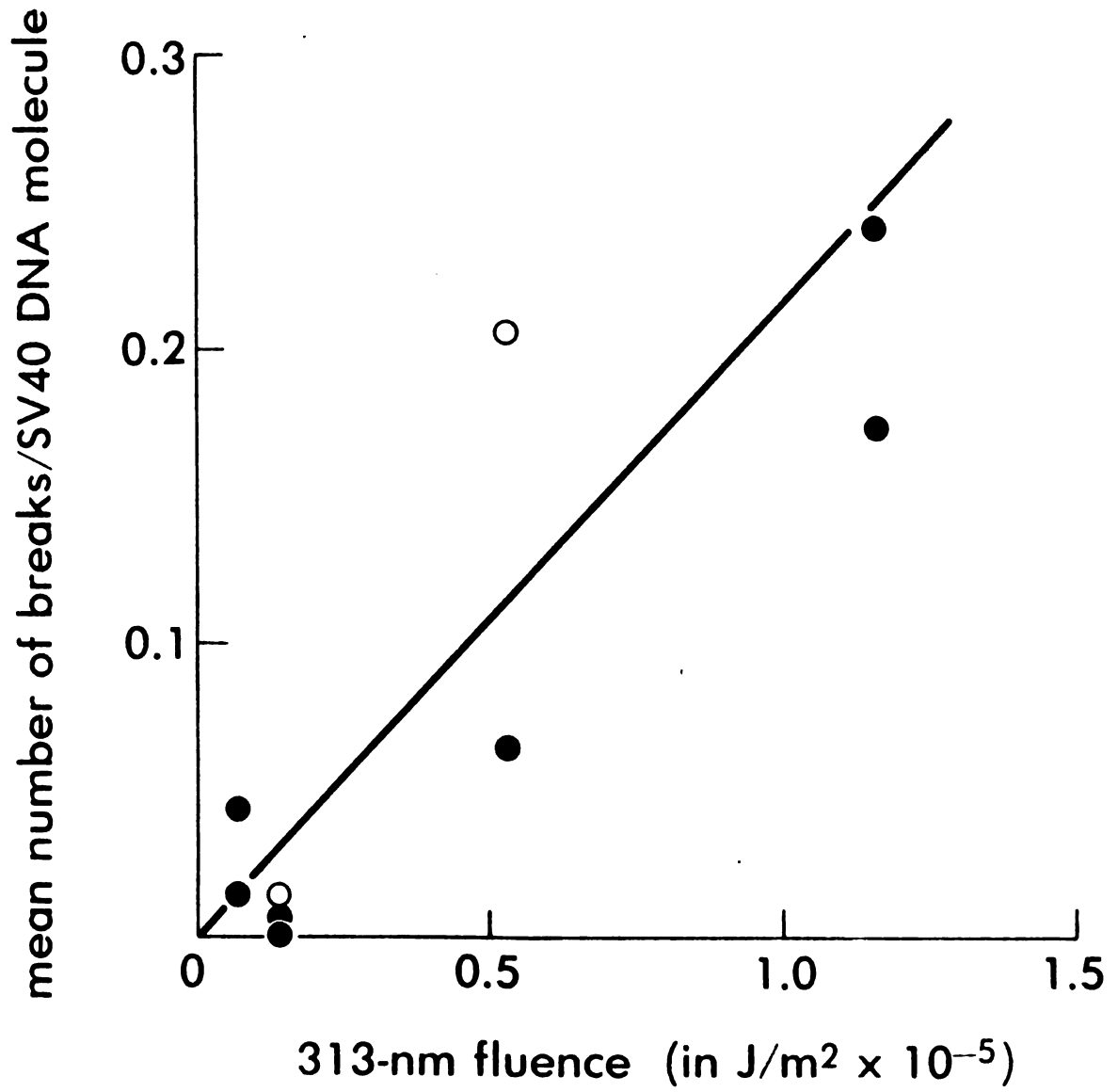
Standard methods of measuring repair replication (21) do not work with SV40 DNA since an infected culture yields less than one CV-1 cell genome equivalent of SV40 DNA. Two

modified approaches were investigated as suggested by the results of J. D. Regan et al (115) and A. R. Lehmann (112).

The BrdUrd photolysis technique measures strand scission of the DNA phosphodiester backbone induced by 313 nm light. This occurs preferentially at sites where BrdUrd has been incorporated as a base residue in place of thymidine (149). The rate at which SV40 DNA molecules were broken by 313 nm light after extraction from CV-1 cultures incubated with 10^{-4} M BrdUrd following UV-irradiation was expected to be significantly greater than the break rate for cultures incubated with 10^{-4} M dThd (Appendix E). However, there was no enhancement of strand breakage for SV40 DNA incubated in the presence of 10^{-4} M BrdUrd. Figure (26) shows SV40 DNA incubated in the dark with 10^{-4} M dThd or 10^{-4} M BrdUrd was broken by 313 nm light with an efficiency of 6.2×10^{-13} breaks/J/m²/dalton. This value was not changed by prior exposure of the SV40 DNA to UV light.

Prelabelling of SV40 DNA molecules with ¹⁴C-dThd as a measure of SV40 DNA content was studied as a second method in repair replication experiments. UV-irradiated cultures were infected with SV40 incubated with ³H-dThd (10 µCi/ml, 11 Ci/mmol) plus 3×10^{-3} M hydroxyurea and 2×10^{-6} M FdUrd for two hours before the SV40 DNA was isolated and analyzed on 5-20% alkaline sucrose gradients with or without prior purification on 5-20% neutral sucrose. Figure (27)

Figure (26). Mean number of breaks per SV40 genome as a function of 313 nm light fluence for SV40 DNA isolated from cultures exposed to 0-70 J/m² of UV light and incubated 7 or 29 hours in mEm supplemented with 10⁻⁴ M dThd (◉) or 10⁻⁴ M BrdUrd (●). The experimental line was fitted by eye. Linear regression analysis of these data points gives a slope of 6.2 x 10⁻³ breaks per J/m² per dalton. There is no discernible correlation between UV dose and number of 313 nm light-induced strand breaks.



shows $^3\text{H}/^{14}\text{C}$ ratios for SV40 Form I DNA as a function of UV dose. There is detectable repair synthesis, but there is also considerable scatter to the data. The scatter is related to the large amount of ^{14}C spillover into the ^3H spectrometer channel; in all experiments, the actual ^3H counts were significantly less than the spurious counts produced in the same channel by ^{14}C decays. Repair replication saturates at about 15 J/m^2 in Figure (27), a fluence that produces about 0.75 dimers per SV40 genome (Figure (24)).

A related attempt to detect repair synthesis in SV40 DNA was made with the protocol used for observing repair replication in CV-1 DNA with three minor modifications: (1) Incubation with ^3H -BrdUrd (25 $\mu\text{Ci/ml}$, 2.3 Ci/mmol) was for four hours; (2) UV-irradiated SV40 DNA that had been prelabelled with ^{14}C -dThd (0.1 $\mu\text{Ci/ml}$, 57 mCi/mmol) was isolated three days after infection by the Hirt extraction procedure and analyzed after extensive dialysis by alkaline CsCl-CsSO_4 isopycnic centrifugation without deproteinization, and (3) the corrected $^3\text{H}/^{14}\text{C}$ ratios (see Appendix A) at the density of light-light DNA was calculated as a measure of base insertion during repair in damaged SV40 DNA molecules. Figure (28) shows the $^3\text{H}/^{14}\text{C}$ count ratio in light-light SV40 DNA for UV doses in the range $0\text{-}37.5 \text{ J/m}^2$. Each data point represents two or three pooled

Figure (27). Repair replication in SV40 DNA after various UV fluences. Cultures pre-labelled with ^{14}C -dThd (0.01-0.20 $\mu\text{Ci/ml}$, 57 mCi/mmole) were exposed to UV light and incubated in the presence of 3×10^{-3} M hydroxyurea with mEm containing ^3H -dThd (10 $\mu\text{Ci/ml}$, 11 Ci/mmole) before SV40 DNA was isolated and $^3\text{H}/^{14}\text{C}$ ratios determined for SV40 Form I DNA molecules by alkaline sucrose isokinetic sedimentation. Data points were corrected for differing initial ^{14}C -concentrations by multiplying all data by the $\mu\text{Ci/ml}$ of ^{14}C -dThd in the prelabelling medium. Data points were also corrected for residual semi-conservative DNA synthesis using Figure (29). A smooth curve was fitted to the data by eye.

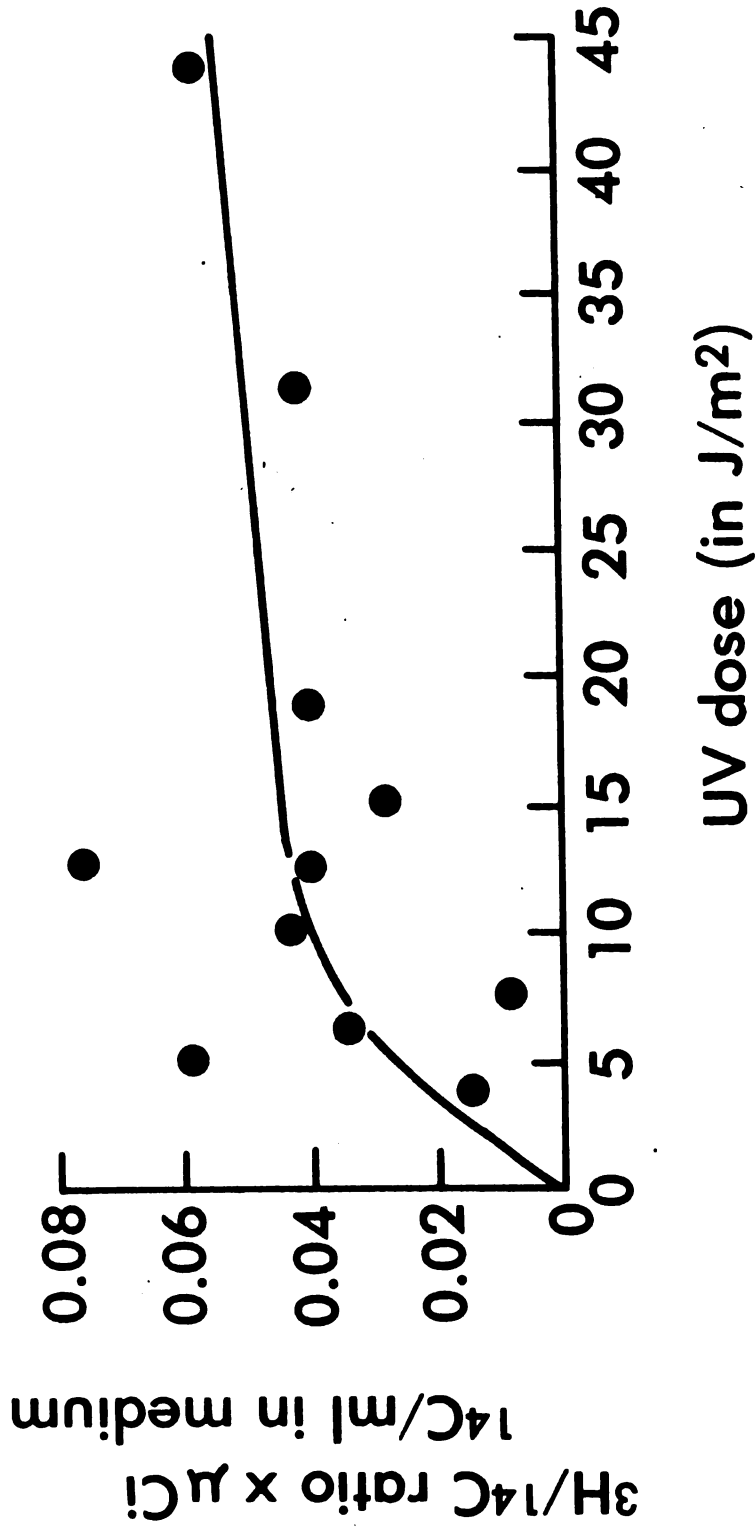
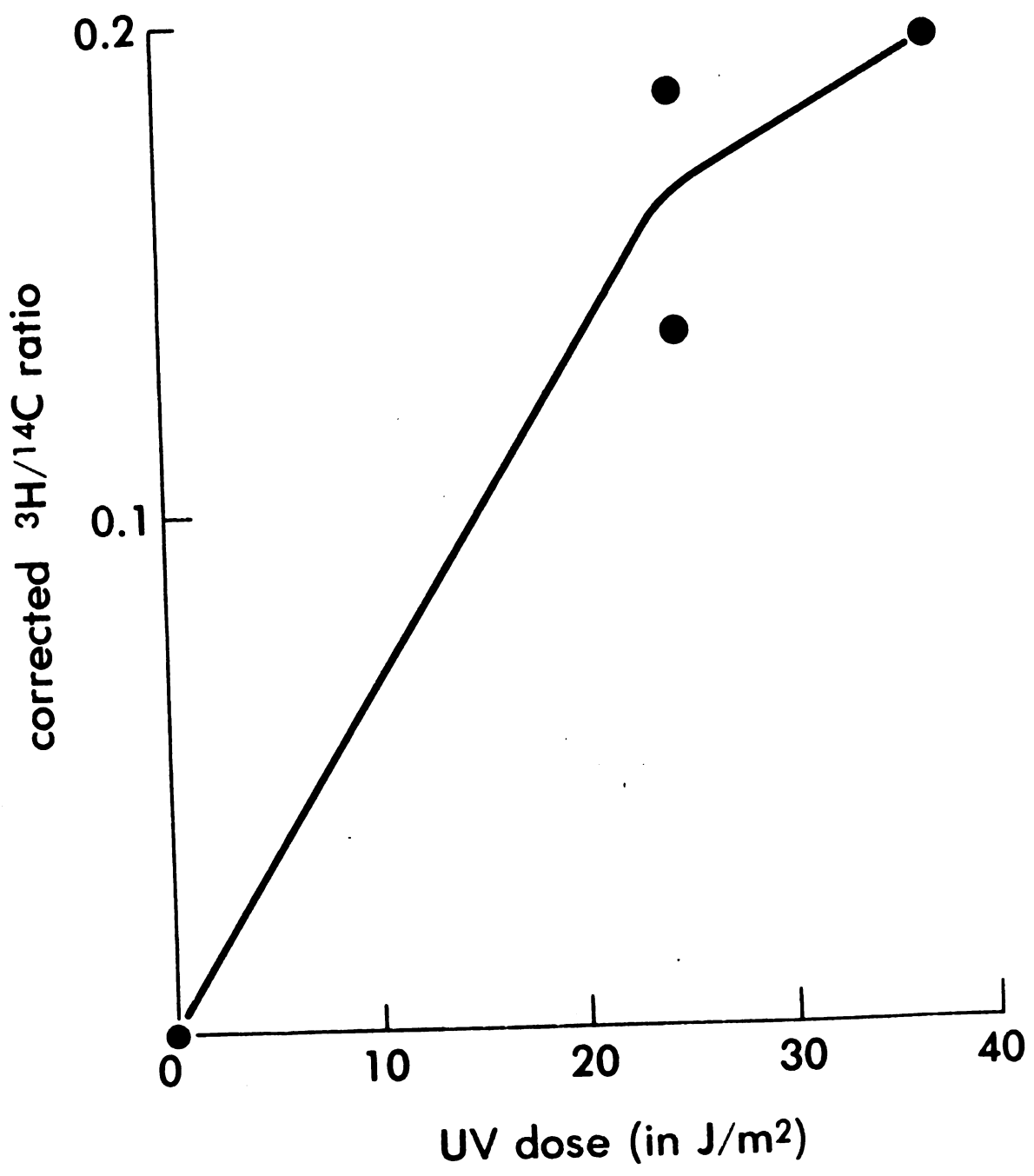


Figure (28). Repair replication in SV40 DNA measured by isopycnic centrifugation. SV40-infected CV-1 cultures prelabelled with ^{14}C -dThd (0.1 $\mu\text{Ci/ml}$, 57 mCi/mmole) were exposed to various UV fluences before being labelled with ^3H -dThd (20 $\mu\text{Ci/ml}$, 11 Ci/mmole) plus 10^{-5} M BrdUrd. The $^3\text{H}/^{14}\text{C}$ radioactivity ratio was determined for Hirt supernatant DNA at the density of light-light DNA in alkaline CsCl-CsSO_4 isopycnic gradients. Data points are corrected for light-light DNA labelled with tritium during semi-conservative DNA synthesis at the ends of replicons; correction factors were inferred from Figure (29).

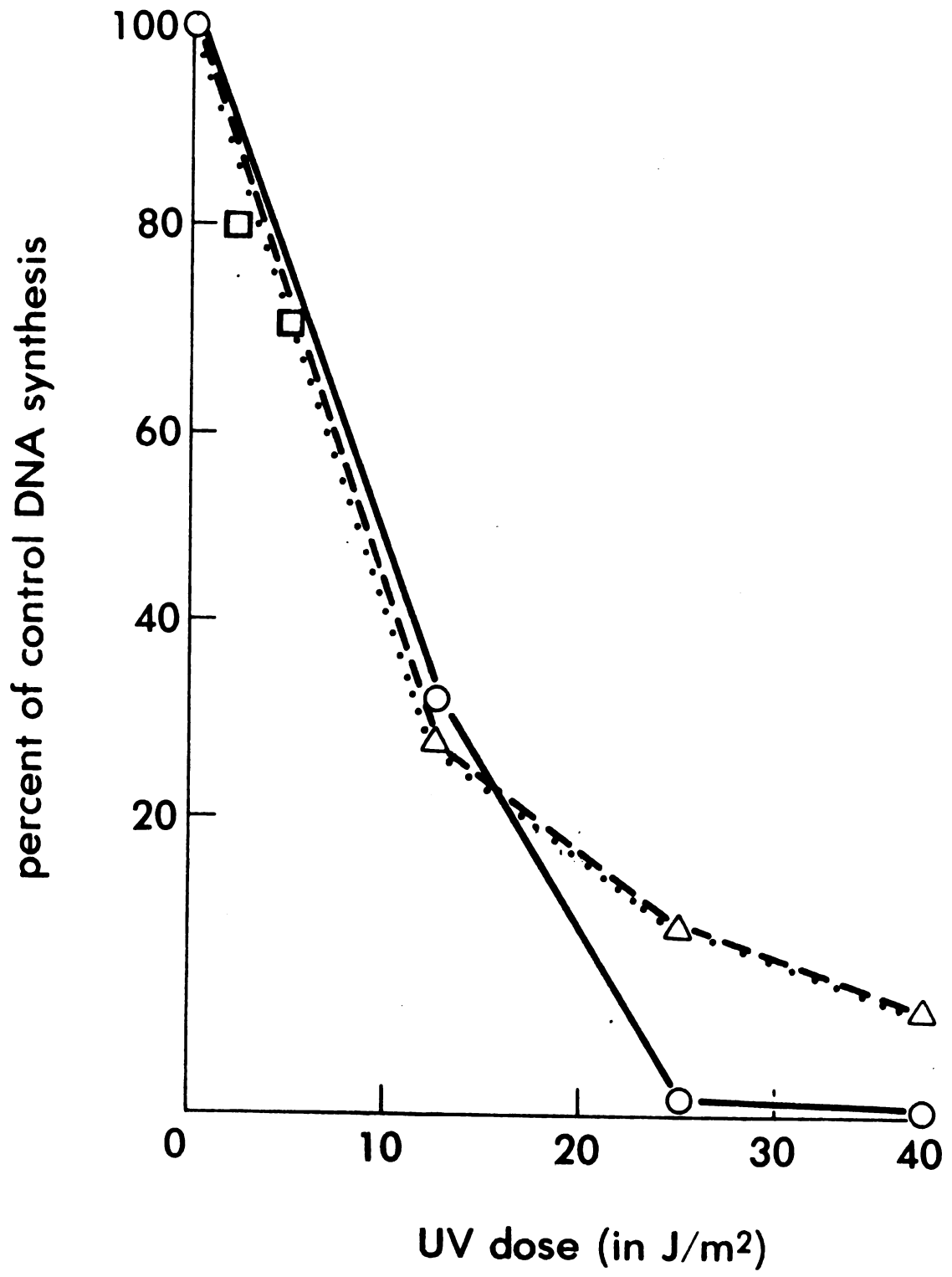


cultures. There is a great deal in common between these data points and those in Figure (28), but the low $^3\text{H}/^{14}\text{C}$ ratios force caution in interpreting these results. It is clear, however, that there are similarities between repair replication in SV40 DNA and CV-1 DNA. This is evident when Figures (27) and (28) are compared to Figure (17).

5. CV-1 DNA Synthesis UV-Irradiated Cultures

DNA synthesis in UV-irradiated mammalian cell cultures is suppressed in a dose-dependent fashion and recovers at later times in surviving cells (150). CV-1 DNA synthesis in uninfected cultures was examined by pulse-labelling 0, 24, or 72 hours after UV-irradiation. Figure (29) shows the percent of ^3H and ^{14}C counts from light-heavy DNA density band of alkaline $\text{CsCl}-\text{CsSO}_4$ isopycnic gradients compared to control values and corrected with total A_{260} values. These results for pulse-labelling immediately after UV-irradiation were obtained from the same isopycnic gradients used to study repair replication in CV-1 DNA. Although the presence of hydroxyurea complicates interpretation of this data since hydroxyurea suppresses DNA replication in a complex fashion (151), there is a clear pattern of inhibition of CV-1 DNA synthesis from both purine and pyrimidine precursors with increasing exposures of UV light. The data in Figure (29) for SV40 DNA synthesis suggests synthesis of SV40 DNA and CV-1 DNA is probably suppressed with UV light

Figure (29). Rate of CV-1 DNA synthesis after various UV fluences in the presence of 2×10^{-3} M hydroxyurea. Data points represent the ratio of specific activities for ^{14}C -labelled (Δ) or ^3H -labelled (\bullet) hybrid DNA (cf. Figures (17), (18), and (22)) exposed to various UV fluences relative to hybrid DNA in unirradiated controls. Two values measuring SV40 DNA replication after UV-irradiation of infected cultures and in the absence of hydroxyurea are included for comparison (\square).



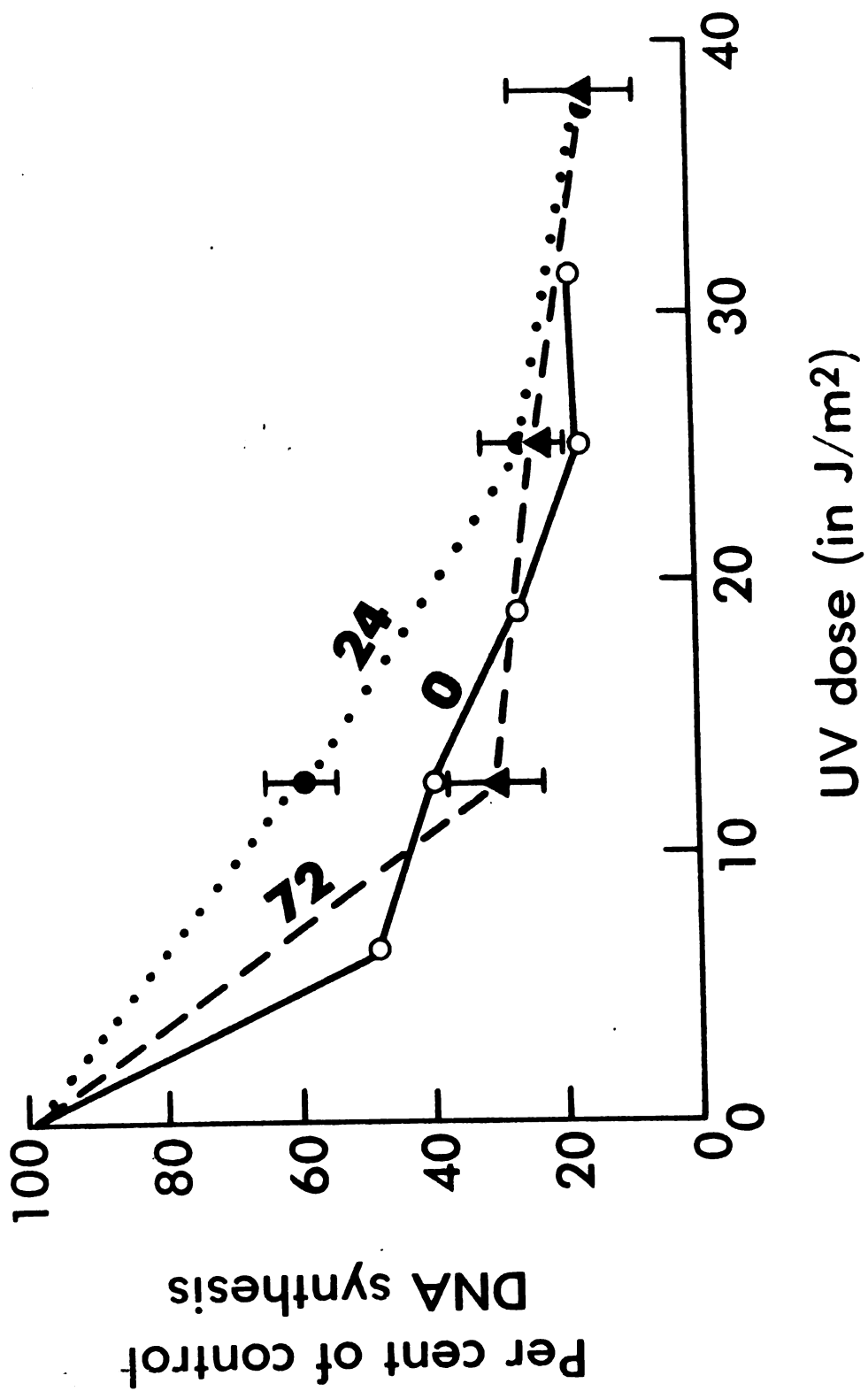
by a similar mechanism.

For comparison, DNA synthesis was measured in CV-1 cultures 24 or 72 hours after UV-irradiation. Figure (30) shows the percent of acid-insoluble radioactive counts in UV-irradiated cultures compared to the acid-insoluble radioactive counts in unirradiated cultures 0, 24, or 72 hours after UV-irradiation. The extent of DNA synthesis is very similar to that shown in Figure (29), but DNA synthesis one or three days after UV irradiation is only carried out by a small percentage of the original cells since most cells are dead or dying (150). Therefore, the DNA synthesis per competent CV-1 cell at a given UV fluence is higher one or three days after UV-irradiation than immediately after UV-irradiation.

6. SV40 DNA Synthesis in SV40-Infected CV-1 Cultures After Exposure to UV Light

Semi-conservative DNA replication in UV-irradiated mammalian cells is considered to be blocked or retarded at UV photoproducts (116,119,125). Pulse-labelling experiments in SV40-infected cells were undertaken to shed further light on the interaction of UV light and semi-conservative DNA synthesis. SV40-infected cells were prelabelled with ^{14}C -dThd (0.1 $\mu\text{Ci/ml}$, 57 mCi/mmol), irradiated with 20 or 40 J/m^2 of UV light, and pulse-labelled 20 minutes with ^3H -dThd (20 $\mu\text{Ci/ml}$, 11 Ci/mmol) before the medium was changed to unlabelled medium and incubation continued for

Figure (30). CV-1 DNA synthesis in UV-irradiated cultures 0 hours (○—○—○), 24 hours (●.....●.....●), or 72 hours (▲---▲---▲) after exposure to UV light. Error bars indicate ranges of DNA synthesis observed in replicate cultures. Hydroxyurea was not present during these experiments.

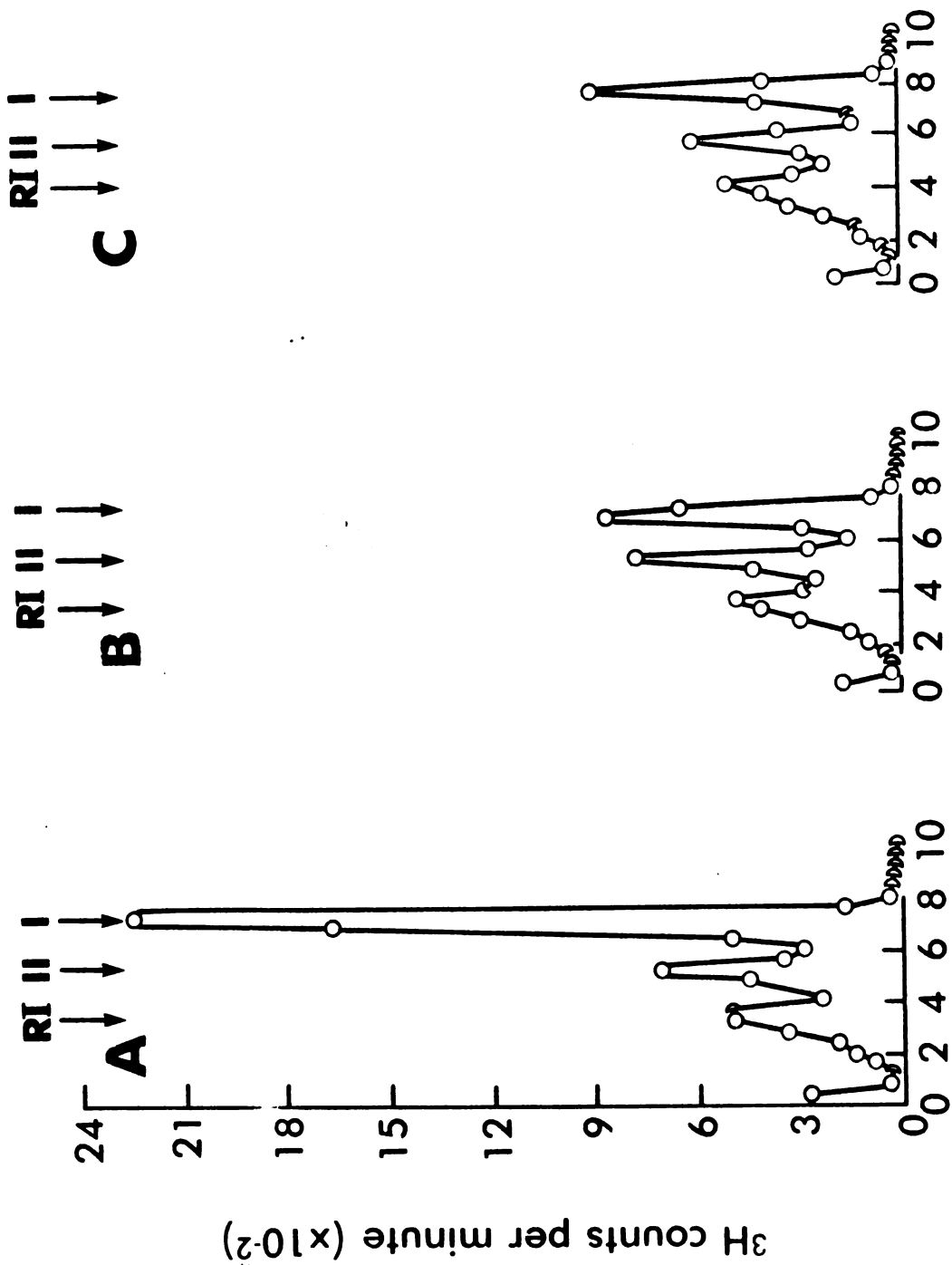


0, 60 or 180 minutes. These UV fluences were chosen to yield an average of 1.0 or 2.0 dimers per SV40 genome (see Figures (21) and (24)).

It was found that the average increase in the $^3\text{H}/^{14}\text{C}$ ratio summed over an entire gel was only 8% after 60 minutes of "chase" and 0% after 180 minutes of "chase." It is apparent that the use of unlabelled 5×10^{-5} M dThd and 5×10^{-5} M dCyd in the "chase" medium efficiently terminated incorporation of ^3H -dThd into SV40 DNA daughter strands. The position of Form I and Form II molecules and replicative intermediates was identified by comparison of agarose tube gel profiles with and without a post-UV "chase" and agrees well with previously reported profiles (77,89). The profiles show the order of increasing electrophoretic mobility is replicative intermediate \leq Form II < Form I with a broad distribution of mobilities for replicative intermediates.

Typical ^3H radioactivity profiles of pulse-labelled SV40 DNA in agarose tube gels are shown in Figures (31a-c) for several UV fluences. There was an increase in the relative proportion of Form II and replicative intermediate molecules (RIs) and a large decrease in Form I molecules, implying UV light interferes with elongation and not initiation of SV40 DNA replication. The net depression of label uptake under these conditions was to 60% of control

Figures (31a-c). Tritium radioactivity profiles for pulse-labelled SV40 DNA analyzed on 1.0% agarose tube gels by electrophoresis. Pulse and pulse-"chase" experiments (not shown) were used to identify the order of increasing electrophoretic mobility in various SV40 DNA molecules. Electrophoresis was from left to right. Analyzed SV40 DNA had received (a) 0 J/m^2 , (b) 20 J/m^2 , and (c) 40 J/m^2 of UV light prior to isolation from infected CV-1 cultures.

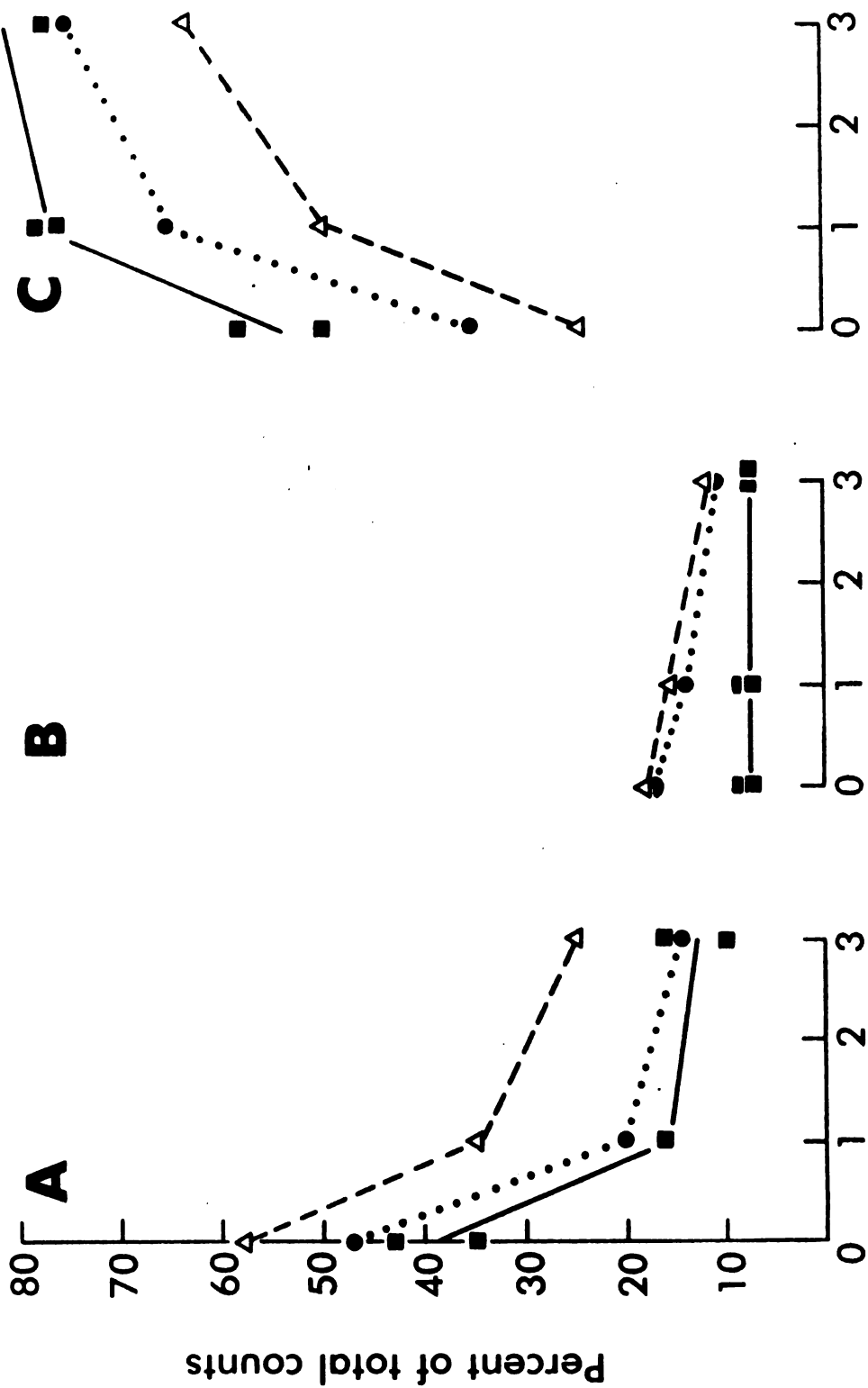


Cm. into 1.0% agarose gel

at 20 J/m^2 and to 44% of control at 40 J/m^2 . These values are higher than usually seen in mammalian cell cultures at these fluences (150, this thesis) and, among other factors, reflect the small replicon size of SV40 DNA. When UV-irradiated cultures that have been pulse-labelled with ^3H are "chased" for 60 or 180 minutes, the relative number of SV40 RIs and Form II molecules decreases and the number of Form I SV40 DNA molecules increases. This shift in number of DNA molecules is summarized in Figures (32a-c). The initial rate of increase in Form I molecules at 20 or 40 J/m^2 of UV light is similar to that seen in unirradiated cultures. The rate of decrease in Form II and replicative intermediate molecules similarly resembles that seen in the unirradiated cultures, although the rate of decrease in replicative intermediate molecules is not as great after 40 J/m^2 of UV light as after 0 or 20 J/m^2 of UV light. This implies that the UV light photoproducts responsible for interruption of semi-conservative DNA synthesis in SV40 DNA molecules are not absolute blocks to further DNA replication. The apparent delay in reaching the same percent of labelled SV40 Form I DNA molecules is about 30 minutes at 20 J/m^2 and 60 minutes at 40 J/m^2 . The importance of these delays is discussed later.

Bidirectional DNA replication of the SV40 genome allows completion of daughter strands at a new termination site if

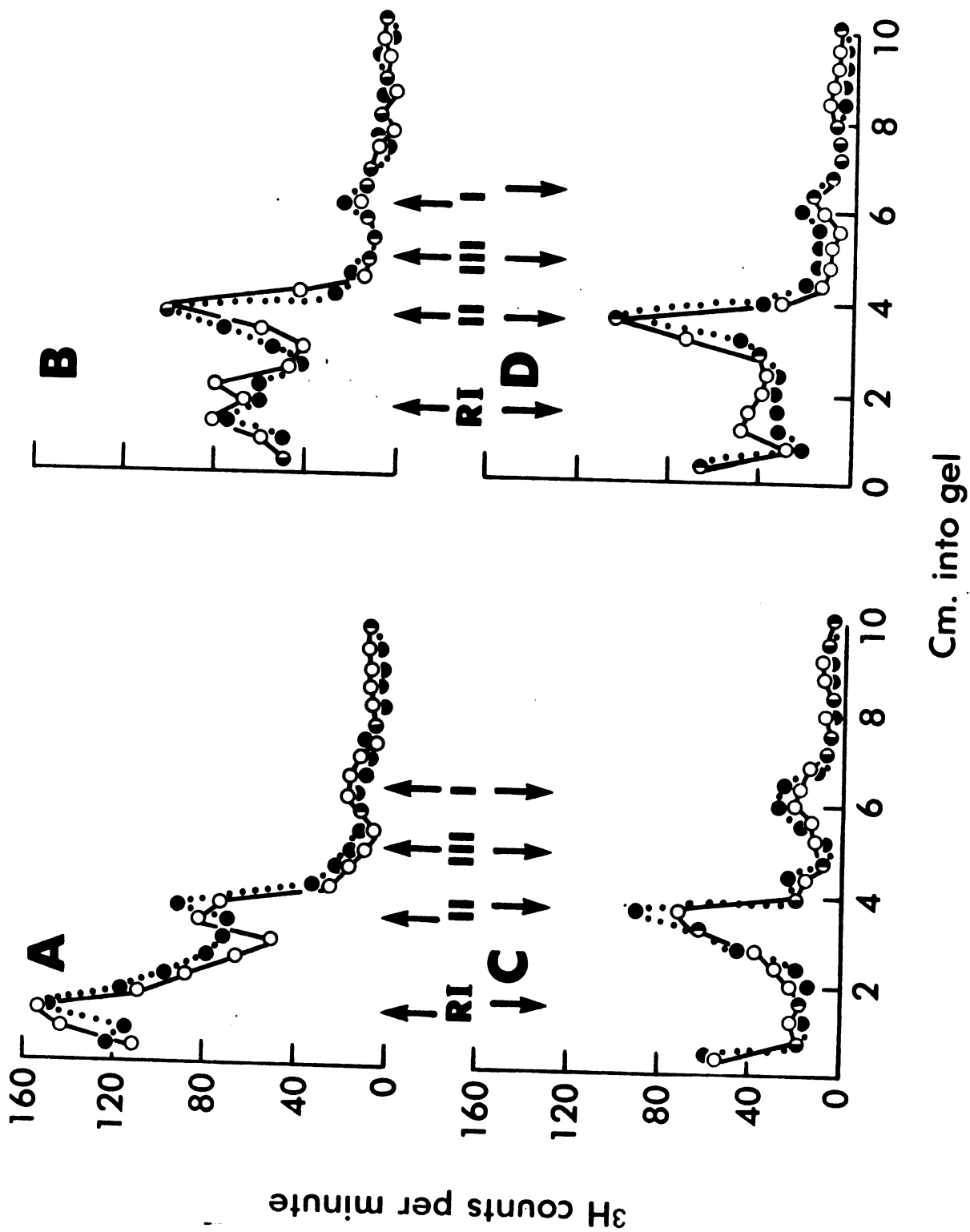
Figures (32a-c). Percent total tritium counts in (a) SV40 replicative intermediates (RI), (b) Form II SV40 DNA molecules, and (c) Form I SV40 DNA molecules after 0 J/m² (■—■—■), 20 J/m² (●.....●.....●), and 40 J/m² (△---△---△) and 0-3 hours of incubation in unlabelled mEm following 20 minutes of post-UV labelling with ³H-dThd (20 μCi/ml, 11 Ci/mmole). Each data point is the mean value taken from three replicate cultures.



Hours of post-labelling "chase"

replication is one arm of a replicating SV40 molecule is blocked or retarded since there is no specific termination site in the SV40 genome (74). This may explain how a replicating SV40 molecule appears to by-pass UV-induced photoproducts. An SV40 DNA molecule which completes DNA synthesis at a new termination site by this mode of replication will have a gap in one daughter DNA strand with a UV-photoproduct opposite the gap in the parent DNA strand. This prediction was tested by isolating pulse-labelled SV40 DNA Form II molecules from the top DNA band in a CsCl-EtBr isopycnic gradient and treating them with T4 endonuclease V after extensive dialysis. This enzyme treatment should convert SV40 Form II to Form III (linear) DNA molecules if the enzyme is active on pyrimidine dimers in single-stranded DNA and there are dimers opposite a gap in the daughter strand. Enzyme-treated SV40 DNA molecules were analyzed on 1.5% agarose tube gels by electrophoresis and evidence was sought for the appearance of Form III molecules. Figures (33a-d) show the tritium radioactivity profiles of pulse-labelled Form II molecules exposed at 0 or 40 J/m² of UV light, incubated in unlabelled medium for 0 or 60 minutes, and then treated 60 minutes with or without T4 endonuclease V. The electrophoretic position of Form III molecules was verified using Form I molecules cleaved by the EcoRI restriction enzyme to linear molecules.

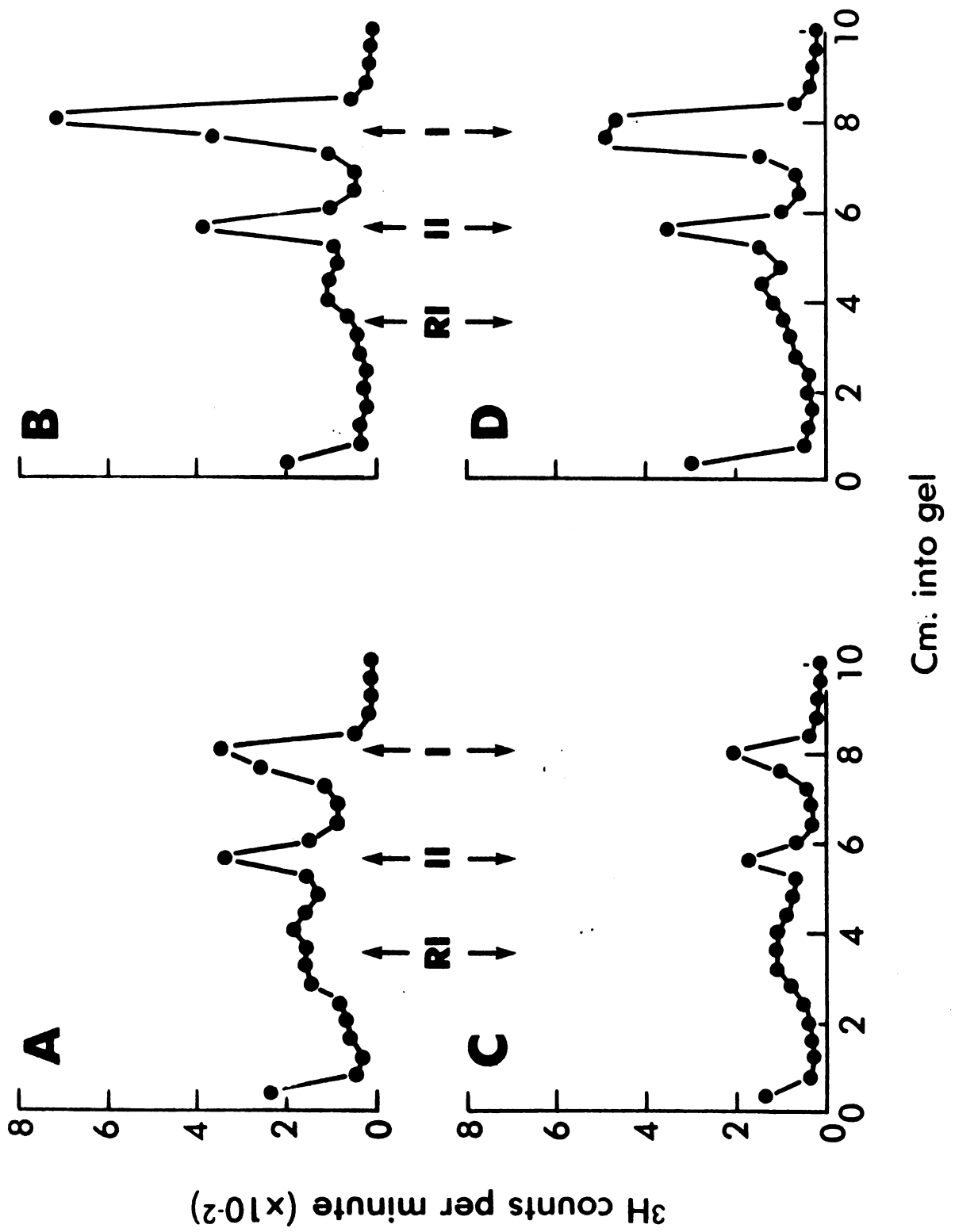
Figures (33a-d). Tritium radioactivity profiles for non-supercoiled SV40 DNA isolated on CsCl-PI₂ isopycnic gradients. SV40 DNA was isolated from infected CV-1 cultures exposed to 0 J/m²(a,c) or 40 J/m²(b,d) of UV light, pulse-labelled 20 minutes with ³H-dThd(10 μCi/ml, 11 Ci/mmole), and either extracted immediately (a,b) or incubated 60 minutes in unlabelled medium before extraction (c,d). Isolated DNA was treated one hour with T4 buffer (○—○—○) or an excess of T4 endonuclease V (●.....●.....●) before analysis on 1.5% agarose tube gels by electrophoresis. Positions of RI, Form I and Form II molecules was determined by pulse and pulse-"chase" experiments (not shown). Electrophoresis was from left to right.



There are substantial amounts of replicative intermediate molecules in these DNA samples at the top of these gels which also served as T4 endonuclease V substrates. There is little or no change in the radioactivity profiles and no buildup of Form III (linear) DNA molecules during the 60 minutes after pulse-labelling. This means either that there are no molecules with gaps in the daughter strand opposite pyrimidine dimers or that T4 endonuclease V is not active on these substrates.

Another hypothesis that might explain the rapid completion of DNA replication in UV-irradiated SV40 DNA molecules is that UV-incuded DNA damage sites are quickly removed in replicating DNA in comparison to lesions in non-replicating DNA. This idea was tested by pulse-labelling SV40-infected CV-1 cultures 20 minutes after UV-irradiation rather than immediately after UV-irradiation and then incubating in nonradioactive medium for 0 or 60 minutes before isolating SV40 DNA. Radioactivity under these conditions primarily enters SV40 DNA molecules which were not replicating at the time of UV-irradiation since the mean replication time for an SV40 DNA molecule is 10-15 minutes (77). Figures (34a-d) show radioactivity profiles for SV40 DNA molecules given 20 J/m^2 of UV light, "chased" for 0 or 60 minutes, and pulse-labelled 0 or 20 minutes after UV irradiation. The apparent rate of decline in Form II and replicative

Figures (34a-d). Tritium radioactivity profiles for SV40 DNA analyzed on 1.0% agarose tube gels by electrophoresis. SV40 DNA in infected CV-1 cultures was exposed to 20 J/m^2 of UV light, pulse-labelled with $^3\text{H-dThd}$ ($20 \text{ }\mu\text{Ci/ml}$, 11 Ci/mmole) for 20 minutes beginning either 0 (a,b) or 20 (c,d) minutes after UV-irradiation, and extracted immediately (a,c) or incubated 60 minutes in unlabelled medium before extraction (b,d). Electrophoresis was from left to right.



intermediate SV40 DNA molecules is the same regardless of whether or not the SV40 DNA population being followed by pulse-labelling was replicating at the time of exposure to UV light. This suggests that either there is no preferential removal of UV-induced DNA lesions from replicating SV40 DNA compared to all non-replicating SV40 DNA molecules or, more specifically, there is no preferential removal of UV-induced lesions from replicating SV40 DNA compared to non-replicating DNA which begins a replication round very soon after exposure to UV light.

IV. DISCUSSION

1. Excision Repair of CV-1 DNA

CV-1 monkey cells efficiently remove and repair UV-induced lesions in DNA. They lose UV-endonuclease-sensitive sites rapidly after UV fluences of 0-25 J/m² (Figure (15)), perform more than 65% of their total repair replication in the first six hours following exposure to 25 J/m² (Figure (18)), and actively remove dimers after UV fluences of 50-75 J/m² (Table (2)) while the percent of surviving and reproductively active cells has dropped to much less than 0.01% (Figure (4)). They also maintain complete viability with more than 10⁵ UV lesions per cell (based on Figure (4)). To gain perspective on these numbers, these values must be compared with data in the available literature for other mammalian cells.

Several reports have made use of either the T4 phage or the M. luteus UV-endonuclease in quantifying the number of UV-induced and endonuclease-sensitive sites in mammalian DNA per unit fluence. The values found with the T4 phage enzyme were 0.33-0.93 sites per 10⁸ daltons of DNA per J/m² in WI38 and HeLa cells (124), 0.70-1.14 in mitochondrial DNA from a variety of mammalian cells (156), 1.42 in monkey CV-1 cells (this thesis), and 1.36 in SV40 DNA from SV40-infected CV-1 cells (this thesis). Similarly, the use of the M. luteus enzyme yielded values of 1.0 sites per 10⁸ daltons of DNA per J/m² in human diploid fibroblasts (157), 0.74-0.82 in CHO cells (116), 2.5 in human and XP primary fibroblasts (107), and 0.4 (low salt assay) or 0.7 (high salt assay) in WI38 human fibroblasts (108).

The number of dimers expected in a DNA double helix of this size per J/m^2 can be calculated from chromatographic data (21) to be about 2.4, so the number of endonuclease-sensitive sites detected in most of these studies is only about one-half the actual number of pyrimidine dimers. There is evidence that the number of endonuclease-sensitive sites is equal to the number of pyrimidine dimers for carefully purified enzyme preparations (107, 158) and it is not clear why the majority of studies fail to detect a significant fraction of pyrimidine dimers. The fact that no report of the number of UV-endonuclease sites exceeds the number of pyrimidine dimers suggests that technical problems are at fault. The T4 phage UV-endonuclease preparation used in this thesis was not purified, but adequate results were obtained with a discrepancy of less than 10% between the number of UV-endonuclease sites and the number of pyrimidine dimers in CV-1 DNA.

UV-endonuclease sites disappear relatively rapidly from CV-1 DNA at fluences below $25 J/m^2$ (Figure (15)). The extent of T4 UV-endonuclease site loss in CV-1 DNA after 24 hours is dose-dependent: 90% at $12.5 J/m^2$, 50% at $25 J/m^2$, and 42% at $37.5 J/m^2$ of UV light. These figures are indicative of an efficient UV-endonucleolytic step in excision repair of CV-1 DNA.

There is an apparent inhibition of UV-endonuclease site loss at $37.5 J/m^2$ (Figure (15)) that may be real or may be related to the small number of experimental observations at this level of UV light exposure. Experiments with UV-endonucleases become prohibitive at similar doses of UV light since the molecular weight changes with enzyme treatment

become so large at these doses that assay on alkaline sucrose gradients becomes questionable (e.g., see Figure (1), ref. (116)). The extent of UV-endonuclease site loss at 37.5 J/m^2 agrees well with the extent of site lost at 25 J/m^2 (Figure (15)), suggesting that there is no inhibition unless the excision repair system compensates by operating at a faster rate at the higher dose once the inhibition is released. This seems unlikely as does direct inactivation of the enzymes involved. The linear rate of dimer removal at 37.5 J/m^2 (Table (2)) would be impossible without an active UV-endonuclease, adding further weight to the argument against inhibition.

Repair replication also occurs rapidly in CV-1 cells. Repair replication saturates at a UV fluence of $25\text{-}35 \text{ J/m}^2$ (Figure (17)), or $1.2\text{-}1.7 \times 10^6$ dimers per cell (Figure (21)) assuming a cell diploid DNA complement of 6 pgms.(159). This suggests that the excision repair enzymes in monkey cells are present in large number or operate very rapidly. The second possibility seems favored since repair replication takes hours to complete, but more than 65% of all repair replication after 25 J/m^2 is complete within six hours of UV-irradiation (Figure (18)). Only bovine fibroblasts have been reported to perform repair replication more rapidly (21, 138).

The patch size inserted during repair replication can be estimated from Figures (17) and (18) of this thesis, Table 2, and references (160) and (161). The percent of thymidine bases removed in 20 hours after 25 J/m^2 of UV light is 0.028%. Repair replication during the first three hours after UV-irradiation is about one-third of the total repair replication during the first 20 hours and about 0.04% of all thymidine

bases are substituted during the first three hours of excision repair.

The number of thymidine bases per repair patch is thus

$$\frac{3 (0.04\%)}{\frac{1}{2} (0.028\%)} = 9 \text{ thymidine bases or}$$

about $9/0.3 = 30$ bases altogether. This agrees with the range of 35-200 bases found in other mammalian cells (21).

There have been only a few reports of experiments that attempted to detect strand breaks and closure of such breaks during excision repair (160, 162, 163, 164). These results are regarded with caution for two reasons: (1) they give contradictory and surprising results for XP fibroblasts (160, 162), and (2) these studies have used alkaline sucrose velocity gradients under conditions where many anomalies may occur such as speed dependence of sedimentation (165) and the presence of DNA in double-stranded conformation (166). The number of strand breaks at any one time is low in comparison to the number of UV-induced lesions (162, 163) and it seems likely that only new techniques (164, 167) will provide further insight into the initial and final stages of excision repair.

The only remaining stage in excision repair that can be monitored is the actual removal of damaged bases. In most mammalian cells, this process occurs at an essentially constant rate ((21), this thesis). It is curious that the extent of dimer removal is generally lower than the extent of UV-endonuclease-sensitive site loss and base insertion. There may be a cell line dependence to explain this discrepancy, but the results of this thesis favor alternative hypotheses. A "patch-

and-cut" mechanism is the most obvious explanation, but other explanations mentioned in the Introduction of this thesis cannot be ruled out.

There are three distinct advantages in studying excision repair with CV-1 cells: (1) their excision repair system is efficient and operates up to $40\text{-}50 \text{ J/m}^2$ (Table (2) and Figure (15)), (2) they offer a technical simplification for long-term repair studies since very few CV-1 cells lyse or become detached from a Petri plate substrate during the 24 hours following UV-irradiation, and (3) they serve as host cells for SV40 and thereby provide the options SV40 offers for DNA repair and mutation experiments. These reasons as well as the results discussed above should focus greater attention on these cells. It is worth noting that monkey cells may be of interest for radiobiological studies since they represent the closest analogue to human cells on an evolutionary scale and may avoid some of the problems encountered with cells from more distantly related animals such as rodents (168). As a final note, primary monkey cells may be an excellent experimental system for testing the aging-DNA repair hypothesis of Hart and Setlow (169) since the monkey's life span of 29 years (170) is close to the middle of animal ages considered by Hart and Setlow.

2. Excision Repair of SV40 DNA

The most sensitive excision repair assay that has been developed is enzymatic detection of UV-induced endonuclease-sensitive sites. This assay can detect as few as one UV-endonuclease-specific site per 10^8 daltons of DNA per J/m^2 (107, 157). Such sensitivity and

specificity for UV-induced lesions is necessary to monitor excision repair in the small SV40 genome. The UV-endonucleases from T4 phage and M. luteus are highly specific, although there is some question about how these endonucleases interact with chromatin or unusual substrate conformations (57, 124). When technical problems are minimized, the 1:1 recognition of UV-endonuclease sites;pyrimidine dimers in mammalian cell DNA can be achieved (107, 158).

The efficiency with which UV-irradiated Form I SV40 DNA molecules were converted to Form II molecules by T4 endonuclease V corresponded to 0.49 UV-endonuclease-sensitive sites per SV40 genome per J/m^2 or 1.36 sites per 10^8 daltons of DNA. When compared to the number of UV-induced pyrimidine dimers per J/m^2 in CV-1 DNA, 1.30 dimers per 10^8 daltons of DNA, it is clear that T4 endonuclease V substrates are pyrimidine dimers in CV-1 DNA and SV40 DNA.

The rate and extent of T4 endonuclease V-sensitive site removal from SV40 DNA would be expected to mimic the extent of removal of these sites from CV-1 DNA if SV40 and CV-1 DNA are similarly accessible within the cell to excision repair enzymes. Using Figures (15) and (25), the number of sensitive sites removed in 24 hours per 10^8 daltons of DNA can be estimated as 7.8 (CV-1) and 10.0 (SV40) at $12.5 J/m^2$, 8.2 (CV-1) and 14.9 (SV40) at $25 J/m^2$, and 8.8 (CV-1) and 15.8 (SV40) at $37.5 J/m^2$ of UV light. These values agree within the range of data points used to estimate them except at $37.5 J/m^2$. It is likely that the CV-1 site value at this fluence is too low because T4 endonuclease V was not present in excess during analysis. The SV40 values indicate an increase in

the number of sites removed as a function of UV fluence that closely resembles the data of Figure (17) on repair replication in CV-1 DNA for the first three hours following UV-irradiation.

The removal of UV-endonuclease sites from SV40 is not simply related to the UV fluence (Figure (25)). Factors that tend to lower the number of sites removed include packaging of viral DNA for export and cell death due to either UV-irradiation or viral-induced lysis. These factors will be important at 6.3 and 12.5 J/m² where the viral infectious cycle is relatively unimpeded. The percentage of SV40 DNA molecules receiving one or more pyrimidine dimers does not exceed 46% at these fluences. This is the obvious explanation of a slower rate of UV-endonuclease site loss at the lower fluences. The infectious cycle is inhibited at the higher UV fluences (Clever, personal communication). This suggests the number of UV-endonuclease sites that are removed increases as the length of time SV40 DNA can be repaired by excision enzymes also increases.

Much of the viral DNA manufactured during the SV40 infectious cycle has begun to appear in the culture medium by four days post-infection (Figure (11)). This suggests that UV-induced lesions unrepaired during the first 24 hours after UV-irradiation may not be repaired at all. At UV fluences of 25 J/m² or greater, it can be calculated that more than half of the viral DNA molecules still carry at least one UV-endonuclease-sensitive site. Some of these molecules will certainly appear in non-infectious virions, but the shallow slope of the UV survival curve for direct irradiation of SV40

virions (50) allows us to estimate that many DNA molecules carrying UV-endonuclease-sensitive sites are still infectious. It is not clear how these molecules will replicate, but apparently they do so while bypassing the sensitive sites. This situation is analogous to that found in some rodent cells where low levels of excision repair still allow cells to survive UV-irradiation (34, 168). This phenomenon is equivalent to the dimer bypass events occurring during "post-replication repair"(35).

Base insertion in UV-irradiated SV40 DNA by excision repair enzymes can be detected with difficulty (Figures (27) and (28)). The data scatter directly resulted from ^{14}C spillover into the ^3H spectrometer channel. This unfortunate circumstance could not be avoided if the amount of SV40 DNA was to be estimated by prelabelling rather than by the A_{260} absorbance. It is clear that more reliable results will require an improved means of estimating the solution concentration of SV40 DNA.

In summary, SV40 DNA does undergo excision repair, but the small genome size of SV40 makes detection difficult. Based on the labor involved, there is no advantage per se in studying excision repair in SV40 DNA. However, the existence of SV40 replication mutants will allow the relation of excision repair to DNA replication and mutagenesis in mammalian cells to be profitably explored in the future using SV40 as an experimental probe.

3. DNA Synthesis in UV-irradiated CV-1 DNA

The sensitivity of ^3H -dThd label uptake in CV-1 cells following

UV-irradiation (Figure (29)) has been previously reported (e.g., 150). The sensitive depression at doses below 20 J/m^2 is due to inhibition of DNA elongation (35, 121). At higher doses, this inhibition is compensated for with continued initiation of DNA replication at previously quiescent origins and elongation up to or near the first UV photoproduct. The increase in the percentage of label uptake relative to controls in CV-1 cells 24 hours after UV-irradiation (Figure (30)) probably reflects a release of DNA synthesis from inhibition in conjunction with the cessation of metabolism in dying cells. The depression of label uptake three days after UV-irradiation is due to cell death. The extent of cell death at this time was assessed morphologically by noting that most cells had lysed or were floating in these cultures. If the percentage of label uptake was corrected for the percentage of reproductively surviving cells, the label uptake per surviving cell would exceed that seen in control cultures. This increase in DNA synthesis per surviving cell is not surprising since the surviving cells are no longer contact-inhibited and therefore can synthesize DNA at a higher rate than the maintenance rate found in contact-inhibited controls.

4. DNA Synthesis in UV-irradiated SV40 DNA

DNA synthesis shortly after UV light treatment of mammalian cells is depressed (150, this thesis). The extent of depression depends directly on the UV fluence, the time elapsed between UV-irradiation and pulse-labelling, and on the length of pulse-labelling. SV40 DNA synthesis as measured by ^3H -dThd pulse-labelling was depressed almost as much after 5 J/m^2 of UV light (measured by a two hour

$^3\text{H-dThd}$ pulse-label) as after 20 J/m^2 of UV light (measured by a 20 minute pulse-label). The generally accepted explanation of this phenomenon is that DNA elongation is preferentially inhibited in comparison to initiation of DNA synthesis and elongation is inhibited to a greater extent compared to controls for a given UV fluence as the pulse-labelling time is increased.

The time of replication of an SV40 DNA molecule was obtained from control pulse-labelling experiments for 5, 10, 15, and 20 minutes of $^3\text{H-dThd}$ pulse. The time of synthesis of an SV40 DNA molecule is the time necessary for the percent of counts in replicative intermediates to decrease to 50% of total counts (171). This was found to be 15-20 minutes, a value also observed by other investigators (77, 171, 172). This value is slightly higher than the actual value since label uptake is initially non-linear (171), but linear uptake was found in this thesis at 5 minutes of pulse label. The correction consequently must be less than 5 minutes and a corrected time of replication would be approximately 15 minutes. The minimum SV40 DNA fork movement rate can be calculated from this time of replication to be about $0.05 \mu\text{m}$ per minute. This value is lower than the rate of $0.5\text{-}2.0 \mu\text{m}$ per minute in most mammalian cell nuclear DNA (120) and close to the value of $0.006 \mu\text{m}$ per minute in mitochondrial DNA (120). The rate of fork movement in SV40 DNA is low enough to suggest there may be a uniqueness to replication of circular DNA molecules in a mammalian cell.

Some features of the technical approach used in the pulse-labelling experiments with UV-irradiated SV40 DNA must be mentioned

before the results are discussed more fully. Pulse-labelling protocols with UV-irradiated mammalian cell DNA usually require a 30-60 minute incubation in unlabelled medium after UV light treatment and before radioactivity is added (113, 116, 119). Replicons that have initiated prior to pulse-labelling but have not yet finished replication or stopped at a dimer will presumably take up very little label under these circumstances. This procedure also limits measurements of DNA strand length to the distance from replication origins to the first dimer on either strand. These protocols also compensate for depressed label uptake in UV-irradiated cultures by lengthening the time of pulse-labelling with increasing UV fluences to reach the same specific activity in DNA as found in control cultures (113). Neither of these precautions were taken in the pulse-labelling experiments described here for three reasons: (1) the average number of dimers per SV40 "replicon" remained small at the UV fluences studied; (2) the size of pulse-labelled SV40 DNA was not as important to these studies as the transition of label between various SV40 DNA conformations during replication, and (3) the Poisson distribution allowed mathematical modelling of label distribution in various SV40 DNA conformations and eliminated the need for lengthening the pulse-label. The decision not to lengthen the pulse-label with SV40 DNA is the major reason that the curves of Figures (32a-c) are shifted with UV fluence and is the cause of the apparent time delay in reaching the distribution of label found in control cultures. This time delay does not affect the following discussion since mathematical modelling has been adjusted to compensate for a constant time of pulse-labelling.

With this additional information, a simple model can be constructed to explain the observed depression of label uptake after UV light exposure. The Poisson distribution predicts that an average of n hits in a large population of targets leaves e^{-n} targets with no hits, ne^{-n} targets with one hit, $\frac{1}{2}n^2e^{-n}$ targets with two hits, and so on. If we assume the SV40 DNA molecules are "targets" and UV photoproducts are "hits," and further assume that 20 J/m^2 of UV light produces about 1.0 dimer per SV40 genome (Figure (24)), then the percent of control label uptake is approximately

$$\% \cong (1 + n + \frac{1}{4}n^2)e^{-n} \quad \text{for } n \text{ dimers per SV40}$$

genome and a 20 minute pulse label. This formula takes into account the length of time it takes an SV40 DNA molecule to replicate and assumes replication in the two replicating arms stops independently at UV photoproducts. It also uses the observation that an average SV40 DNA molecule is 1/3 replicated during a 20 minute pulse label. The percent of $^3\text{H-dThd}$ uptake at 20 ($n=1$) and 40 ($n=2$) J/m^2 of UV light predicted by this equation is $\% = 0.81(n=1)$ and $0.56(n=2)$. These values do not differ greatly from the observed values of $0.60(n=1)$ and $0.44(n=2)$.

The profiles of Figure (31) show that Form I molecule formation is sensitive to UV light while replicative intermediate formation is resistant. This agrees with the models of Edenberg (119), Clarkson and Hewitt (116), and others (35, 117) that DNA elongation is inhibited by UV photoproducts while initiation is resistant to UV light exposure. The proportional decrease in Form II molecules with UV-irradiation can be attributed to inhibition of DNA synthesis in

the daughter strand opposite a parental strand containing one or more UV photoproducts. Painter has proposed that the adjacent gap found in the daughter strand is downstream from a dimer in the direction of replication (125), but it is more likely true that the gap is within a very few nucleotides of the dimer.

There is a resistant subpopulation of replicative intermediates which are difficult to chase into Form I molecules. This is most evident at 40 J/m² (Figure 32a) where more than 10% of all label is contained in replicative intermediates that otherwise would have successfully completed replication. The origin of this subpopulation is confused by the constant re-entrance of Form I molecules into the pool of replicating molecules (77, Figure (32a) of this thesis). This subpopulation probably is comprised of molecules carrying more than one dimer in the unreplicated DNA region. If we assume the probability of more than one dimer in the unreplicated region of an "average" SV40 DNA molecule that is 1/3 replicated is P and also assume replication is stopped on both parental strands at a growing fork which encounters a dimer, then P is approximately given by

$$P \cong \left(\frac{1}{12} + \frac{n}{27} \right) n^2 e^{-n} . \quad \text{Equation (1)}$$

This equation takes into account the decreased label uptake into this replicating molecule (see Appendix E). Thus

$$P(40 \text{ J/m}^2) \cong P(n=2) \cong 0.09.$$

If we assume that replication can continue to completion on a daughter strand copying an undamaged template strand at a growing fork which has encountered a dimer, then the equation for P is

modified (see Appendix E):

$$P \cong \frac{1}{3} \left(\frac{1}{12} + \frac{1}{27}n \right) n^2 e^{-n}. \quad \text{Equation (2)}$$

Now we find $P(n=2) \cong 0.03$. The results from equation (1) are in better agreement with the results of Figure (32a) than those from equation (2). The model for equation (1) is also more reasonable on an ad hoc basis since it is likely that replication on both parental strands at a growing fork is coordinated to prevent large single-stranded DNA regions from exposure to endogenous nucleases.

The conclusion that replication stops on both parental strands of a growing fork halted at or near a dimer contradicts the conclusions of Clarkson and Hewitt (116) and raises the issue of single-stranded DNA regions that appear at or near dimers (112, 117, 118). Clarkson and Hewitt based their model partly on the supposition that newly synthesized DNA that is pulse-labelled one hour after UV-irradiation must consist entirely of DNA in replicons that have not yet encountered a dimer after initiating replication. However, their model and the results of other investigators (112, 117, 118) suggest the replication blocks are bypassed within a few hours. In this instance, some pulse-label must go into molecules longer than the average interdimer distance even when time is allowed to elapse after UV-irradiation and before pulse-labelling begins. The average length of labelled daughter molecules may then approximate the average interdimer distance despite retardation of both daughter strands at a dimer. Models that postulate either one or both daughter DNA strands are

retarded will then explain the literature observations equally well.

The presence of single-stranded regions must then be considered in light of the SV40 data. One explanation for these regions is that the DNA strands ahead of a growing fork must open up in preparation for replication. A revised model of DNA synthesis on UV-irradiated templates would then predict that the dimer somehow interferes with the polymerization of small nascent DNA on the UV-damaged DNA strand but not on the undamaged strand (117). Bypass of the dimer would then close this gap. The data of Menighini using the *N. crassa* single-strand-specific endonuclease shows the presence of single-stranded regions in UV-irradiated template DNA that disappear within two hours post-UV (117). These regions would be predicted to be adjacent to dimers in the template strands.

The contribution of two growing forks meeting at a dimer to the state of mammalian DNA shortly after UV-irradiation is small since there are about 10 dimers induced per replicon at 10 J/m^2 of UV light (112). However, the circular structure and small size of SV40 DNA increases the likelihood of a dimer serving as a new termination site for UV fluences producing an average of 1 or 2 dimers per SV40 genome (20 and 40 J/m^2 , respectively). The percent of Form II molecules is initially increased by UV-irradiation, as expected if dimers define new termination sites and temporarily inhibit ring closure. However, Figure (32b) shows that Form II molecules do not accumulate in UV-irradiated SV40 DNA. This suggests that ring closure occurs more rapidly than the time necessary to finish

replication in replicative intermediates. Thus, the time to close a small gap opposite a dimer in a Form II molecule must be less than 15 minutes. We can infer that the time to bypass a dimer blocking replication in mammalian cell DNA will be at least this long and that mammalian cells have the capacity to polymerize across a dimer without removing the dimer. This may be the origin of increased frequencies of mutation in XP variant cells (126) where elongation of nascent DNA in UV-irradiated cells is slower than in XP or normal human fibroblasts.

A prediction from these ideas is that a substantial fraction of Form II molecules in UV-irradiated CV-1 cells will contain a small gap of only a few nucleotides opposite a dimer. The tests for such gaps with T4 endonuclease V proved negative. This result means either the gaps are not opposite dimers or T4 endonuclease V is not active against this DNA conformation for some unknown reason. Menighini and Hanawalt failed to detect gaps with T4 endonuclease V in WI38 or HeLa cells in a similar experiment (124). Since the DNA conformation at an interrupted mammalian DNA growing fork (three double helical DNA strands at a gap site) differs from that in a Form II SV40 molecule (two double helical DNA strands at a gap site), the DNA conformation may not be the problem. However, both these DNA conformations differ from the known active substrates for T4 endonuclease V, namely single or double-stranded DNA containing dimers and no gaps (128). A peculiarity of both DNA conformations may somehow prevent T4 endonuclease V from making single-strand nicks at dimers interrupting replication.

Some other possible reasons for the failure of T4 endonuclease

V to create double-strand breaks at a dimer site in replicating DNA can be postulated. It is possible that gaps may appear opposite dimers in Form II molecules, but, as mentioned above, the gaps may close so quickly that detection is impossible. Alternatively, replication enzymes may bind very tightly at a growing point and block T4 endonuclease V activity at that site. The high salt conditions used to isolate SV40 tend to deproteinize DNA (173), but DNA samples were dialyzed afterwards against a low salt buffer (T4 buffer) in the presence of the same proteins. These proteins may have bound again or remained bound at the dimer site in replicating molecules, masking the dimer to T4 endonuclease V. Discrimination between these two hypotheses and the claim that gaps are not opposite dimers is not possible from the available data. A similar ambiguity may explain the failure to detect dimers opposite gaps with the UV-specific M. luteus endonuclease (116).

The Clarkson and Hewitt model (116) and the Menighini model (117) both explain the failure to detect dimers opposite gaps and the existence of single-stranded gaps in daughter DNA copying a UV-damaged template. However, their models are based on data from alkaline sucrose velocity gradients after UV-endonuclease treatment. It is possible that their enzyme preparations contained a contaminant that produced alkali-labile sites in the substrate DNA under the conditions of assay and that these sites were converted to single-strand breaks only in alkali. If their UV-endonucleases could not work at dimers near growing forks, then their conclusions would be based on misleading results. There is no precedent for this type of behavior for UV-endonuclease preparations in the literature, but

definitive sedimentation experiments under non-alkaline denaturing conditions (e.g., in formamide) have not been done. Consequently, this unlikely hypothesis cannot be entirely disregarded.

It is symptomatic of the state of the art that Menighini and Hanawalt invoked possible substrate problems in their studies (124) despite clear evidence in alkali sedimentation profiles that their T4 endonuclease V enzyme preparation led to strand breaks in parental DNA. Their caution in stating their conclusions was possibly motivated by the activity of T4 endonuclease V against daughter DNA strands as well as parental strands. Technical problems also may have affected the results of Clarkson and Hewitt (116). Their neutral sucrose sedimentation profiles show much of their DNA pelleting to the bottom and it may be that their calculations of median molecular weights in these skewed radioactivity profiles obscured real decreases in the size of large DNA. Other means of detecting single-stranded gaps in parental DNA and relating them to the location of dimers in parental DNA must be developed before further progress in this area can be made. Menighini has used one such method (117); others must be found.

V. A MODEL FOR DNA SYNTHESIS
IN UV-IRRADIATED SV40 DNA

Information on DNA synthesis in UV-irradiated mammalian cells can be combined with the observations of this thesis to restate more succinctly some of the above conclusions and to provide a more accurate picture of "post-replication repair" in mammalian cells. The model necessarily is limited to DNA synthesis in UV-irradiated SV40 DNA, but the similarities in SV40 and mammalian cell DNA synthesis do allow tentative generalization of the model to mammalian cell DNA.

A replicating fork in SV40 DNA is stopped at or near a pyrimidine dimer after UV-irradiation of an infected culture. The dimer probably blocks replication from continuing on both parental strands at the growing fork, but the DNA ahead of the growing fork opens enough for a small section of daughter DNA to be inserted and ligated opposite the undamaged parental strand. This leaves a small single-stranded region adjacent to the daughter DNA copying the UV-damaged parental strand. This gap is closed by one of two mechanisms:

(1) The replicating arm proceeding in the opposite direction from the blocked replicating arm arrives distal to the blocked replicating fork, one daughter molecule completes replication normally, and the second daughter molecule seals the small single-stranded gap opposite the dimer within 15 minutes of daughter molecule segregation. It is an open question whether the dimer directly opposes the daughter strand gap, but it seems likely that only

technical problems have prevented the collection of evidence for the dimer-gap apposition.

(2) The second replicating arm is also blocked by a UV photoproduct, principally another dimer, and the pyrimidine dimers are bypassed slowly. The time to bypass the replication block is dependent on the mode of replication at a growing fork (116, 117). For SV40 DNA, replication is discontinuous on both strands (67) and the growing fork will almost certainly be blocked if the dimer is in the parental strand upon which a daughter molecule is synthesized in the 5'→3' direction (117). A dimer in the parental strand of opposite polarity may allow the growing fork to move on in mammalian cells, leaving a small gap opposite the dimer (116, 117). However, this situation also stops the growing fork in SV40 DNA. It is not known if single-stranded gaps as described by Menighini (117) appear in daughter SV40 DNA, but it seems likely they are quickly sealed in analogous fashion to the closure of gaps in SV40 Form II molecules (see case (1) above). These blocks are eventually overcome by an unknown mechanism after at least three hours.

As a speculation, it is plausible that the gap filling proceeds as a function of the cellular replication complex associated with a growing fork. Small gaps opposite dimers remain open for 15-120 minutes after the replication complex is stopped by a dimer (117, this thesis). During this time, the replication machinery can remain attached at the site of interrupted DNA elongation, or, if dissociating, must reattach before elongation can resume. One can thus

picture the dimer block forcing the replication machinery to "idle," attempting to overcome an energetically unfavorable situation while single base residues are continually tested for a good "fit" opposite the dimer. Finally the energy block is surmounted in a stochastic process with or without the properly inserted bases. Removal of incorrect bases and/or of the dimer can then be accomplished by the excision repair system with potentially mutagenic consequences.

Appendix A. Calculation of repair replication in SV40 DNA from infected cultures after exposure to UV light:

The corrected ratio of ^3H counts to ^{14}C counts in the SV40 Form I DNA peak resolved on alkaline sucrose isokinetic gradients was calculated as a measure of repair replication in SV40 DNA. Correction for ^{14}C count spillover into the ^3H spectrometer channel was done from correction curves using external ^{14}C -labelled DNA standards. The contribution of semi-conservative DNA synthesis to the ^3H counts was also corrected for using the results in Figure (29) with the assumption that SV40 DNA and CV-1 DNA synthesis are similarly suppressed when similar UV doses and labelling conditions are used. Two observations of SV40 DNA synthesis using the above protocol with the omission of hydroxyurea are plotted on Figure (29) for comparison and bear out this assumption.

The corrected $^3\text{H}/^{14}\text{C}$ ratio for repair replication in SV40 DNA can be expressed by the formula:

$$^3\text{H}/^{14}\text{C} \left| \begin{array}{l} \text{repair} \\ \\ \text{UV fluence} = d \end{array} \right. = \frac{h_d - \text{BF}_{h_d}}{c_d - \text{BG}_{c_d}} - f_1 - \left[\frac{h_o - \text{BG}_{h_o}}{c_o - \text{BG}_{c_o}} \times f_2 \right]$$

where $\text{BG}_{h_d} = \text{BG}_{h_o} =$ background counts in ^3H channel,

$BG_{c_d} = BG_{c_o} =$ background counts in ^{14}C channel,

$h_d =$ tritium counts at UV fluence of $d \text{ J/m}^2$,

$h_o =$ tritium counts at UV fluence of 0 J/m^2 ,

$c_d =$ carbon-14 counts in ^{14}C channel at UV fluence of $d \text{ J/m}^2$,

$c_o =$ carbon-14 counts in ^{14}C channel at UV fluence of 0 J/m^2 ,

$f_1 =$ fraction of ^{14}C counts (c_d) spilling into ^3H channel,

and $f_2 =$ fraction of control DNA synthesis at UV dose of $d \text{ J/m}^2$; taken from Figure (29).

Appendix B. Calculation of number average DNA molecular weight (M_n) and weight average DNA molecular weight (M_w) from SW40 rotor alkaline sucrose gradient radioactivity profiles:

$$M_n \text{ is defined as } M_n = \frac{\sum_i M_i n_i}{\sum_i n_i}$$

and

$$M_w \text{ is defined as } M_w = \frac{\sum_i M_i^2 n_i}{\sum_i M_i n_i}, \text{ where } M_i \text{ is the mass}$$

of a DNA molecule sedimenting to the center of the i th alkaline sucrose gradient fraction and n_i is the number of molecules with mass M_i (39). The fractional distance sedimented by DNA at the center of each alkaline sucrose gradient fraction was calculated with corrections for the mean position of the DNA starting zone and the presence of a 0.60 ml high density ($\rho = 1.62$) CsCl cushion at the bottom of each SW40 gradient. It was experimentally found that the mean position of the DNA starting zone was approximately the interface between the sample-lysis layer solution and the alkaline sucrose gradient solution. If the counts per minute in the i th fraction is designated C_i and the corrected fractional distance sedimented to the center of the i th fraction as r_i , then

$$S_i = \text{sedimentation coefficient in svedbergs (10}^{-13} \text{ sec)} = \frac{\alpha r_i}{\omega^2 T}$$

$$M_i = (S_i / .0528)^{2.5} \text{ by the Studier relation (176 ;} \\ \text{also see 177, 178)}$$

and

$$M_n = \frac{0.5 \times C_T}{\sum_i C_i (\omega^2 T / r_i)^{2.5}} \quad \text{equation (1)}$$

$$M_w = \frac{0.5 \times \sum_i C_i (r_i / \omega^2 T)^{2.5}}{C_T} \quad \text{equation (2)}$$

where $C_t = \sum_i C_i$, α is an empirical calibration constant given by the slope of a curve of fractional distance an SV40 Form I DNA molecule sedimented vs. time of sedimentation at 39,000 rpm, ω is the centrifuge angular speed in rpm, and T is the time of centrifugation in minutes.

The sedimentation of SV40 DNA was found to be linear with time although the alkaline sucrose distribution in the alkaline gradients was not exponential and therefore not strictly isokinetic (179). Because of this observation, these gradients are referred to in this thesis as isokinetic on the basis of restricting sedimenting DNA to a constant velocity. After correcting for unit changes (minutes to seconds), the sedimenting coefficient α was found to be 0.040 ± 0.002 Svedbergs $\times \text{sec}^{-1}$ (data not shown). Equations (1) and (2) rely completely on experimental quantities and were used to calculate M_n and M_w after ignoring the top and

bottom three fractions in each gradient for the calculations (180, 181).

Appendix C. Calculation of the number of T4 endonuclease V-sensitive sites per 10^8 daltons of CV-1 DNA from alkaline sucrose gradient radioactivity profiles:

Number average DNA molecular weight (M_n) and weight average DNA molecular weight (M_w) values were calculated from alkaline sucrose gradient radioactivity profiles as described in Appendix B. Paired alkaline sucrose gradients which contained DNA handled identically except for the use of T4 endonuclease V on the DNA of one gradient just prior to centrifugation yielded the four molecular weights $M_n(-T4\ endo)$, $M_n(+T4\ endo)$, $M_w(-T4\ endo)$, and $M_w(+T4\ endo)$. When the ratio of M_w to M_n in a single gradient fell in the range 1.6-2.4, the alkaline sucrose gradient profile was assumed monodisperse (182, 183) and the corrected number N_{uv}^f of T4 endonuclease V-sensitive sites per 10^8 daltons of DNA after a UV flux of $f\ J/m^2$ was calculated as:

(monodisperse)

$$N_{uv}^f = 10^8 \left[\left(\frac{1}{M_n(+T4\ endo)_f} - \frac{1}{M_n(-T4\ endo)_f} \right) - \left(\frac{1}{M_n(+T4\ endo)_{f=0}} - \frac{1}{M_n(-T4\ endo)_{f=0}} \right) \right]$$

In some circumstances, skewed radioactivity profiles occurred and gave M_w/M_n ratios greater than 2.4. This frequently happened at UV doses equal or greater than $25\ J/m^2$.

When the radioactivity profile was skewed towards the bottom of the alkaline sucrose gradient, the observation was discarded since diffusion of the CsCl high density cushion produced anomalous sedimentation in this region of the gradient. Observations were also discarded if an excess of T4 endonuclease V was not used to analyze for UV-specific endonuclease-sensitive sites; this meant the following empirical relation had to be satisfied (data not shown):

$$(\text{cpm}) \times (f_{\text{uv}}) \times (\mu\text{l}) \leq 4 \times 10^4$$

where cpm = counts per minute in 5 μl of CV-1 DNA sample

$$f_{\text{uv}} = 0.8 \times \text{UV dose (in J/m}^2\text{)}$$

and μl = μl CV-1 DNA sample used per 5 μl of T4 endonuclease V.

When radioactivity profiles were skewed towards the top of an alkaline sucrose gradient, M_n values were considered unreliable since they are drastically altered by changes near the top of the gradient (see equation (1), Appendix B). In these cases, the number N_{uv}^f of T4 endonuclease V-sensitive sites per 10^8 daltons of DNA was calculated as:

(skewed)

$$N_{uv}^f = 2 \times 10^8 \left[\left(\frac{1}{M_w(+T4 \text{ endo})_f} - \frac{1}{M_w(-T4 \text{ endo})_f} \right) - \left(\frac{1}{M_w(+T4 \text{ endo})_{f=0}} - \frac{1}{M_w(-T4 \text{ endo})_{f=0}} \right) \right]$$

Appendix D. Calculation of the corrected percentage of tritium label found in the pyrimidine dimer peak on thin layer chromatograms:

True background counts in all fractions of a chromatogram profile were determined by counting phantom 0.6 cm x 2.0 cm chromatogram strips that had not been exposed to radioactivity. The percentage of counts in each fraction of a cell lysate chromatogram was calculated after correcting for true background and a histogram constructed of the percentage counts per fraction (see Figure (19)). Five fractions spanning the dimer peak region were chosen on all chromatograms including controls and the total percentage counts P_{uv} in these fractions determined. The percentage $P_{f_{uv}}$ of total counts attributable to pyrimidine dimers at a UV fluence f_{uv} was then calculated as the difference in P_{uv} values found at the fluence f_{uv} and unirradiated controls:

$$P = P_{uv}(f=f_{uv}) - P_{uv}(f=0).$$

This method was chosen to correct for technical problems that might have led to high background counts. The method of Cook & Friedberg (140) was not used for this reason and also because high fluences of UV light will raise the apparent background as judged by the minima on either side of the

dimer peak. These two methods give essentially identical results for most chromatograms (unpublished observation; Friedberg, personal communication).

Appendix E. Calculation of the maximum expected increase in DNA strand breakage by 313 nm light in SV40 DNA molecules which contain BrdUrd in place of dThd as a base residue in repaired regions of the SV40 genome:

Based on the data for endonuclease-sensitive sites in CV-1 and SV40 DNA and the loss of pyrimidine dimers from CV-1 DNA, we can estimate the maximum number of repaired regions in an SV40 DNA molecule during the 24 hours after UV-irradiation as 0.6. Let us assume that the average number of bases inserted at a site repaired by the excision repair system is 50 (21) and that 30% of the inserted bases are dThd since the G-C content of SV40 DNA is about 40% (67). The maximum number of BrdUrd bases which can then be inserted into a SV40 DNA molecule by excision repair is $0.6 \times 50 \times 0.3 = 9$ out of a total of 3000 dThd bases in an SV40 DNA molecule. Hutchinson reports the efficiency of 313 nm light breakage at a BrdUrd base residue is in the range of 20-2000 times that at a dThd residue (¹⁸⁴), so the maximum increase expected in conversion of SV40 Form I DNA molecules substituted with BrdUrd to Form II molecules is $9 \times \frac{(20-2000)}{3000} = (6-600) \%$ times that observed in unsubstituted SV40 DNA molecules.

Appendix F. Equations for the fraction of pulse label in UV-irradiated SV40 replicative intermediates (RIs) that persists for several hours after pulse-labelling:

For simplification only average effects will be considered. Under the conditions used (see text of Discussion), an average pulse-labelled SV40 molecule is $1/3$ replicated. Two cases are thought to be possible under the assumptions stated in the Discussion:

Case (1): Replication stops at both parental strands at a UV photoproduct (presumably a pyrimidine dimer). Then the fraction of label that persists in RIs is that found in molecules with two or more dimers in the unreplicated region. If $P(n)$ is the fraction of label in molecules with n dimers in the unreplicated region, then $P = P(2) + P(3) + \sum_{n=2}^{\infty} P(n)$. The contribution of these terms diminishes rapidly as n increases, so only the first two terms will be considered, or

$$P \cong P(2) + P(3)$$

The fraction of label in a molecule of given n is a function of the location of the dimers (that is, on one or both strands) and the amount of unreplicated DNA between the dimer and the growing fork approaching it. There is reason to believe one arm of the bidirectional replication can copy the entire SV40 genome if necessary (67,74), so calculation of the amount of label entering a replicating molecule must

take this fact into account. Let us designate the amount of label entering a single DNA daughter strand that is of SV40 genome length as $\frac{3}{2}L$, so that the length of the uncopied region on a single parental strand in the average SV40 replicating molecule is L . For $P(2)$, the probability of two dimers both being in the unreplicated region is $\frac{2}{3} \times \frac{2}{3} = \frac{4}{9}$ and there are four possible distributions of two dimers ahead of the replicating forks. Thus,

$$P(2) = \frac{4}{9} \left(\frac{1}{2}n^2 e^{-n} \right) \left[\frac{2 \times \frac{1}{2}L + 2 \times L}{8L} \right] \text{ using average}$$

positions of the dimers ahead of the growing forks (the average positions are $\pm \frac{1}{6}$ genome lengths ($\pm \frac{1}{4} L$) from the normal termination site),

$$P(2) = \frac{6}{72} n^2 e^{-n} \approx \frac{1}{12} n^2 e^{-n}$$

Similarly,

$P(3) = \frac{17}{27} \left(\frac{1}{6}n^3 e^{-n} \right) [S]$ where $[S]$ is a complex function containing nine terms. S is less than the term in brackets for $P(2)$ above, so a maximum expression for $P(3)$ is

$$P(3) = \frac{17}{27} \left(\frac{1}{6}n^3 e^{-n} \right) \left(\frac{3}{8} \right) \approx \frac{1}{27} n^3 e^{-n}$$

$$\text{Thus } P \approx \left(\frac{1}{12} + \frac{1}{27}n\right) n^2 e^{-n}. \quad \text{Equation (1)}$$

Case (2): If replication is allowed to continue on the undamaged parental strand, then $P(2)$ and $P(3)$ decrease since several cases considered above lead to completion of replication on at least one parental strand. The expression in brackets above for $P(2)$ becomes

$$\frac{2 \times \frac{1}{2}L + 2 \times 0}{8L} = \frac{1}{8} \quad \text{since only in the two cases where}$$

both dimers are on the same parental strand does replication halt for at least one parental strand. Thus

$$P(2) \approx \frac{4}{9} \left(\frac{1}{2}n^2 e^{-n}\right) \frac{1}{8} \approx \frac{1}{36}n^3 e^{-n}$$

and the maximum $P(3)$ is $P(3) \approx \frac{17}{27} \left(\frac{1}{6}n^3 e^{-n}\right) \left(\frac{1}{8}\right) \approx \frac{1}{81} n^3 e^{-n}$

$$P \approx \frac{1}{3} \left(\frac{1}{12} + \frac{1}{27}n\right) n^2 e^{-n} \quad \text{Equation (2)}$$

VI. LIST OF REFERENCES

1. J. Bergonié and L. Tribondeau, Archivés d'électricité médicale, 14, 779 (1906).
2. Ibid., 14, 822 (1906).
3. Ibid., 14, 874 (1906).
4. Ibid., 14, 911 (1906).
5. D. E. Lea, Actions of Radiations on Living Cells, Cambridge at the University Press, London (1955).
6. Z. M. Bacq and P. Alexander, Fundamentals of Radiobiology, Pergamon Press, New York (1961).
7. K. K. Sanford, W. R. Earle, and G. Likely, J. of Natl. Cancer Inst., 9, 229 (1948).
8. H. Eagle, Science, 122, 501 (1955).
9. T. T. Puck and P. I. Marcus, Proc. natn. Acad. Sci. U.S.A., 41, 432 (1955).
10. L. Hayflick and P. S. Moorhead, Exptl. Cell Res., 25, 585 (1961).
11. T. T. Puck and P. I. Marcus, J. Exptl. Med, 103, 653 (1956).
12. M. M. Elkind and H. Sutton, Nature, 184, 1293 (1959).
13. M. M. Elkind, H. Sutton, and W. B. Moses, J. Cell Comp. Physiol., 58 (supp. 1), 113 (1961).
14. M. M. Elkind and G. F. Whitmore, The Radiobiology of Cultured Mammalian Cells, Gordon and Breach, New York (1967).
15. R. E. Zirkle and C. A. Tobias, Arch. Biochem. Biophys., 47, 282 (1953).
16. H. Dertinger and H. Jung, Molecular Radiation Biology, Springer-Verlag, New York (1970).
17. A. Kelner, Proc. natn. Acad. Sci. U.S.A., 35, 73 (1949).

18. F. L. Gates, J. Gen. Physiol., 13, 231 (1929).
19. A. D. McLaren and D. Shugar, Photochemistry of Proteins and Nucleic Acids, Pergamon Press, Long Island City, N.Y. (1964).
20. P. Todd, T. P. Coohill, and J. A. Mahoney, Radiat. Res., 35, 390 (1968).
21. J. E. Cleaver, Advances in Radiation Biology, Vol. 4, pp. 1-75, Academic Press, New York (1974).
22. J. Jagger, Introduction to Research in Ultraviolet Photobiology, Prentice-Hall, Englewood Cliffs, N.J. (1967).
23. S. Okada, Radiation Biochemistry, Volume I: Cells, Academic Press, New York (1970).
24. P. Howard-Flanders, British Medical Bulletin, 29, 226 (1973).
25. R. B. Painter and R. E. Rasmussen, Nature, 201, 162 (1964).
26. R. Becker, J. Ijlstra, and W. Berends, Recueil Travaux Chimiques des Pays-Bas, 78, 883 (1959).
27. R. Becker and W. Berends, Biochim. Biophys. Acta, 41, 550 (1960).
28. R. B. Setlow and J. K. Setlow, Proc. natn. Acad. Sci. U.S.A., 48, 1250 (1962).
29. P. C. Hanawalt, Photophysiology, Vol. 4, pp. 204-252, Academic Press, New York (1968).
30. J. K. Setlow, M. E. Boling, and F. J. Bollum, Proc. natn. Acad. Sci. U.S.A., 53, 1430 (1965).
31. R. B. Setlow and W. L. Carrier, Proc. natn. Acad. Sci. U.S.A., 51, 226 (1964).
32. R. P. Boyce and P. Howard-Flanders, Proc. natn. Acad. Sci. U.S.A., 51, 293 (1964).
33. W. D. Rupp, E. Zipser, C. von Essen, D. Reno, L. Prosnitz, and P. Howard-Flanders, Time and Dose Relationships in Radiation Biology as Applied to Radiotherapy, Brookhaven National Laboratory, Upton, N.Y. (1969).

34. R. B. Painter, Current Topics in Radiation Research, 7, 45 (1970).
35. A. R. Lehman, Life Sciences, 15, 2005 (1974).
36. H. F. Stich, R. H. C. San, J. A. Miller and E. C. Miller, Nature (London) New Biol., 238, 9 (1972).
37. J. E. Cleaver, Cancer Research, 33, 362 (1973).
38. J. E. Cleaver, Nature, 218, 652 (1968).
39. J. E. Cleaver, Methods in Cancer Research, Vol. 11, pp. 123-165, Academic Press, New York (1975).
40. J. Pontén, Biochim. Biophys. Acta, 458, 397 (1976).
41. G. Chan and J. B. Little, Nature, 264, 442 (1976).
42. T. Boveri, The Origin of Malignant Tumors, Williams and Wilkens, Baltimore (1929).
43. J. E. Trosko, D. Krause, and M. Isoun, Nature, 228, 358 (1970).
44. A. Kornberg, DNA Synthesis, W. H. Freeman and Co., San Francisco, (1974).
45. B. A. Bridges and R. J. Munson, Mol. Gen. Genet., 103, 266 (1968).
46. L. J. Stadler, Cold Spring Harbor Symposium on Quantitative Biology, 9, 168 (1941).
47. F. T. Kao and T. T. Puck, J. Cell Physiol., 74, 245 (1969).
48. B. A. Bridges and J. Huckle, Mutation Res., 10, 141 (1970).
49. R. M. Humphrey, W. C. Dewey and A. Cork, Radiat. Res., 19, 247 (1963).
50. J. E. Cleaver and S. Weil, J. of Virology, 16, 214 (1975).
51. K. H. Kraemer, E. A. de Weerd-Kastelein, J. H. Robbins, W. Keijzer, S. F. Barret, R. A. Petinga, and D. Bootsma, Mutation Res., 33, 327 (1975).

52. J. E. Cleaver, J. Invest. Dermat., 58, 124 (1972).
53. A. R. Lehmann, S. Kirk-Bell, C. F. Arlett, M. C. Paterson, P. H. M. Lohman, E. A. de Weerd-Kastelein, and D. Bootsma, Proc. natn. Acad. Sci. U.S.A., 72, 219 (1975).
54. M. C. Paterson, B. P. Smith, P. H. M. Lohman, A. K. Anderson, and L. Fishman, Nature, 260, 444 (1976).
55. J. E. Cleaver, Metabolic Basis of Inherited Disease, Vol. 4, McGraw-Hill, New York (1976).
56. J. E. Cleaver, Proceedings of 5th International Congress of Human Genetics, Mexico City, in press (1976).
57. K. Cook, E. C. Friedberg, H. Slor, and J. E. Cleaver, Nature, 256, 235 (1975).
58. A. S. Rabson, S. A. Tyrell and F. Y. Legallais, Proc. Soc. Exptl. Biol. Med., 132, 802 (1969).
59. R. S. Day III, Photochem. and Photobiol., 19, 9 (1974).
60. S. A. Aaronson and C. D. Lytle, Nature, 228, 359 (1970).
61. P. J. Abrahams and A. J. Van der Eb, Mutation Res., 35, 13 (1976).
62. E. K. Wagner, M. Rice, and B. Sutherland, Nature, 254, 627 (1975).
63. R. S. Day III, A. S. Giuffrida, and C. W. Dingman, Mutation Res., 33, 311 (1975).
64. C. J. Lai and D. Nathans, Cold Spring Harbor Symposium on Quantitative Biology, 39, 53 (1974).
65. N. H. Seemayer and V. Defendi, J. of Virology, 13, 36 (1974).
66. B. H. Sweet and M. R. Hilleman, Proc. Soc. Exptl. Biol. Med., 105, 420 (1960).
67. J. Tooze, The Molecular Biology of Tumour Viruses, Cold Spring Harbor Laboratory, N. Y. (1973).
68. M. A. Martin, L. D. Gelb, C. Garon, K. K. Takemoto, T. N. H. Lee, G. H. Sack, and D. Nathans, Virology, 59, 179 (1974).

69. J. Y. Chou and R. G. Martin, J. of Virology, 13, 1101 (1974).
70. L. Polisky and B. McCarthy, Proc. natn. Acad. Sci. U.S.A., 72, 2895 (1975).
71. R. L. Mackey and R. A. Consigli, J. of Virology, 19, 620 (1976).
72. J. Griffith, Science, 187, 1202 (1975).
73. A. J. Levine, Biochim. Biophys. Acta, 458, 213 (1976).
74. C. J. Lai and D. Nathans, J. molec. Biol., 97, 113 (1975).
75. D. R. Dubbs, M. Rachmeler, and S. Kit, Virology, 57, 161 (1974).
76. P. J. Laipis, A. Sen, A. J. Levine, and C. Mulder, Virology, 68, 115 (1975).
77. P. Tegtmeyer and F. Macasaet, J. of Virology, 10, 599 (1972).
78. A. Roman and R. Dulbecco, J. of Virology, 16, 70 (1975).
79. W. W. Brockman, T. N. H. Lee, and D. Nathans, Virology, 54, 384 (1973).
80. N. Frenkel, S. Lavi, and E. Winocour, Virology, 60, 9 (1974).
81. F. Holzel and F. Sokol, J. molec. Biol., 84, 423 (1974).
82. I. Prasad, D. Zouzias, and C. Basilico, J. of Virology, 16, 897 (1975).
83. M. A. Martin, P. M. Howley, J. C. Byrne, and C. F. Garon, Virology, 71, 28 (1976).
84. R. Gingery and H. Echols, Cold Spring Harbor Symposium on Quantitative Biology, 33, 721 (1968).
85. M. R. Botchan, B. Ozanne, W. Sugden, P. Sharp, and J. Sambrook, Proc. natn. Acad. Sci. U.S.A., 4183 (1974).
86. K. N. Subramian, J. Pan, S. Zain, and S. M. Weissman, Nucleic Acids Research, 1, 727 (1974).

87. J. Carbon, T. E. Shenk, and P. Berg, Proc. natn. Acad Sci. U.S.A., 72, 1392 (1975).
88. T. E. Shenk, J. Carbon, and P. Berg, J. of Virology, 18, 664 (1976).
89. C. Aaij and P. Borst, Biochim. Biophys. Acta, 269, 192 (1972).
90. J. Sambrook, B. Sugden, W. Keller, and P. A. Sharp, Proc. natn. Acad. Sci. U.S.A., 70, 3711 (1973).
91. R. Laterjet, R. Cramer, and L. Montagnier, Virology, 33, 104 (1967).
92. T. Ide and K. Andoh, Virology, 66, 568 (1975).
93. J. E. Cleaver and G. H. Thomas, Biochem. Biophys. Res. Commun., 36, 203 (1969).
94. J. C. Kaplan, S. M. Wilbert, J. J. Collins, T. Rakusanova, G. B. Zamansky, and P. H. Black, Virology, 68, 200 (1975).
95. J. C. Kaplan, L. F. Kleinman, and P. H. Black, Virology, 68, 215 (1975).
96. C. D. Lytle, S. G. Benane, and J. E. Stafford, Photochem and Photobiol., 23, 331 (1976).
97. B. M. Sutherland and R. Oliver, Biochim. Biophys. Acta, 442, 358 (1976).
98. K. Mortelmans, J. E. Cleaver, G. H. Thomas, B. Smith, M. Paterson, and E. C. Friedberg, Biochim. Biophys. Acta (1977), in preparation.
99. R. S. Day III, Mutation Res., 33, 321 (1975).
100. R. B. Setlow, F. M. Faulcon and J. D. Regan, Int. J. Radiat. Biol., 29, 125 (1976).
101. L. Grossman, Advances in Radiation Biology, Vol. 4, pp. 76-129, Academic Press, New York (1974).
102. J. D. Regan and R. B. Setlow, Cancer Res., 34, 3318 (1974).

103. J. Duncan, H. Slor, K. Cook, and E. C. Friedberg, Molecular Mechanisms for Repair of DNA, Part B, pp. 643-649, Plenum Publishing Co., New York (1975).
104. G. Pawl, H. Slor, and E. C. Friedberg, J. of Bacteriology, 122, 341 (1975).
105. R. B. Painter and B. R. Young, Mutation Res., 14, 225 (1972).
106. H. Edenberg and P. C. Hanawalt, Biochim. Biophys. Acta, 324, 206 (1973).
107. M. C. Paterson, P. H. M. Lohman, and M. L. Sluyter, Mutation Res., 19, 245 (1973).
108. R. J. Wilkins and R. W. Hart, Nature, 247, 35 (1974).
109. J. R. Gautschi, B. R. Young, and J. E. Cleaver, Exptl. Cell Res., 76, 87 (1973).
110. A. M. Rauth, Radiat. Res., 31, 121 (1967).
111. R. E. Meyn and R. M. Humphrey, Biophys. J., 11, 295 (1971).
112. A. R. Lehmann, J. molec. Biol., 66, 319 (1972).
113. S. F. H. Chiu and A. M. Rauth, Biochim. Biophys. Acta, 259, 164 (1972).
114. W. D. Rupp and P. Howard-Flanders, J. molec. Biol., 31, 291 (1968).
115. J. D. Regan, R. B. Setlow and R. D. Ley, Proc. natn. Acad. Sci. U.S.A., 68, 708 (1971).
116. J. M. Clarkson and R. R. Hewitt, Biophys. J., 16, 1155 (1976).
117. R. Menighini, Biochim. Biophys. Acta, 425, 419 (1976).
118. S. N. Buhl, R. B. Setlow, and J. D. Regan, Int. J. Radiat. Biol., 22, 417 (1972).
119. H. J. Edenberg, Biophys. J., 16, 849 (1976).
120. H. J. Edenberg and J. A. Huberman, Ann. Rev. Genetics, 9, 245 (1975).

121. L. F. Povirk and R. B. Painter, Biophys. J., 16, 883 (1976).
122. A. R. Lehmann, Eur. J. Biochem., 31, 438 (1972).
123. S. N. Buhl, R. B. Setlow, and J. D. Regan, Biophys. J., 13, 1265 (1973).
124. R. Meneghini and P. Hanawalt, Biochim. Biophys. Acta. 425, 428 (1976).
125. R. B. Painter, Molecular Mechanisms for Repair of DNA, Part B, pp. 595-600, Plenum Publishing Co., New York (1975).
126. V. M. Maher, L. M. Ouellette, R. D. Curren, and J. J. McCormick, Nature, 261, 593 (1976).
127. G. Kimura and R. Dulbecco, Virology, 49, 394 (1972).
128. E. C. Friedberg and J. J. King, J. of Bacteriology, 106, 500 (1971).
129. R. Dulbecco and M. Vogt, J. Exptl. Med., 99, 167 (1954).
130. H. J. Burki, S. Bunker, M. Ritter, and J. E. Cleaver, Radiat. Res., 62, 299 (1975).
131. B. Hirt, J. molec. Biol, 26, 365 (1967).
132. J. E. Cleaver, J. of Virology, 14, 1607 (1974).
133. R. Goth and J. E. Cleaver, Mutation Res., 36, 105 (1976).
134. L. Povirk and R. B. Painter, Biochim. Biophys. Acta, 432, 267 (1976).
135. C. Mulder and H. Delius, Proc. natn. Acad. Sci. U.S.A., 69, 3215 (1972).
136. J. F. Morrow and P. Berg, Proc. natn. Acad. Sci. U.S.A., 69, 3365 (1972).
137. C. S. Lange and D. F. Liberman, Anal. Biochem., 59, 129 (1974).
138. J. E. Cleaver, G. H. Thomas, J. E. Trosko, J. T. Lett, Exptl. Cell Res., 74, 67 (1972).


139. B. Hudson, W. B. Upholt, J. Deviny, and J. Vinograd, Proc. natn. Acad. Sci. U.S.A., 62, 813 (1969).
140. K. H. Cook and E. C. Friedberg, Anal. Biochem., 73, 411 (1976).
141. The American Tissue Culture Collection Registry of Animal Cell Lines, Rockville, Maryland (1972).
142. D. Gershon, L. Sachs, and E. Winocour, Proc. natn. Acad. Sci. U.S.A., 56, 918 (1966).
143. E. Ritzi and A. J. Levine, J. of Virology, 5, 686 (1969).
144. P. Liberti, L. Fischer-Fantuzzi, and C. Vesco, J. molec. Biol., 105, 263 (1976).
145. J. M. Boyle and R. B. Setlow, J. molec. Biol., 51, 131 (1970).
146. L. C. Klotz and B. H. Zimm, J. molec. Biol., 72, 779 (1972).
147. S. Kondo, Genetics, 78, 149 (1974).
148. J. H. Zar, Biostatistical Analysis, Prentice-Hall, Englewood Cliffs, N.J. (1974).
149. K. C. Smith, Biochem. Biophys. Res. Commun., 6, 458 (1962).
150. M. Domon and A. M. Rauth, Radiat. Res., 35, 350 (1968).
151. J. E. Cleaver, Radiat. Res., 37, 334 (1969).
152. P. C. Hanawalt, Photochem. Photobiol., 5, 1 (1966).
153. J. E. Cleaver, Int. J. Radiat. Biol., 18, 557 (1970).
154. J. E. Cleaver, Thymidine metabolism and cell kinetics, John Wiley and Sons, Inc., New York (1967).
155. H. Turler, J. of Virology, 15, 1158 (1975).
156. D. A. Clayton, J. N. Doda, and E. C. Friedberg, Proc. natn. Acad. Sci., U.S.A., 71, 2777 (1974).
157. R. J. Wilkins, Int. J. Radiat. Biol., 24, 609 (1973).

158. E. C. Friedberg and D. A. Clayton, Nature, 237, 99 (1972).
159. S. Abrahamson, M. A. Bender, A. D. Conger, and S. Wolff, Nature, 245, 460 (1973).
160. J. E. Cleaver, Molecular and Cellular Repair Processes, pp. 195-211, John Hopkins University Press, Baltimore, Md. (1972).
161. J. E. Cleaver, Photochem. and Photobiol., 12, 17 (1970).
162. C. W. Dingman and T. Kakunaga, Int. J. Radiat. Biol., 30, 55 (1976).
163. I. G. Walker and R. Sridhar, Chem-Biol. Interactions, 12, 229 (1976).
164. A. J. Fornace, Jr., K. W. Kohn, and H. E. Kann, Jr., Proc. natn. Acad. Sci., U.S.A., 73, 39 (1976).
165. B. H. Zimm, Biophys. Chem., 1, 279 (1974).
166. J. E. Cleaver, Biochem. Biophys. Res. Commun., 59, 92 (1974).
167. G. Ahnstrom and K. Erixon, Int. J. Radiat. Biol., 23, 285 (1973).
168. R. B. Painter and J. E. Cleaver, Radiat. Res., 37, 451 (1969).
169. R. W. Hart and R. B. Setlow, Proc. natn. Acad. Sci., U.S.A., 71, 2169 (1974).
170. W. S. Spector, ed., Handbook of Biological Data, p. 182, W. B. Saunders Co., Philadelphia, Pa. (1956).
171. S. Manteuil, J. Pages, D. Stehilin and M. Girard, J. of Virology, 11, 98 (1973).
172. A. J. Levine, H. S. Kang, and F. E. Billheimer, J. molec. Biol., 50, 549 (1970).
173. H. H. Ohlenbusch, B. M. Olivera, D. Tuan, and N. Davidson, J. molec. Biol., 25, 299 (1967).
176. F. W. Studier, J. molec. Biol., 11, 373 (1965).
177. A. Charlesby, Proc. Royal Society A, 224, 120 (1954).
178. E. Burgi and A. D. Hershey, Biophys. J., 3, 309 (1963).
179. H. Noll, Nature, 215, 360 (1967).
180. J. E. Cleaver, Radiat. Res., 57, 207 (1974).

181. C. J. Koch and R. B. Painter, Radiat. Res., 64, 256 (1975).
182. U. K. Ehmann and J. T. Lett, Radiat. Res., 54, 152 (1973).
183. J. T. Lett, I. Caldwell, and J. G. Little, J. molec. Biol., 48, 395 (1970).
184. F. Hutchinson, Quar. Rev. Biophys., 6, 201 (1973).

FOR REFERENCE

NOT TO BE TAKEN FROM THE ROOM

 CAT. NO. 23 012

PRINTED
IN
U.S.A.

